ABSTRACT

LIU, RAN. Modeling and Simulation of Nonstationary Non-Poisson Processes. (Under the direction of Dr. James R. Wilson.)

We develop and experimentally evaluate various methods for modeling and simulating nonstationary non-Poisson point processes (NNPPs) with the following key properties:

(i) a given mean-value function over a finite time horizon of interest;

(ii) a given "rate" function whose integral yields the given mean-value function over that time horizon; and

(iii) a given finite positive asymptotic value for the ratio of the process variance to its mean-value function as the time horizon for the process increases.

Recent research has focused on inversion and thinning methods for modeling and simulating NNPPs. Unfortunately the inversion method is limited to mean-value functions with an inverse that is analytically or numerically tractable; and the current thinning methods are not guaranteed to yield the desired dispersion (variance-to-mean) ratio for the given process even approximately. In this dissertation we propose CIAT, a combined inversion-and-thinning method for simulating NNPPs that avoids the disadvantages of the methods of inversion and thinning while retaining the advantages of each method.

First we construct a strictly positive step function that majorizes and closely approximates the given rate function and that also has an easily invertible majorizing mean-value function over the given time horizon. Next we generate a stationary renewal process whose interrenewal times have mean one and the desired variance-to-mean ratio; and finally the resulting sequence of renewal epochs is transformed via the inverse of the majorizing mean-value function to generate the associated "majorizing" point process. To complete CIAT we apply the thinning method to the arrival epochs of the majorizing NNPP to obtain the desired sequence of arrival epochs from an NNPP with the given rate function and the desired asymptotic dispersion ratio as follows. Each arrival epoch in the majorizing NNPP is independently selected for inclusion in the desired NNPP with probability equal to the ratio of the following : (i) the given rate function evaluated at the current arrival epoch in the majorizing NNPP; and (ii) the majorizing rate function evaluated at the same arrival epoch. CIAT is specifically designed so that at every arrival epoch in the majorizing NNPP, the ratio of (i) to (ii) is close to one, guaranteeing that a high percentage of the generated arrival epochs survive the thinning step of CIAT.

We establish the following key properties of a CIAT-generated NNPP:

- The resulting point process has the desired mean-value function over the given time horizon.
- If the desired mean-value function grows without bound as the time horizon increases, then the resulting point process asymptotically achieves the desired dispersion ratio, provided that the step

rate function for the majorizing process is based on a sufficiently fine subdivision of the time horizon into subintervals over which the step function is constant.

In an experimental performance evaluation involving a wide range of test processes, we examine the quality of CIAT-generated NNPPs and the efficiency of CIAT by evaluating the following:

(i) the closeness between the estimated mean-value function of the CIAT-generated NNPP and the corresponding desired mean-value function, and the closeness between the estimated asymptotic dispersion ratio and the desired asymptotic dispersion ratio;

(ii) the convergence rate of CIAT, expressed by the warm-up time, after which the estimated confidence intervals for the mean-value function and dispersion ratio of the CIAT-generated NNPP include their desired respective values; and

(iii) the computational cost for CIAT to generate 50 realizations of selected NNPPs over the given time horizon.

We also develop CIATL, a simplified version of CIAT using lognormal distributions for the interrenewal times in the underlying stationary renewal process. In the selected test processes, the performance of CIATL was similar to that of CIAT.

Modeling and Simulation of Nonstationary Non-Poisson Processes

by
Ran Liu

A dissertation submitted to the Graduate Faculty of
North Carolina State University
in partial fulfillment of the
requirements for the Degree of
Doctor of Philosophy

Operations Research

Raleigh, North Carolina

2013

APPROVED BY:

Dr. Peter Bloomfield	Dr. Julie Ivy
Dr. Michael G. Kay	Dr. Yunan Liu

Dr. James R. Wilson
Chair of Advisory Committee

BIOGRAPHY

Ran Liu received his bachelor's degree in applied mathematics from Peking University, Beijing, in June 2006. To pursue advanced degrees, he came to the United States in August 2006. He received a master's degree in applied mathematics from Wayne State University in August 2008. He joined the Ph.D. program in Operations Research at North Carolina State University in Fall 2008. His primary research interest includes simulation modeling, analysis, and optimization. During his Ph.D. study, he also served as a teaching assistant and was a student intern at the SAS Institute.

ACKNOWLEDGEMENTS

I would like to express my sincere gratitude to my advisor Dr. James R. Wilson for his supervision, thoughtful advice, kindness, patience, and his continued support and encouragement throughout my Ph.D. study. His guidance toward being a professional is an invaluable asset which I will carry in the future. I thank Dr. Peter Bloomfield for serving on my committee, and I have benefited a lot from Dr. Bloomfield's time series course. I thank Dr. Julie Ivy for serving on my committee, and I highly enjoyed her applied stochastic models course which inspired me a lot in my research. Many thanks go to Dr. Yunan Liu for serving on my committee and his comments and enlightening advice on my work. Special thanks go to Dr. Michael G. Kay for serving on my committee. Dr. William Stewart's queueing systems course was the most joyful course I have ever taken, which affected my dissertation path significantly.

I also would like to thank Rong Huang, one of the most important persons in my life who is always there for me. Finally, I would like to express my gratitude to my parents Yunxiu Sun and Taoxi Liu for their motivation and support for me all the time.

TABLE OF CONTENTS

LIST OF TABLES

LIST OF FIGURES

Chapter 1

Introduction

1.1. Motivation

Arrival processes with time-varying arrival rates are routinely encountered in practical applications of industrial and systems engineering techniques. Discrete-event stochastic simulation is almost always used to analyze and improve system operation in such situations. Consequently, in order to perform meaningful simulation experiments, developing and implementing high-fidelity probabilistic input models is of great importance.

A homogeneous Poisson process (HPP) has interarrival times that are independent and identically distributed (i.i.d.) exponential random variables; and HPPs are often used because over a finite time horizon, they yield random arrivals with a constant arrival rate. However, interarrival times are frequently not i.i.d. exponential random variables. For instance, in many locales, the storm-arrival process [23] depends on the season of the year and exhibits greater variability than a homogeneous Poisson process. On the other hand, in many manufacturing systems, customer orders have an arrival rate that exhibits daily, weekly, and monthly effects as well as long-term trends; and yet the associated point process describing the buildup of orders over time exhibits less variability than the homogenous Poisson process [8].

Nonhomogeneous Poisson processes (NHPPs) have been widely used to model complex time-dependent arrival processes in a broad range of application domains [27, 31]. A noteworthy application involved organ-transplantation policy decisions. In the analysis of the cadaveric liver-allocation system in the United States, the United Network for Organ Sharing (UNOS) applied the NHPP techniques for modeling and simulating patient- and donor-arrival streams in the development and use of the UNOS Liver Allocation Model (ULAM); see [13]. ULAM incorporated NHPP models of the following: (a) the streams of liver-transplant patients arriving at 115 transplant centers; and (b) the streams of donated organs arriving at 61 organ procurement organizations in the United States. Virtually all these arrival streams exhibited strong dependencies on the time of day, the day of the week, and the season of the year as well as pronounced geographic effects.

Although NHPPs are used to model a large class of nonstationary arrival processes, there exist a number of situations, including some applications in manufacturing, telecommunications, marketing, and other areas, where NHPPs are inappropriate to represent arrivals. In some cases, the key characteristics of the designated arrival process (for example, its variability about its mean-value function) deviate considerably from those of an NHPP, which may invalidate the resulting simulation-based estimates of overall system performance. A study of wide-area traffic has shown that modeling TELNET packet arrivals by Poisson processes grossly underestimates the burstiness of TELNET traffic [30]. Studies in consumer behavior reveal that the purchasing process for frequently purchased goods follows a more regular distribution and has a smaller coefficient of variation than a Poisson process [33]. Thus, the simulation input models for nonstationary non-Poisson (NNPP) arrival processes are highly desired.

1.2. Problem Statement

Suppose that $\{N(t) : t \geq 0\}$ is a given nonstationary arrival process defined by

$$N(t) = \text{number of arrivals in } (0, t] \text{ for } t \geq 0 \tag{1.1}$$

that may be non-Poisson and that we wish to estimate, validate, and simulate efficiently. This arrival process has the *mean-value function*

$$\mu(t) \equiv \mathrm{E}[N(t)] \quad \text{for} \quad t \geq 0 \tag{1.2}$$

that by assumption can be expressed in the form

$$\mu(t) = \int_0^t \lambda(u)du \quad \text{for} \quad t \geq 0, \tag{1.3}$$

where the *"rate" function* $\lambda(u)$ is assumed to be nonnegative and (Lebesgue) integrable on $\mathbb{R}_+$, the nonnegative real numbers. The associated *variance function* is

$$\mathrm{Var}[N(t)] \equiv \mathrm{E}\{[N(t) - \mu(t)]^2\} \quad \text{for} \quad t \geq 0; \tag{1.4}$$

and the process $\{N(t) : t \geq 0\}$ is assumed to have a limiting variance-to-mean ratio

$$C \equiv \lim_{t\to\infty} \frac{\mathrm{Var}[N(t)]}{\mathrm{E}[N(t)]}, \quad \text{where } 0 < C < \infty, \tag{1.5}$$

that we call the *asymptotic dispersion ratio*. Now all HPPs and NHPPs have the variance-to-mean ratio of 1 for all $t \geq 0$; and thus when the designated process $\{N(t) : t \geq 0\}$ has asymptotic dispersion ratio

$C \neq 1$, the latter process must be a nonstationary non-Poisson (NNPP) process for which we require new methods for efficient estimation, validation, and simulation. The main objective of the proposed research is to develop such methods.

To facilitate the rest of the discussion, we introduce some basic notation that will be used throughout this dissertation. Let X_n denote the interarrival time between the $(n-1)$st and nth arrivals in the process $\{N(t) : t \geq 0\}$ for $n = 1, 2, \ldots$. Let $S_0 \equiv 0$; and for $n = 1, 2, \ldots$, let $S_n = \sum_{i=1}^{n} X_i$ denote the nth arrival epoch so that

$$N(t) \equiv \max\{n : S_n \leq t\} \text{ for } t \geq 0.$$

To simulate the designated nonstationary non-Poisson process with rate function $\lambda(t)$ and asymptotic dispersion ratio C, we start from a stationary renewal process $\{N^\circ(t) : t \geq 0\}$ with mean-value function $\mu^\circ(t) \equiv \mathrm{E}[N^\circ(t)] = t$ for $t \geq 0$ so that renewals occur at the constant rate of one new renewal per time unit. Here we are using analogous notation to that used for the designated arrival process $\{N(t), t \geq 0\}$, so that we let X_n° denote the interrenewal time between the $(n-1)$st and nth renewals in the process $\{N^\circ(t) : t \geq 0\}$ for $n = 1, 2, \ldots$. We let $S_0^\circ \equiv 0$; and for $n = 1, 2, \ldots$, and we let $S_n^\circ = \sum_{i=1}^{n} X_i^\circ$ denote the nth renewal epoch so that

$$\begin{aligned} N^\circ(t) &\equiv \max\{n : S_n^\circ \leq t\} \text{ for } t \geq 0 \\ &= \text{number of renewals in } (0, t] \text{ for } t \geq 0; \end{aligned} \tag{1.6}$$

and if $\mathrm{Var}[X_n^\circ] = C$ for $n \geq 2$, then it can be shown that the stationary renewal process $\{N^\circ(t) : t \geq 0\}$ has the required limiting variance-to-mean ratio

$$C \equiv \lim_{t\to\infty} \frac{\mathrm{Var}[N^\circ(t)]}{\mathrm{E}[N^\circ(t)]} \tag{1.7}$$

as detailed in Section 2.2.1 below.

First we construct a step rate function $\widetilde{\lambda}(t)$ that satisfies $\widetilde{\lambda}(t) > 0$ for $t \geq 0$ and $\widetilde{\lambda}(t)$ majorizes and closely approximates the designated rate function $\lambda(t)$, and that consequently has an invertible mean-value function $\widetilde{\mu}(t) = \int_0^t \widetilde{\lambda}(u)du$ for all $t \in [0, S]$; and we use the method of inversion (the inverse-transform method) to generate the associated point process $\{\widetilde{N}(t) : t \geq 0\}$ with asymptotic variance-to-mean ratio C and arrival epochs $\{\widetilde{S}_n : n = 1, 2, \ldots\}$, where $\widetilde{S}_i = \mu^{-1}(S_i^\circ)$, for $i = 1, 2, \ldots$. To complete the combined inversion and thinning procedure, we apply the method of thinning [28] to the arrival epochs $\{\widetilde{S}_n : n = 1, 2, \ldots\}$ to obtain the desired sequence of arrival epochs $\{S_j : j = 1, 2, \ldots\}$ from the point process with the designated rate function $\lambda(t)$ as follows: the epoch $\widetilde{S}_n$ is independently accepted for inclusion in $\{S_j : j = 1, 2, \ldots\}$ with probability $\lambda(\widetilde{S}_n)/\widetilde{\lambda}(\widetilde{S}_n)$. Then the arrival process generated by the combined inversion-and-thinning method with arrival epochs $\{S_j\}$, that is

$$\begin{aligned} N(t) &\equiv \max\{j : S_j \le t\} \text{ for } t \ge 0 \\ &= \text{number of arrivals in } (0, t] \text{ for } t \ge 0, \end{aligned} \tag{1.8}$$

is the designated arrival process with mean value function $\mathrm{E}[N(t)] = \mu(t)$ and asymptotic variance to mean ratio $C \equiv \lim_{t\to\infty} \mathrm{Var}[N(t)]/\mathrm{E}[N(t)]$.

1.3. Organization of the Dissertation

The remainder of the dissertation is organized as follows. Chapter 2 reviews several methods for modeling and simulating nonstationary arrival processes, including nonparametric, parametric, and semiparametric methods for estimating an NHPP from observed arrival streams. Chapter 2 also surveys methods based on inversion and thinning for generating independent realizations of the fitted NHPP. Chapter 3 introduces the theoretical background and techniques used in this research, and explains the combined inversion-and-thinning (CIAT) method for modeling and simulation of nonstationary non-Poisson processes. Chapter 4 summarizes the results of an extensive performance evaluation for this new method. In Chapter 5 we summarize the main contributions and conclusions of this research, and we make recommendations to future work.

Chapter 2

Literature Review

In this chapter we will initially review different methods for modeling and simulating nonhomogeneous point processes.

2.1. Nonhomogeneous Poisson Processes (NHPPs)

A nonhomogeneous Poisson process $\{N(t) : t \geq 0\}$ is nonstationary point (arrival) process that is a generalization of a Poisson process in which the instantaneous arrival rate $\lambda(t)$ at time t is a nonnegative (Lebesgue) integrable function of time. The arrival times are defined by

$$S_n = \begin{cases} 0, & \text{if } n = 0, \\ \displaystyle\sum_{i=1}^{n} X_i, & \text{if } n \geq 1, \end{cases}$$

where X_n is the time between the $(n-1)$st arrival and the nth arrival (X_1 is the time to first arrival). Therefore $N(t) = \max\{n : S_n \leq t\}, t \geq 0$ is the total number of arrivals in $(0, t]$. The mean-value function of the NHPP is defined by

$$\mu(t) \equiv \mathrm{E}[N(t)] = \int_0^t \lambda(z)\,\mathrm{d}z \ \text{ for all } \ t \geq 0,$$

and the variance of $\{N(t) : t \geq 0\}$ is

$$\mathrm{Var}[N(t)] = \mu(t) \ \text{ for all } \ t \geq 0,$$

which implies that the variance-to-mean ratio for an NHPP is

$$\frac{\mathrm{Var}[N(t)]}{\mathrm{E}[N(t)]} = 1 \ \text{ for all } \ t \geq 0.$$

An NHPP has the following properties (Çinlar 1975):
(i) $\{N(t) : t \geq 0\}$ is a counting process;
(ii) $N(0) = 0$;
(iii) $\{N(t+s) - N(t) : s \geq 0\}$ is independent of $\{N(u) : 0 \leq u < t\}$ for all $t \geq 0$;
(iv) $\Pr\{N(t+h) - N(t) = 1\} = \lambda(t)h + o(h)$ for all $t \geq 0$ and $h > 0$; and
(v) $\Pr\{N(t+h) - N(t) \geq 2\} = o(h)$ for all $t \geq 0$ and $h > 0$.
In the above properties, the function $f(\cdot)$ is said to be $o(h)$ if $\lim_{h \to 0} f(h)/h = 0$. From these properties we observe that the rate or mean-value function of the NHPP $\{N(t) : t \geq 0\}$ completely characterizes the probabilistic behavior of the process.

Researchers have developed nonparametric, parametric, and semiparametric methods for estimating an NHPP from observed arrival streams; and for generating independent realizations of the fitted NHPP, methods based on inversion and thinning have been developed.

2.1.1 Generating NHPPs by Inversion

The exact simulation procedures for simulating an NHPP are generally based on the inverse transform method or the method of thinning. For joint application with standard variance reduction techniques, the inverse transform method is preferred because this method facilitates (a) synchronized use of random number inputs across different simulation experiments, and (b) arrangement of a monotonic dependence of the simulation outputs on the random number inputs. However, the inverse transform method is limited to special forms of the rate function for which the mean-value function of the next interevent time can be inverted. For example, the rate functions that have used the inversion method for NHPP generation include functions that are piecewise-linear [16], trigonometric [6], and piecewise-constant [14].

If the random variable X has cumulative distribution function (CDF) $F_X(x) \equiv \Pr\{X \leq x\}$ for all real x, then the inverse CDF of X is defined by $F_X^{-1}(u) \equiv \min\{x : F_X(x) \geq u\}$, $0 \leq u \leq 1$. If U is uniformly distributed on [0,1], then $Y \equiv F_X^{-1}(U)$ has CDF $F_X(x)$, this can be seen from $F_Y(y) \equiv \Pr\{Y \leq y\} = \Pr\{U \leq F_X(y)\} = F_X(y)$ for all real y; and thus the random variable Y has the same distribution as the random variable X. This is the *method of inversion* or the *inverse-transform method* for generating random samples from a given distribution. By analogy with this general inverse transform method, the inversion method for generating NHPPs was introduced by Çinlar [9]. An NHPP $N(t)$ with a continuous mean-value function $\mu(t)$ can be transformed into a homogeneous Poisson process, with arrival rate of 1 arrival per time unit.

THEOREM 1. *If the arrival process with interarrival times $\{N(t) : t \geq 0\}$ is an NHPP with rate function $\lambda(t)$, continuous mean-value function $\mu(t)$ for $t \geq 0$, and arrival times $\{S_n : n = 0, 1, \ldots\}$*

where $S_0 \equiv 0$*, then*

$$S_n^\circ = \mu(S_n) = \int_0^{S_n} \lambda(u)du, \text{ for } n = 0, 1, \ldots$$

define an arrival process

$$N^\circ(w) = \max\{n : S_n^\circ \le w\} \text{ for } w \ge 0$$

that is a homogeneous Poisson process with rate $\lambda^\circ = 1$ *and mean-value function*

$$\mu^\circ(w) = \int_0^{w} 1dz = w, \text{ for all } s \ge 0.$$

Going the other way, Çinlar defines the inverse of a continuous mean-value function $\mu(t)$ for a given NHPP $\{N(t) : t \ge 0\}$ as follows:

$$\mu^{-1}(w) = \inf\{t : \mu(t) \ge w\},\ w \ge 0.$$

The following theorem [9] establishes that such an NHPP can be obtained by transforming a homogeneous Poisson process of rate 1.

THEOREM 2. *If the arrival process* $\{N^\circ(w) : w \ge 0\}$ *with arrival times* $\{S_n^\circ : n = 0, 1, \ldots\}$ *where* $S_0^\circ = 0$*, is a homogeneous Poisson process with rate* $\lambda^\circ = 1$ *and mean value function* $\mu^\circ(w) = w$ *for* $w \ge 0$*, then the transformed arrival times*

$$S_n = \mu^{-1}(S_n^\circ) \quad \text{for} \quad n = 0, 1, \ldots$$

define an arrival process

$$N(t) = \max\{n : S_n \le t\} \quad \text{for} \quad t \ge 0$$

that is an NHPP with mean-value function $E[N(t)] = \mu(t)$*, for* $t \ge 0$*.*

2.1.2 Generating NHPPs by Thinning

The inversion method may not be useful if the rate function is difficult to invert numerically or is analytically intractable. For an arbitrary rate function with a an easily identified upper bound, the thinning method is simple to apply and can be relatively efficient. The thinning method was introduced by Lewis and Shedler [28] based on the following theorem.

THEOREM 3. *Consider an NHPP* $\{\widetilde{N}(t) : t \ge 0\}$ *with rate function* $\widetilde{\lambda}(t)$ *for* $t \ge 0$*. Suppose that* $\widetilde{S}_1, \widetilde{S}_2, \ldots, \widetilde{S}_{\widetilde{n}}$ *are the event epochs of this process in the interval* $(0, t_0]$ *and that* $0 \le \lambda(t) \le \widetilde{\lambda}(t)$ *and* $\widetilde{\lambda}(t) > 0$ *for all* $t \in (0, t_0]$*. If for* $i = 1, 2, \ldots, \widetilde{n}$*, we delete the event epoch* $\widetilde{S}_i$ *with probability* $1 - \lambda(\widetilde{S}_i)/\widetilde{\lambda}(\widetilde{S}_i)$*, then the remaining event epochs form an NHPP with rate function* $\lambda(t)$ *in the interval* $(0, t_0]$*.*

At the ith event epoch $\widetilde{S}_i$, thinning can be performed by sampling a random number U_i and rejecting $\widetilde{S}_i$ if $U_i > \lambda(\widetilde{S}_i)/\widetilde{\lambda}(\widetilde{S}_i)$. The following is the algorithmic statement of the thinning method in [28].

[1] Generate points of the NHPP $\{\widetilde{N}(t) : t \geq 0\}$ with rate function $\widetilde{\lambda}(t)$ in the fixed interval $[0, t_0]$. If the number of points generated, $\widetilde{n}$, is such that $\widetilde{n} = 0$, then exit because there are no points in the current realization of process$\{N(t) : 0 \leq t \leq t_0\}$; otherwise, **goto [2]**.

[2] Let $\widetilde{S}_1, \widetilde{S}_2, \ldots, \widetilde{S}_{\widetilde{n}}$ denote the observed arrival epochs in the process $\{\widetilde{N}(t) : 0 \leq t \leq t_0\}$. Set $i = 1$ and $k = 0$.

[3] Generate $U_i \sim$ Uniform(0, 1) independently of all other random variables. If $U_i \leq \lambda(\widetilde{S}_i)/\widetilde{\lambda}(\widetilde{S}_i)$, then take $k \leftarrow k + 1$ and $S_k \leftarrow \widetilde{S}_i$.

[4] Set $i \leftarrow i + 1$. If $i \leq \widetilde{n}$, then **goto [3]**; otherwise **goto [5]**.

[5] Return $S_1, S_2, \ldots, S_k$, where $N(t) \leftarrow k$.

Figure 2.1: Algorithmic statement of the NHPP thinning simulation procedure of [28].

2.1.3 Nonparametric NHPP Methods

In this section we review the nonparametric methods proposed by Leemis [3, 24, 25] for estimating and simulating an NHPP over a given time interval $[0, S]$. Suppose that k independent realizations of the arrival process $\{N(t) : t \geq 0\}$ over the interval $[0, S]$ have been observed so that we have n_i arrivals on the ith realization for $i = 1, 2, \ldots, k$; and thus we have a total of $n = \sum_{i=1}^{k} n_i$ arrivals accumulated over all realizations of the arrival process. Let $\{t_{(i)} : i = 1, \ldots, n\}$ denote the sequence of all arrival times taken over all k realizations of the arrival process and sorted in increasing order.

We take $t_{(0)} \equiv 0$ and $t_{(n+1)} \equiv S$ so that for $t_{(i)} < t \leq t_{(i+1)}$ and $i = 1, 2, \ldots, n$, a piecewise linear nonparametric estimator of $\mu(t)$ is

$$\widehat{\mu}(t) = \frac{in}{(n+1)k} + \left\{ \frac{n[t - t_{(i)}]}{(n+1)k[t_{(i+1)} - t_{(i)}]} \right\}; \tag{2.1}$$

see [24]. Figure 2.3 shows the layout of $\widehat{\mu}(t)$. Equation (2.1) and Figure 2.3 provide a basis for modeling

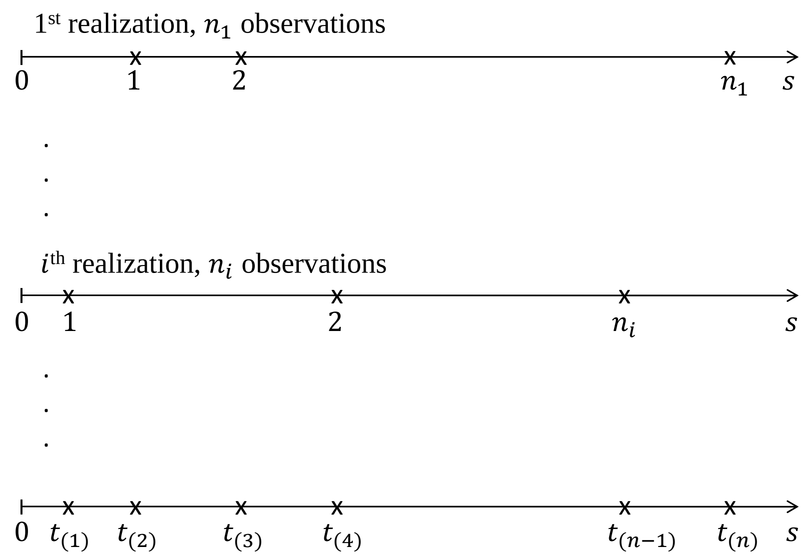

Total over k realizations, $\sum_{i=1}^{k} n_i = n$ observations

Figure 2.2: The partition of interval $(0, S]$

and simulating the given arrival process when the arrival rate exhibits a strong dependence, for example, on the time of day, or the day of the week.

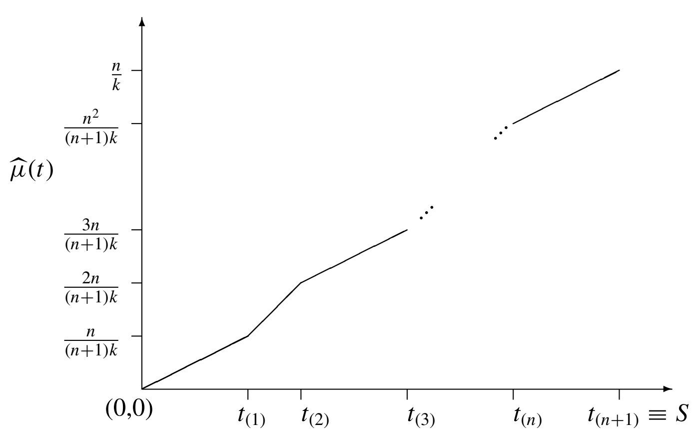

Figure 2.3: Nonparametric estimator of mean-value function.

Given the estimated mean-value function $\widehat{\mu}(t)$ of the form (2.1), we can use the inversion procedure of [24] to generate a new stream of arrival times $\{S_i : i = 1, 2, ...\}$ over the time interval $(0, S]$ with approximately the same general pattern of dependence on time as in (2.1). Figure (2.4) provides an algorithm statement of this inversion procedure.

[1] Set $i \leftarrow 1$ and $N \leftarrow 0$.

[2] Generate $U_i \sim$ Uniform(0, 1).

[3] Set $B_i \leftarrow -\ln(1 - U_i)$.

[4] **while** $B_i < n/k$ **do**

Begin

Set $m \leftarrow \left\lfloor \frac{(n+1)kB_i}{n} \right\rfloor$;

Set $S_i = \leftarrow t_{(m)} + \{t_{(m+1)} - t_{(m)}\}\left\{\frac{(n+1)kB_i}{n} - m\right\}$;

Set $N \leftarrow N + 1$; set $i \leftarrow i + 1$;

Generate $U_i \sim$ Uniform(0, 1);

Set $B_i = B_{i-1} - \ln(1 - U_i)$.

End

Figure 2.4: Algorithmic statement of the NHPP simulation procedure of [24].

The advantage of this nonparametric method for modeling and simulating NHPPs is that it does not require the assumption of any arbitrary parameters of the arrival rate function $\lambda(t)$. And the author proves that when $k \to \infty$ so that the number of realizations of the designated arrival process becomes large, the estimated mean-value function $\widehat{\mu}(t)$ of Equation (2.1) converges to the true mean-value function $\mu(t)$ for all $t \in (0, S]$ with probability 1.

Arkin and Leemis [3] propose an extension of the nonparametric estimator (2.1) to handle overlapping realizations. The time interval $(0, S]$ is partitioned into the smallest possible number of subintervals r such that in each subinterval $(s_j, s_{j+1}]$ there is a compete set of k_{j+1} realizations (in other words, each of k_{j+1} observed realizations of the NHPP *completely covers* the subinterval $(s_j, s_{j+1}]$ for $j = 0, 1, \ldots, r-1$). In this partition, the end points are $s_0 = 0$ and $s_r = S$. Let n_{j+1} denote the total number of observed events over all realizations during the time interval $(s_j, s_{j+1}]$ for $j = 0, 1, \ldots, r-1$ as depicted in Figure 2.5. Define $n = \sum_{q=1}^{r} n_q$ to be the total number of events observed on the interval $(0, S]$. Let $t_{(0)}, t_{(1)}, \ldots, t_{(n+r)}$ denote the nondecreasing sequence time points in $[0, S]$ that consists of the following: (a) all arrival times taken over all realizations of the designated arrival process; and (b) the subinterval boundaries $s_0, s_1, \ldots s_r$. It follows that $t_{(0)} = s_0 = 0, t_{(n+r)} = s_r = S$. The subinterval boundaries $s_0, s_1, \ldots, s_r$ will not be counted as events when constructing $\widehat{\mu}(t)$, though they are included in the sequence $\{t_{(i)} : i = 0, 1, \ldots, n + r\}$ that has been sorted in increasing order. If $t \in (t_{(i)}, t_{(i+1)}]$ and $t \in (s_j, s_{j+1}]$, then the piecewise-linear estimator of the mean-value function has the form:

$$\widehat{\mu}(t) = \sum_{q=1}^{j} \left\{ \frac{n_q}{k_q} + \frac{\left[i - \sum_{q=1}^{j}(n_q + 1)\right] n_{j+1}}{(n_{j+1} + 1) k_{j+1}} \right\} + \left[\frac{n_{j+1}[t - t_{(i)}]}{(n_{j+1} + 1) k_{j+1} [t_{(i+1)} - t_{(i)}]} \right],$$

where $0 \le i \le n + r - 1$ and $0 \le j \le r - 1$.

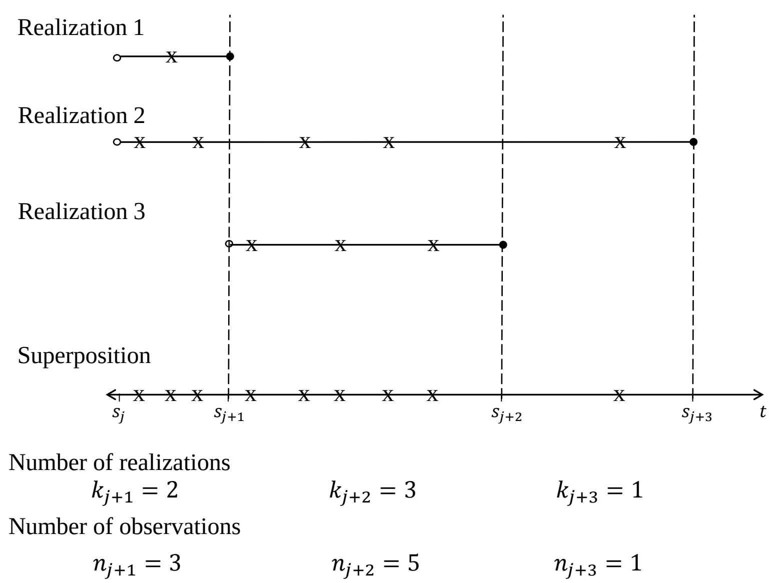

Figure 2.5: Nonparametric estimator of mean-value function.

In [25], Leemis consider k independent, *completely overlapping* realizations of an NHPP over the time horizon $(0, S)$, which is arbitrarily partitioned into subintervals $\{(a_{i-1}, a_i] : i = 1, \ldots, m\}$, where $a_0 = 0$ and $a_m = S$. The subintervals do not necessarily have equal widths. For $i = 1, \ldots, m$, let n_i

denote the total number of observed events in the subinterval $(a_{i-1}, a_i]$ taken over all k realizations of the arrival process.

If the rate function $\lambda(t)$ of the designated NHPP is piecewise constant on each subinterval of the partition $(a_0, a_1], (a_1, a_2], \ldots, (a_{m-1}, a_m]$, then the maximum likelihood estimator of the average intensity function on the interval $(a_{i-1}, a_i]$ is

$$\hat{\lambda}(t) = \frac{n_i}{k(a_i - a_{i-1})}, \quad \text{for } a_{i-1} < t \leq a_i, \text{ and } i = 1, \ldots, m,$$

for $i = 1, 2, \ldots, m$, because on each realization of the NHPP, the expected number of arrivals in the ith subinterval $(a_{i-1}, a_i]$ is

$$\mu(a_i) - \mu(a_{i-1}) = \lambda_i(a_i - a_{i-1}), \tag{2.2}$$

where λ_i is the constant arrival rate on that subinterval; and clearly n_i/k is the maximum likelihood estimator of this expected value. It follows that the associated estimator of the mean-value function $\mu(t)$ is a continuous, piecewise-linear function on $(0, S]$ having the form

$$\widehat{\mu}(t) = \left(\sum_{j=1}^{i-1} \frac{n_j}{k}\right) + \left[\frac{n_i(t - a_{i-1})}{k(a_i - a_{i-1})}\right], \quad \text{for } a_{i-1} < t \leq a_i, \text{ and } i = 1, \ldots, m.$$

2.1.4 Parametric NHPP methods

Parametric models for the rate function of an NHPP have been developed to represent arrival processes that exhibit systematic changes in the arrival rate over time, such as long term trends or periodicities. Cox and Lewis [10] present an exponential-polynomial function (EPF) of the form $\lambda(t) = \exp\{\alpha_0 + \alpha_1 t\}$ to approximate the rate function of an NHPP. This rate function has an exponential form to ensure the arrival rate always remains positive. To model the arrival of patients at an intensive-care unit, Lewis [26] introduced a exponential-polynomial-trigonometric function (EPTF) rate function of the form $\lambda(t) = \exp\left\{\sum_{i=0}^{2} \alpha_i t^i + \gamma \sin(\omega t + \phi)\right\}$, a quadratic trend is also included in this rate function. MacLean [29] proposes using an exponential polynomial rate function of degree m,

$$\lambda(t) = \exp\left\{\sum_{i=0}^{m} \alpha_i t^i\right\}, \tag{2.3}$$

since the rate function (2.3) can approximate any continuous rate function arbitrarily closely .

To simulate and model the occurrence of storms in the Arctic Sea, Lee, Wilson, and Crawford [23] use an NHPP displaying cyclic behavior with rate function of the form

$$\lambda(t) = \exp\{h(t; m, \boldsymbol{\Theta})\}, \tag{2.4}$$

where $h(t; m, \mathbf{\Theta}) = \sum_{i=0}^{m} \alpha_i t^i + \gamma \sin(\omega t + \phi)$, and $\mathbf{\Theta} = [\alpha_0, \alpha_1, \ldots, \alpha_m, \gamma, \phi, \omega]$ is the vector of continuous parameters. To reduce the computation time in simulating of an NHPP with the rate function (2.4), the authors formulate `maxline`, an algorithm to construct a positive piecewise linear rate function $\widetilde{\lambda}(t)$ that closely approximates $\lambda(t)$ while majorizing $\lambda(t)$ on $[0, S]$; that is, $\widetilde{\lambda}(t) \geq \lambda(t)$ and $\widetilde{\lambda}(t) > 0$ for all $t \in [0, S]$. The advantage of this approach is that the corresponding mean-value function $\tilde{\mu}(t) = \int_0^t \widetilde{\lambda}(u)\,\mathrm{d}u$ is piecewise quadratic and thus is easily inverted so that a sequence of arrival epochs $\{\widetilde{S}_n\}$ for this process is easily generated by the method of inversion. Then the authors simulate the fitted NHPP by thinning a realization of the majorizing process. The authors apply the thinning scheme of [28] to generate arrival epochs $\{S_j\}$ from an NHPP with rate function $\lambda(t)$ as follows: the epoch $\widetilde{S}_n$ is independently accepted for inclusion in $\{S_j\}$ with probability $\lambda(\widetilde{S}_n) / \widetilde{\lambda}(\widetilde{S}_n)$ for $n = 1, 2, \ldots$.

Kuhl, Wilson, and Johnson [21] and Kuhl and Wilson [20] extended the work of [23] to handle arrival processes with a general trend or multiple periodicities. The model for the arrival process is an NHPP with rate function of the form

$$\lambda(t) = \exp\{h(t; m, p, \mathbf{\Theta})\}, \quad \text{for } t \in (0, S], \tag{2.5}$$

where $h(t; m, p, \mathbf{\Theta}) = \sum_{i=0}^{m} \alpha_i t^i + \sum_{k=1}^{p} \gamma_k \sin(\omega_k t + \phi_k)$, and $\mathbf{\Theta} = [\alpha_0, \alpha_1, \ldots, \alpha_m, \gamma_1, \ldots, \gamma_p, \phi_1, \ldots, \phi_p, \omega_1, \ldots, \omega_p]$ is the vector of continuous parameters. Kuhl, Wilson, and Johnson use inversion for simulating NHPPs with a rate function of the form (2.5). Rate functions of this type were originally used in the UNOS Liver Allocation Model [31]; and although the resulting fits were remarkably accurate, the times to generate realizations of the fitted NHPPs by inversion were too large in practice.

In this research, we propose an algorithm in Section 3.1 to construct a piecewise constant rate function $\widetilde{\lambda}(t)$ that closely approximates $\lambda(t)$ while majorizing it; thus the corresponding mean-value function $\tilde{\mu}(t) = \int_0^t \widetilde{\lambda}(u)\,\mathrm{d}u$ is piecewise linear and easily inverted. This algorithm could facilitate a rapid simulation of NHPPs using the rate function (2.5) by reducing the times to generate realizations of the fitted NHPPs.

2.1.5 Semiparametric NHPP methods

To model and simulate NHPPs having a long-term trend or nontrigonometric cyclic effects, Kuhl and Wilson [22] formulate a semiparametric method which combines the flexibility of nonparametric methods with the smooth, continuous representations of parametric models. Called a “multiresolution” procedure because of its ability to handle nested cyclic effects, this procedure has been implemented by Kuhl, Sumant, and Wilson [19] in Web-based software.

The procedure of [19] involves the following steps at each resolution level corresponding to a basic cycle: (a) transforming the cumulative relative frequency of arrivals within the cycle to obtain a statistical model with approximately normal, constant-variance responses; (b) fitting a specially formulated polynomial to the transformed responses; (c) performing a likelihood ratio test to determine the degree of the fitted polynomial; and (d) fitting to the original (untransformed) responses a polynomial of the same form as in (b) with the degree determined in (c).

Extending the semiparametric method of [19] to model more general nonstationary behavior, Kuhl, Deo, and Wilson [18] introduce an alternative method to model the mean-value function of the NHPP. The final estimate is obtained for the mean-value function of the following form: $\mu(t) = \mu(S)R(t)$ for $t \in [0, S]$, where $R(t)$ is a monotone increasing degree-r polynomial of the form

$$R(t) = \begin{cases} t/S, & \text{if } r = 1, \\ \displaystyle\sum_{k=1}^{r-1} \beta_k (t/S)^k + \left(1 - \sum_{k=1}^{r-1} \beta_k\right)(t/S)^r, & \text{if } r > 1. \end{cases}$$

This methodology can be used to fit an NHPP to one or more realizations of data from the process under study. The primary advantage of this method is that it fits a smooth (differentiable) mean-value function over the interval $[0, S]$.

2.1.6 Smoothing the Rate Function of an NHPP

Continuous nonnegative rate functions of NHPPs are sometimes approximated as piecewise constant functions. Chen and Schmeiser [7] present the I-SMOOTH (Iterated Smoothing via Mean-constrained Optimized-Objective Time Halving) algorithm to calculate progressively refined nonnegative approximations to the original rate function such that over each subinterval, the integral of the latest approximation matches the integral of the original function; and the limiting approximation is a nonparametric continuous function. I-SMOOTH applies to finite-horizon functions as well as periodic functions.

Suppose we are given an NHPP with piecewise constant rate function $\lambda(t)$ so that $\lambda(t) = \lambda_i$ for $t_{i-1} < t \le t_i$, where $t_i = i$ for $i = 1, 2, \ldots, k$ and $\lambda(t_0) = \lambda_1$. The authors aim to get a smoother nonnegative rate function $\tau(t)$ over the time horizon $[0, S]$ (or over the integral multiples of this time horizon), where $S = k$, and maintain the mean-value function over each subinterval $(t_{i-1}, t_i]$ so that we have

$$\int_{t_{i-1}}^{t_i} \tau(t)dt = \int_{t_{i-1}}^{t_i} \lambda(t)dt \quad \text{for } i = 1, \ldots, k,$$

where $\lambda(t) = \lambda_{i(t)}$ with $i(t) = \min\{1 \le i \le k : (t - \lfloor t/t_k \rfloor t_k)\} < t_i\}$.

The authors use a definition of "smoothness" (for which they do not give a reference), that is actually a measure of the curvature of a twice continuously differentiable function $f(t)$ on an interval $[a, b]$,

$$z = \int_a^b \left[\frac{d^2 f(u)}{du^2}\right]^2 du;$$

see, for example, Section 6.24 of [1].

Followed their definition of the "smoothness" of a continuous function, the authors define the "smoothness" for a piecewise-constant function by

$$z_F = \sum_{i=1}^{k-2} [\lambda_{i+2} - 2\lambda_{i+1} + \lambda_i]^2 \tag{2.6}$$

when the problem horizon is finite. At each iteration, the new rate function is:

$$\tau(t) = \begin{cases} \lambda_i - \gamma_i, & \text{for } t_{i-1} < t \leq (t_{i-1} + t_i)/2, \\ \\ \lambda_i + \gamma_i, & \text{for } (t_{i-1} + t_i)/2 < t \leq t_i. \end{cases}$$

To obtain nonnegative rates, the constraints

$$|\gamma_i| \leq \lambda_i \quad \text{for} \quad i = 1, 2, \ldots, k \tag{2.7}$$

must be satisfied. The authors then minimize the smoothness function (2.6), subject to the nonnegativity constraints in Equation (2.7) to obtain the optimal values of $\gamma_1, \ \ldots, \ \gamma_k$.

Figure 2.6 illustrates successive iterations in the operation of I-SMOOTH. The original piecewise-constant rates, shown in the first subplot of Figure 2.6, are the yearly live-donor kidney-donation numbers of the period 1988–2010 that were obtained from the web site for the Organ Procurement and Transplantation Network of the United States (OPTN 2011). The authors apply I-SMOOTH to the original rate function because the actual donation-rate function is not piecewise constant, but rather continuous. The second through fourth subplots show the progress of I-SMOOTH iterations 1, 2, and 3, which have 46, 92, and 184 intervals respectively.

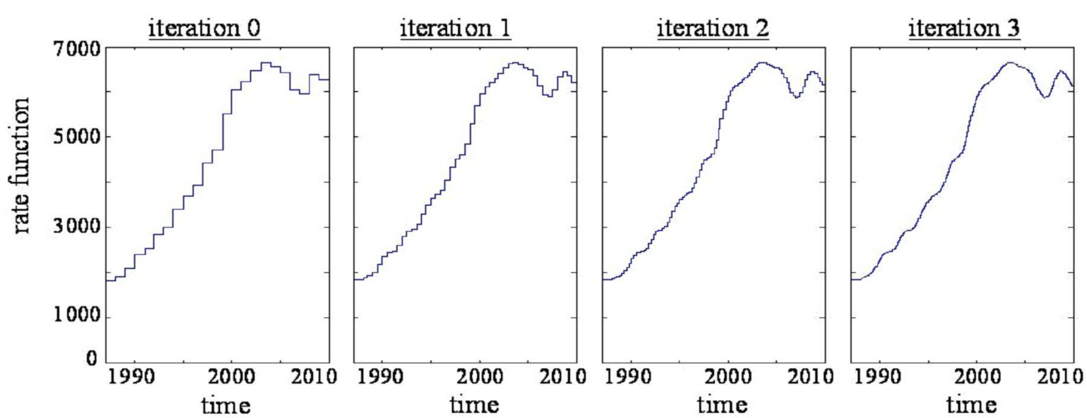

Figure 2.6: I-SMOOTH procedure applied to the rate function of liver-donor kidney-donation data from 1988 through 2010.

2.2. Nonstationary Non-Poisson Processes (NNPPs)

2.2.1 Preliminaries on Equilibrium Renewal Processes

Normally, when nonstationary arrival processes are required, it is natural to assume Poisson arrivals with a time-varying arrival rate. However, real-life studies of many systems, including telecommunication networks, manufacturing systems, and consumer behavior have revealed that arrival processes may be either more or less variable than Poisson processes.

To model such processes, first we consider a set of nonnegative interarrival times $\{X_n^\circ : n = 1, 2, \ldots\}$, where the subset $\{X_n^\circ : n = 2, 3, \ldots\}$ are independent and identically distributed with cumulative distribution function G, while X_1°, the time until the first event, may have a different distribution. As usual, we let S_n° denote the time of the nth event, and we let $N^\circ(t)$ denote the number of events observed on or before time t. Such a renewal process $N^\circ(t)$ is called a delayed renewal process or general renewal process; and it is generated by taking $\{X_n^\circ : n = 2, 3, \ldots\} \overset{\text{iid}}{\sim} G$, where $\tau = \mathrm{E}[X_j^\circ], \sigma^2 = \mathrm{Var}[X_j^\circ]$, and $\mathrm{CV}[X_j^\circ] = \sigma/\tau$, for $j \geq 2$.

If X_1° has the equilibrium distribution associated with G, specifically,

$$G_e(t) \equiv \Pr\{X_1^\circ \leq t\} = \frac{1}{\tau}\int_0^t [1 - G(u)]du \quad \text{for } t \geq 0,$$

then $N^\circ(t)$ is a stationary renewal process, so by Equations (16) and (17) of [11], we have

$$\mathrm{E}[N^\circ(t)] = \frac{t}{\tau} \quad \text{for } t \geq 0,$$

and

$$\mathrm{Var}[N^\circ(t)] = \frac{t}{\tau} - \left(\frac{t}{\tau}\right)^2 + \frac{2}{\tau}\int_0^t E[N^\#(u)]du \quad \text{for } t \geq 0, \tag{2.8}$$

where $N^\#(t)$ is the ordinary renewal process with i.i.d interarrival times $\{X_n^\#, n = 1, 2, \ldots\}$ all having the common distribution G. According to [32],

$$\begin{aligned}
\mathrm{E}\{N^\#(t)\} &= \frac{t}{\mathrm{E}[X_n^\#]} + \left\{\frac{\mathrm{E}[(X_n^\#)^2]}{2\mathrm{E}^2[X_n^\#]} - 1\right\} + o(1) \quad \text{as } t \to \infty \\
&= \frac{t}{\tau^2} + \frac{\sigma^2 - \tau^2}{2\tau^2} + o(1) \quad \text{as } t \to \infty,
\end{aligned} \tag{2.9}$$

where $\mathrm{E}[X_n^\#] = \tau, \mathrm{E}[(X_n^\#)^2] = \mathrm{Var}[X_n^\#] + \mathrm{E}^2[X_n^\#] = \sigma^2 + \tau^2$. Combining Equations (2.8) and (2.9), we have

$$\begin{aligned}
\mathrm{Var}\{N^\circ(t)\} &= \frac{t}{\tau} - \left(\frac{t}{\tau}\right)^2 + \frac{2}{\tau}\int_0^t \mathrm{E}[N^\#(u)]du \\
&= \frac{t}{\tau} - \left(\frac{t}{\tau}\right)^2 + \frac{2}{\tau}\Big[\frac{t^2}{2\tau} + \left(\frac{\sigma^2-\tau^2}{2\tau^2}\right)t + o(t)\Big] \\
&= \left(\frac{\sigma^2}{\tau^3}\right)t + o(t) \quad \text{as } t \to \infty. \qquad (2.10)
\end{aligned}$$

Thus, for the stationary renewal process $\{N^\circ(t);\ t \geq 0\}$ with $X_1^\circ \sim G_e$ and $X_n^\circ \sim G$ for $n = 2, 3, \ldots,$ we have the dispersion ratio

$$\mathrm{Var}\{N^\circ(t)\}/\mathrm{E}\{N^\circ(t)\} \sim \mathrm{CV}^2 = \sigma^2/\tau^2 \quad \text{as } t \to \infty.$$

2.2.2 Inversion Method for NNPPs

Building on the basic properties of equilibrium renewal processes outlined in Section 2.2.1, Gerhardt and Nelson [12] propose methods for modeling and simulating a point process that allow the user to achieve desired values of both the mean-value function $\mu(t)$ and the ratio $\mathrm{Var}[N(t)]/\mathrm{E}[N(t)]$ of the process. Starting from a stationary renewal process $\{N^\circ(t)\}$ with $\tau = 1$ and the desired asymptotic dispersion ratio $\lim_{t\to\infty} \mathrm{Var}[N^\circ(t)]/\mathrm{E}[N^\circ(t)] = C$, the authors first generate a corresponding sequence of renewal epochs $\{S_n^\circ : n = 1, 2, \ldots\}$ for the process $\{N^\circ(t)\}$. Finally the authors obtain a point process $\{N(t)\}$ with the desired mean-value function $\mu(t)$ and the corresponding arrival epochs $\{S_n : n = 1, 2, \ldots\}$ by inversion: $S_n = \mu^{-1}(S_n^\circ)$ for $n = 1, 2, \ldots$ as detailed in Figure 2.7.

[1] Set $n \leftarrow 1$, and $S_0 \leftarrow 0$. Generate $S_1^\circ \sim G_e$. Set $S_1 \leftarrow \mu^{-1}(S_1^\circ)$.

[2] Return the interarrival time $X_n \leftarrow S_n - S_{n-1}$;

[3] Set $n \leftarrow n + 1$. Generate $X_n^\circ \sim G$. Set $S_n^\circ \leftarrow S_{n-1}^\circ + X_n^\circ$ and $S_n = \mu^{-1}(S_n^\circ)$.

[4] **Goto** step **2**.

Figure 2.7: Algorithmic statement of the inversion method of [12].

The authors show that their inversion procedure yields $\mathrm{E}[N(t)] = \mu(t)$ for all $t \geq 0$ and $\lim_{t\to\infty} \mathrm{Var}[N(t)]/\mathrm{E}[N(t)] = C$. The inversion method is useful when $\mu(t)$ is easily invertible. Functional forms for the rate function $\mu(t)$ that use the inversion method for NHPP generation include piecewise-linear, trigonometric, and piecewise-constant functions. The disadvantage of this method is that in many applications $\mu(t)$ (or an estimate of this function) is not easily invertible.

2.2.3 Thinning Method for NNPPs

Gerhardt and Nelson [12] also propose a method for achieving an arrival process $\{N(t)\}$ with the desired mean-value function $\mu(t)$ based on thinning. If the corresponding rate function $\lambda(t) = \frac{\mathrm{d}}{\mathrm{d}t}\mu(t)$ has finite upper bound $\widetilde{\lambda}$, then the authors start from a stationary renewal process $\{\widetilde{N}(t)\}$ with rate $\widetilde{\lambda}$, arrival epochs $\{\widetilde{S}_n : n = 1, 2, \ldots\}$, and the desired variance-to-mean ratio C; and the corresponding sequence of arrival epochs $\{S_j : j = 1, 2, \ldots\}$ from a point process with the desired mean-value function $\mu(t)$ is obtained as follows: each arrival epoch $\widetilde{S}_n$ is independently accepted for inclusion in $\{S_\ell\}$ with probability $\lambda(\widetilde{S}_n)/\widetilde{\lambda}$ for $n = 1, 2, \ldots$. The algorithmic statement of this procedure is given in Figure 2.8. The authors show that the resulting thinned point process $\{N(t) : t \geq 0\}$ has mean-value function $\mathrm{E}[N(t)] = \mu(t)$ for all $t \geq 0$; the authors also show that in the case $\lambda(t) = \overline{\lambda}$ for all $t \geq 0$ so that the rate function is constant, the asymptotic variance-to-mean ratio $\lim_{t\to\infty} \mathrm{Var}[N(t)]/\mathrm{E}[N(t)] = \left[1-\overline{\lambda}/\widetilde{\lambda}\right] + \left(\overline{\lambda}/\widetilde{\lambda}\right) C$. Unfortunately, it is not in general true that $\lim_{t\to\infty} \mathrm{Var}[N(t)]/\mathrm{E}[N(t)] = C$. The other disadvantage of this method is that it may be computationally inefficient if $\lambda(t) \ll \widetilde{\lambda}$ for a substantial range of values of t.

[1] Set $n \leftarrow 1$, $j \leftarrow 1$ and $\widetilde{S}_0 \leftarrow 0$ and $S_0 \leftarrow 0$. Generate $\widetilde{S}_1 \sim G_e$

[2] Generate $U_1 \sim$ Uniform$(0, 1)$. If $U_1 \le \lambda(\widetilde{S}_1)/\widetilde{\lambda}$ then

- **[2a]** Set $S_1 \leftarrow \widetilde{S}_1$;
- **[2b]** Return interarrival time $X_1 \leftarrow S - S_0$;
- **[2c]** Set $j \leftarrow j + 1$.

[3] Set $n \leftarrow n + 1$. Generate $\widetilde{X}_n \sim G$. Set $\widetilde{S}_n \leftarrow \widetilde{S}_{n-1} + \widetilde{X}_n$.

[4] Generate $U_n \sim$ Uniform$[0, 1]$. If $U_n \le \lambda(\widetilde{S}_n)/\widetilde{\lambda}$, then

- **[4a]** Set $S_j \leftarrow \widetilde{S}_n$;
- **[4b]** Return interarrival time $X_j \leftarrow S_j - S_{j-1}$;
- **[4c]** Set $j \leftarrow j + 1$.

[5] **Goto** step **3**.

Figure 2.8: Algorithmic statement of the thinning method of [12].

Chapter 3

CIAT: A Combined Inversion-and-Thinning Procedure for Nonstationary Non-Poisson Processes

In this chapter, we propose a combined inversion-and-thinning (CIAT) method that is constructed to overcome the disadvantages of the inversion and thinning methods of [12] while retaining the attractive features of each method. First we seek a strictly positive step function $\widetilde{\lambda}_Q(t)$ that majorizes and closely approximates the designated rate function $\lambda(t)$ and that also has an easily invertible mean-value function $\widetilde{\mu}_Q(t) = \int_0^t \widetilde{\lambda}_Q(u)du$ for all $t \in (0, S]$; and we use inversion to generate the associated point process $\{\widetilde{N}_Q(t) : t \geq 0\}$ with asymptotic variance-to-mean ratio C and arrival epochs $\{\widetilde{S}_n : n = 1, 2, \ldots\}$. To complete the combined inversion-and-thinning procedure, we apply the thinning method to the arrival epochs $\{\widetilde{S}_n : n = 1, 2, \ldots\}$ to obtain the desired sequence of arrival epochs $\{S_j^\circ : j = 1, 2, \ldots\}$ from the point process with the designated rate function $\lambda(t)$ as follows: the epoch $\widetilde{S}_n$ is independently accepted for inclusion in $\{S_j^\circ : j = 1, 2, \ldots\}$ with probability $\lambda(\widetilde{S}_n)/\widetilde{\lambda}_Q(\widetilde{S}_n)$. We then introduce the CIAT procedure with a lognormal distribution for interarrival times, called CIATL, and we highlight the key differences between the original CIAT and CIATL.

3.1. Initial Step: Seeking a Positive Step Function That Majorizes $\lambda(t)$

Throughout the rest of this dissertation, we assume that the designated rate function $\lambda(t)$ satisfies the following property on $(0, S]$:

Property FD: $\lambda(t)$ has at most a finite number of discontinuities in $(0, S]$; and at each of these discontinuities, $\lambda(t)$ is either right-continuous with a left-hand limit, or left-continuous with a right-hand limit.

Property FD ensures that the designated mean-value function $\mu(t)$ is continuous at every $t \in [0, S]$; and except at the discontinuities of $\lambda(t)$, we have $\frac{d}{dt}\mu(t) = \lambda(t)$. In most practical applications, either $\lambda(t)$ or $\mu(t)$ must be estimated by an appropriate statistical method; and in such applications Property FD is usually satisfied.

In mathematics, two quantities are in the golden ratio if the ratio of the sum of the quantities to the larger quantity is equal to the ratio of the larger quantity to the smaller one. The golden ratio is the irrational mathematical constant $\varphi = (1 + \sqrt{5})/2 \approx 1.61803$. The golden section search is a technique for finding the extremum (minimum or maximum) of a unimodal function on a finite interval $[a, b]$ by successively narrowing the range of values inside which the extremum is known to exist. The technique derives its name from the fact that the algorithm maintains the function values for triples of points whose distances form a golden ratio. Throughout the following discussion of the golden section search, we assume that the method is used to find the maximum of a continuous unimodal function $f(x)$ on the finite interval $[a, b]$.

We make the assignments $x_1 \leftarrow a + (2 - \varphi)(b - a)$, and $x_2 \leftarrow a + (\varphi - 1)(b - a)$ so that we have $a < x_1 < x_2 < b$. If $f(x_1) < f(x_2)$, then the desired maximum is inside $[x_1, b]$, and we make the assignments $a \leftarrow x_1, x_1 \leftarrow x_2, x_2 \leftarrow a + (\varphi - 1)(b - a)$. Otherwise if $f(x_1) \geq f(x_2)$ then the desired maximum value is inside $[a, x_2]$, and we make the assignments $b \leftarrow x_2, x_2 \leftarrow x_1, x_1 \leftarrow a + (2 - \varphi)(b - a)$. After the interval of uncertainty $[a, b]$ has been updated, we check for the termination condition $(b - a) < \delta$, where $\delta > 0$ is the user-specified maximum length of the final interval of uncertainty. If $f(x)$ is not unimodal, then the golden section search method may only give one of the local extremum values.

To achieve the strictly positive step function that majorizes $\lambda(t)$, the time interval $(0, S]$ needs to be partitioned in a proper way so that in each subinterval $(z_i, z_{i+1}]$, the golden search method will give the unique maximum value of $\lambda(t)$ in that subinterval. If we have the information that $\lambda(t)$ reaches its local extreme values at $\{t_i, i = 1, 2, \ldots, L\}$, then we can partition the interval $(0, S]$ into Q equal length subintervals $(z_0, z_1], (z_1, z_2], \ldots, (z_{Q-1}, z_Q]$, where $z_0 = 0, z_Q = S$, and the length of each subinterval is $S/Q \leq \min\{t_{i+1} - t_i : i = 1, \ldots, L - 1\}$, so that $\lambda(t)$ is unimodal in each subinterval. For a general function without such information, we may take at least 200 subintervals and visually examine the accuracy of the majorizing procedure. Finally, the majorizing function is given by

$$\tilde{\lambda}(t) = \tilde{\lambda}_Q(t) = \left\{ \sum_{i=1}^{Q} \lambda_{\max,i} \mathbb{I}_{(z_{i-1}, z_i]}(t) \right\} \quad \text{for } 0 \leq t \leq S,$$

where

$$\mathbb{I}_{(z_{i-1}, z_i]}(t) = \begin{cases} 1, & \text{if } z_{i-1} < t \leq z_i, \\ 0, & \text{otherwise ;} \end{cases}$$

and in terms of an arbitrarily small positive constant ε (say, $\varepsilon = 10^{-20}$) together with the quantities

$$\lambda_i^* \equiv \max\{\lambda(t) : t \in [z_{i-1}, z_i]\} \text{ for } i = 1, \ldots, Q, \tag{3.1}$$

as completed by golden section search in $[z_{i-1}, z_i]$, we take

$$\lambda_{\max,i} \equiv \left\{ \begin{array}{ll} \lambda_i^*, & \text{if } \lambda_i^* > 0, \\ \varepsilon, & \text{if } \lambda_i^* = 0; \end{array} \right\} \text{ for } i = 1, \ldots, Q.$$

This step ensures that $\widetilde{\lambda}(t)$ is strictly positive for all $t \in [0, S]$. The algorithmic statement of this procedure is given in Figure 3.1.

[1] Given the interval $[0, S]$, divide it into Q subintervals $\{[z_{i-1}, z_i] : i = 1, \ldots, Q\}$. Set $z_0 \leftarrow 0$, $z_Q \leftarrow S$, $z_i \leftarrow iS/Q$, $\delta = 10^{-4}$, and $\varepsilon = 10^{-20}$.

[2] For $i \leftarrow 1$ **to** Q **do begin**

[2a] Set $a \leftarrow z_{i-1}, b \leftarrow z_i,\ x_1 \leftarrow a + (2-\varphi)(b-a)$,
$x_2 \leftarrow a + (\varphi - 1)(b-a)$.

[2b] While $(b-a) \geq \delta$ **do begin**

[2b.i] If $\lambda(x_1) < \lambda(x_2)$, **then** set $a \leftarrow x_1, x_1 \leftarrow x_2$,
$$x_2 \leftarrow a + (\varphi - 1)(b-a),\ \lambda_{\max,i} \leftarrow \left\{ \begin{array}{ll} \lambda(x_2), & \text{if } \lambda(x_2) > 0, \\ \varepsilon, & \text{if } \lambda(x_2) = 0; \end{array} \right.$$

[2b.ii] Else set $b \leftarrow x_2, x_2 \leftarrow x_1, x_1 \leftarrow a + (2-\varphi)(b-a)$,
$$\lambda_{\max,i} \leftarrow \left\{ \begin{array}{ll} \lambda(x_1), & \text{if } \lambda(x_1) > 0, \\ \varepsilon, & \text{if } \lambda(x_1) = 0. \end{array} \right.$$

[2c] End

[3] End

[4] Define the piecewise constant function $\widetilde{\lambda}_Q(\cdot)$ over $[0, S]$ as follows:

$$\widetilde{\lambda}_Q(t) = \left\{ \sum_{i=1}^{Q} \lambda_{\max,i} \mathbb{I}_{(z_{i-1}, z_i]}(t) \right\} \text{ for } t \in [0, S].$$

[5] End

Figure 3.1: Algorithmic statement of seeking a positive step function that majorizes $\lambda(t)$ procedure.

3.2. Constructing the Majorizing Mean-Value Function

To construct the majorizing mean-value function corresponding to $\widetilde{\lambda}_Q(t)$, we must suitably account for the zeros of the given rate function $\lambda(t)$. The set of zeros of $\lambda(t)$,

$$\mathcal{Z} \equiv \{t \in [0, S] :\ \lambda(t) = 0\}, \tag{3.2}$$

consists of the following:

(i) the set of *isolated zeros* of $\lambda(t)$,

$$\mathcal{T} \equiv \{\tau_g :\ g = 1, 2, \ldots\}, \tag{3.3}$$

such that $\lambda(\tau_g) = 0$ but in some neighborhood $\mathcal{N}(\tau_g)$ of τ_g, we have $\lambda(t) > 0$ for $t \in \mathcal{N}(\tau_g)\backslash\{\tau_g\}$; and

(ii) a countable collection

$$\mathcal{W} \equiv \bigcup_{l=1}^{\infty} \mathcal{W}_\ell \tag{3.4}$$

of nonoverlapping subintervals $\mathcal{W}_\ell \subset [0, S]$ on which $\lambda(t)$ identically vanishes,

$$\lambda(t) \equiv 0 \ \text{ for all } \ t \in \mathcal{W}_\ell,\ \ell = 1, 2, \ldots, \tag{3.5}$$

so that we have the partition

$$\mathcal{Z} = \mathcal{T} \cup \mathcal{W}. \tag{3.6}$$

By construction of the majorizing step rate function $\widetilde{\lambda}_Q(t)$ with Q equal-length steps, we have

$$\widetilde{\lambda}_Q(t) \searrow \lambda(t) \text{ uniformly on } [0, S]\backslash\mathcal{Z} \text{ as } Q \to \infty \tag{3.7}$$

and

$$\widetilde{\lambda}_Q(t) = \varepsilon \ \text{ for } t \in \mathcal{Z}. \tag{3.8}$$

With this formulation of the majorizing rate function, we define the majorizing mean-value function $\widetilde{\mu}_Q(t)$ as follows:

$$\widetilde{\mu}_Q(t) \equiv \int_0^t \widetilde{\lambda}_Q(u)\big(1 - \mathbb{I}_{[u\in\mathcal{W}]}\big)du \quad \text{ for } 0 \le t \le S \tag{3.9}$$

so that we have

$$\widetilde{\mu}_Q(t) \searrow \mu(t) \text{ uniformly on } [0, S] \text{ as } Q \to \infty. \tag{3.10}$$

3.3. Case 1: $C \geq 1$

Phase-type exponential distributions (also called hyperexponential distributions) have larger coefficients of variation than the exponential distribution. For the 2-phase hyperexponential distribution, with probability $\alpha_1 \in (0,1)$, the upper exponential phase with parameter μ_1 is taken; and with probability $\alpha_2 = 1 - \alpha_1$ the lower exponential phase with parameter μ_2 is taken.

The density function of the 2-phase hyperexponential distribution is given by

$$f_X(x) = \begin{cases} 0, & x < 0, \\ \alpha_1 \mu_1 e^{-\mu_1 x} + \alpha_2 \mu_2 e^{-\mu_2 x}, & x \geq 0, \end{cases}$$

while the cumulative distribution function is

$$F_X(x) = \begin{cases} 0, & \text{if } x < 0, \\ \alpha_1(1 - e^{-\mu_1 x}) + \alpha_2(1 - e^{-\mu_2 x}), & \text{if } x \geq 0. \end{cases}$$

The first and second noncentral moments of the hyperexponential random variable $X \sim F_X(\cdot)$ are respectively given by

$$\mathrm{E}[X] = \frac{\alpha_1}{\mu_1} + \frac{\alpha_2}{\mu_2} \quad \text{and} \quad \mathrm{E}[X^2] = \frac{2\alpha_1}{\mu_1^2} + \frac{2\alpha_2}{\mu_2^2}.$$

The squared coefficient of variation of X is

$$(\mathrm{CV}[X])^2 = \frac{\mathrm{Var}(X)}{(\mathrm{E}[X])^2} = \frac{\mathrm{E}[X^2] - (\mathrm{E}[X])^2}{(\mathrm{E}[X])^2} = \frac{\mathrm{E}[X^2]}{(\mathrm{E}[X])^2} - 1 = \frac{2\alpha_1/\mu_1^2 + 2\alpha_2/\mu_2^2}{(\alpha_1/\mu_1 + \alpha_2/\mu_2)^2} - 1 \geq 1. \quad (3.11)$$

The proof that squared coefficient of variation is not less than 1 is equivalent to showing that

$$(\alpha_1/\mu_1 + \alpha_2/\mu_2)^2 \leq \alpha_1/\mu_1^2 + \alpha_2/\mu_2^2. \quad (3.12)$$

We have

$$\begin{aligned}
(\alpha_1/\mu_1 + \alpha_2/\mu_2)^2 &= \left(\sqrt{\alpha_1}\frac{\sqrt{\alpha_1}}{\mu_1} + \sqrt{\alpha_2}\frac{\sqrt{\alpha_2}}{\mu_2}\right)^2 && (3.13) \\
&\leq \left[(\sqrt{\alpha_1})^2 + (\sqrt{\alpha_2})^2)\right] \left\{\left(\frac{\sqrt{\alpha_1}}{\mu_1}\right)^2 + \left(\frac{\sqrt{\alpha_2}}{\mu_2}\right)^2\right\}, && (3.14) \\
&= (\alpha_1 + \alpha_2)\left(\frac{\alpha_1}{\mu_1^2} + \frac{\alpha_1}{\mu_1^2}\right) && (3.15) \\
&= \frac{\alpha_1}{\mu_1^2} + \frac{\alpha_2}{\mu_2^2}, \quad \text{since } \alpha_1 + \alpha_2 = 1. && (3.16)
\end{aligned}$$

where (3.14) follows Cauchy-Schwartz inequality, and (3.16) follows from the normalizing condition

$\alpha_1 + \alpha_2 = 1$. This completes the proof of inequalities (3.11) and (3.12).

In this case, we exploit the two-phase balanced-means hyperexponential distribution with CDF

$$\begin{aligned} G(x) &= p(1 - e^{-2px}) + (1-p)(1 - e^{-2(1-p)x}) \\ &= 1 - pe^{-2px} - (1-p)e^{-2(1-p)x} \quad \text{for } x \geq 0 \end{aligned} \tag{3.17}$$

so that the interrenewal times $\{X_i^\circ : i = 2, 3, \ldots\} \overset{\text{iid}}{\sim} G(x)$ have the moments $\tau \equiv \mathrm{E}[X_i^\circ] = 1$ and $\sigma^2 \equiv \mathrm{Var}[X_i^\circ] = C$.

For $i = 2, 3, \ldots$, we have

$$\begin{aligned} \mathrm{E}[(X_i^\circ)^2] &= p\mathrm{E}[Y_1^2] + (1-p)\mathrm{E}[Y_2^2] \\ &= p\frac{2}{(2p)^2} + (1-p)\frac{2}{[2(1-p)^2]} \\ &= \frac{1}{2p} + \frac{1}{2(1-p)} \end{aligned}$$

where Y_1 is an exponentially distributed random variable with $\mathrm{E}[Y_1] = 1/(2p)$ and Y_2 is an exponentially distributed random variable with $\mathrm{E}[Y_2] = 1/[2(1-p)]$ and

$$\begin{aligned} \mathrm{Var}(X_i^\circ) &= \mathrm{E}[(X_i^\circ)^2] - \mathrm{E}^2[X_i^\circ] \\ &= \frac{1}{2p} + \frac{1}{2(1-p)} - 1. \end{aligned}$$

To achieve

$$\left(\mathrm{CV}[X_i^\circ]\right)^2 = C \text{ for } i = 2, 3, \ldots$$

for a given value of $C \in [1, \infty)$, we must solve the following quadratic equation for $p \in (0, 1)$:

$$\frac{1 - 2p(1-p)}{2p(1-p)} = C.$$

It follows that we have

$$p = \frac{1 + C \pm \sqrt{C^2 - 1}}{2(1+C)}. \tag{3.18}$$

Note that both roots of Equation (3.18) belong to the unit interval $(0, 1)$ and effectively yield the same 2-phase balanced-means hyperexponential distribution.

Finally the CDF of the first interarrival time is

$$\begin{aligned}
G_e(t) = \Pr\{X_1^\circ < t\} &= \int_0^t [1 - G(u)]du \\
&= \frac{1}{2}\int_0^t \left[2pe^{-2pu} + 2(1-p)e^{-2(1-p)u}\right] du \\
&= \frac{1}{2}[1 - e^{-2pt} + 1 - e^{-2(1-p)t}] \\
&= 1 - \frac{1}{2}e^{-2pt} - \frac{1}{2}e^{-2(1-p)t} \quad \text{for } t \geq 0. \qquad (3.19)
\end{aligned}$$

3.4. Case 2: $C < 1$

The hyper-Erlang distribution gives smaller coefficients of variation than the exponential distribution. For the hyper-Erlang distribution, with probability $0 \leq p < 1$, we sample the upper Erlang distribution with shape parameter $k - 1$ (k is an integer with $k \geq 2$) and scale parameter β; and with probability $q = 1 - p$, we sample the lower Erlang distribution with shape parameter k and scale parameter β.

The density function of an Erlang distribution with shape parameter k and scale parameter β is given by

$$f_k(x) \equiv f_X(x; k, \beta) = \frac{\beta^k x^{k-1} e^{-\beta x}}{\Gamma(k)}, \quad \text{for } x \geq 0, \beta > 0 \text{ and } k \in \mathbb{N}^*,$$

where $\mathbb{N}^*$ denotes the positive integers, and is otherwise equal to zero, while the cumulative distribution function is given

$$F_k(x) \equiv F_X(x; k, \beta) = \int_0^x \frac{\beta^k u^{k-1} e^{-\beta u}}{\Gamma(k)} du, \quad \text{for } x, \beta > 0 \text{ and } k \in \mathbb{N}^*,$$

and $F_k(x) = 0$ for $x < 0$. The first and second moments of this distribution are respectively given by

$$\mathrm{E}[X] = \frac{k}{\beta} \quad \text{and} \quad \mathrm{E}[X^2] = \frac{k(k+1)}{\beta^2}.$$

When $C < 1$, the interrenewal times $\{X_i^\circ, i = 2, 3, \ldots\}$ follow the hyper-Erlang distribution with $\tau \equiv \mathrm{E}[X_i^\circ] = 1$ and $\sigma^2 \equiv \mathrm{Var}[X_i^\circ] = C < 1$. Choose $k \in \mathbb{N}^* - \{1\}$ such that

$$\frac{1}{k} \leq C < \frac{1}{k-1}.$$

For $i \geq 2$, we have

$$\begin{aligned}
\mathrm{E}[X_i^\circ] &= p\left(\frac{k-1}{\beta}\right) + (1-p)\frac{k}{\beta} \\
&= \frac{k-p}{\beta} = 1,
\end{aligned}$$

so that we must have $\beta = k - p$. Moreover for $i \geq 2$, we have

$$\begin{aligned}
\mathrm{E}[(X_i^\circ)^2] =& p\mathrm{E}[Y_{k-1}^2] + (1-p)\mathrm{E}[Y_k^2] \\
=& p\frac{(k-1)k}{\beta^2} + (1-p)\frac{k(k+1)}{\beta^2} \\
=& \frac{k(k+1-2p)}{\beta^2},
\end{aligned}$$

where Y_{k-1} follows the upper Erlang distribution with density function

$$f_{k-1}(y) = \frac{\beta^{k-1} y^{k-2} e^{-\beta y}}{\Gamma(k-1)}, \quad \text{for } y \geq 0, \beta > 0 \text{ and } k = 2, 3, \ldots;$$

and Y_k follows the lower Erlang distribution with density function

$$f_k(y) = \frac{\beta^k y^{k-1} e^{-\beta y}}{\Gamma(k)}, \quad \text{for } y \geq 0, \beta > 0 \text{ and } k = 2, 3, \ldots$$

so that

$$\begin{aligned}
\mathrm{Var}[X_i^\circ] =& \mathrm{E}[(X_i^\circ)^2] - (\mathrm{E}[X_i^\circ])^2 \\
=& \frac{k(k+1-2p)}{\beta^2} - 1 \\
=& \frac{k-p^2}{\beta^2}.
\end{aligned}$$

To achieve

$$(\mathrm{CV}[X_i^\circ])^2 = C \quad \text{for } i \geq 2,$$

where $C \in (0, 1)$ is given, we must solve the following quadratic equation for p:

$$C = \frac{k-p^2}{(k-p)^2}.$$

Solving for p in the above equation, we have

$$p = \frac{Ck \pm \sqrt{k(1+C) - k^2C}}{1+C}. \tag{3.20}$$

Note that in Equation (3.20) the solution achieved by taking the root corresponding to the plus sign yields a value of p outside the unit interval [0,1) :

$$\frac{kC + \sqrt{k(1+C) - k^2C}}{1+C} = \frac{kC + \sqrt{k(1+C-kC)}}{1+C} > \frac{kC + (1+C-kC)}{1+C} = 1$$

since $k \geq 2 > 1 + (1-k)C$.
The other solution,

$$p = \frac{kC - \sqrt{k(1+C) - k^2C}}{1+C},$$

belongs to the interval [0,1). This is true because when we chose $k \in \mathbb{N}^* - \{1\}$ and $\frac{1}{k} \leq C < \frac{1}{k-1}$, we have $\sqrt{k + kC - k^2C} \leq \sqrt{k + kC - k} \leq Ck$, so that $p \geq 0$; moreover, $Ck - (1 + C) = C(k-1) - 1 < 0$ implies $Ck < 1 + C$, and $\sqrt{k + kC - k^2C} > 0$ so that $p < 1$.

For for $i \geq 2$, the CDF for the hyper-Erlang interarrival times $\{X_i^\circ\}$ is

$$G(t) = pF_{k-1}(t) + (1-p)F_k(t) \quad \text{for all } t, \tag{3.21}$$

where

$$F_k(t) = 0 \text{ for } t \leq 0,$$

and

$$\begin{aligned} F_k(t) &= \int_0^t \frac{\beta^k u^{k-1}}{(k-1)!} e^{-\beta u} du \\ &= 1 - e^{-\beta t} \sum_{n=0}^{k-1} \frac{(\beta t)^n}{n!} \quad \text{for } t \geq 0. \end{aligned}$$

Finally it follows that for the CDF for the first interarrival time X_1 is given by

$$
\begin{aligned}
G_e(t) &= \int_0^t [1 - G(x)]dx && (3.22)\\
&= \int_0^t [1 - pF_{k-1}(x) - (1-p)F_k(x)]dx && (3.23)\\
&= [1 - pF_{k-1}(x) - (1-p)F_k(x)]x \Big|_0^t + \int_0^t x[pf_{k-1}(x) + (1-p)f_k(x)]dx && (3.24)\\
&= [1 - pF_{k-1}(t) - (1-p)F_k(t)]t && (3.25)\\
&\quad + p\int_0^t xf_{k-1}(x)dx + (1-p)\int_0^t xf_k(x)dx && (3.26)\\
&= [1 - pF_{k-1}(t) - (1-p)F_k(t)]t && (3.27)\\
&\quad + p\int_0^t x\frac{\beta^{k-1}x^{k-2}e^{-\beta x}}{\Gamma(k-1)}dx + (1-p)\int_0^t x\frac{\beta^k x^{k-1}e^{-\beta x}}{\Gamma(k)}dx && (3.28)\\
&= [1 - pF_{k-1}(t) - (1-p)F_k(t)]t + \frac{p(k-1)}{\beta}F_k(t) + \frac{(1-p)k}{\beta}F_{k+1}(t) && (3.29)\\
&= \left\{1 - pF_{k-1}(t) - (1-p)\left[F_{k-1}(t) - \frac{e^{-\beta t}(\beta t)^{k-1}}{(k-1)!}\right]\right\} t && (3.30)\\
&\quad + \frac{p(k-1)}{\beta}F_k(t) + \frac{(1-p)k}{\beta}\left(F_k(t) - \frac{e^{-\beta t}(\beta t)^k}{(k)!}\right) && (3.31)\\
&= [1 - F_{k-1}(t)]t + F_k(t) \quad \text{for all } t \geq 0. && (3.32)
\end{aligned}
$$

3.5. Algorithmic Statement of CIAT

Given a designated rate function $\lambda(t)$, and the corresponding mean-value function $\mu(t) = \int_0^t \lambda(u)du$, the desired variance-to-mean ratio $C = \mathrm{Var}[N_Q(t)]/\mathrm{E}[N_Q(t)]$, first we seek a strictly positive step function $\widetilde{\lambda}_Q(t)$ that majorizes and closely approximates the designated rate function $\lambda(t)$; and we use inversion to generate the associated point process $\{\widetilde{N}_Q(t) : t \geq 0\}$ with asymptotic variance-to-mean ratio C and arrival epochs $\{\widetilde{S}_n : n = 1, 2, \ldots\}$. To complete the combined inversion-and-thinning procedure, we apply the thinning method to the arrival epochs $\{\widetilde{S}_n : n = 1, 2, \ldots\}$ to obtain the desired sequence of arrival epochs$\{S_j : j = 1, 2, \ldots\}$ from the point process with the designated rate function $\lambda(t)$ as follows: the epoch $\widetilde{S}_n$ is independently accepted for inclusion in $\{S_j : j = 1, 2, \ldots\}$ with probability $\lambda(\widetilde{S}_n)/\widetilde{\lambda}(\widetilde{S}_n)$ as detailed in Figure 3.2

[1] Construct the majorizing rate function $\widetilde{\lambda}_Q(t)$ with easily invertible mean-value function $\widetilde{\mu}_Q(t) = \int_0^t \widetilde{\lambda}_Q(u)du$ using the algorithm in Figure 3.1;

[2] Generate the point process $\{N_Q(t) : 0 \leq t \leq S\}$ with $\mathrm{E}[N_Q(t)] = \int_0^t \lambda(u)du$ for all $t \geq 0$ and $\lim_{t\to\infty} \lim_{Q\to\infty} \mathrm{Var}[N_Q(t)]/\mathrm{E}[N_Q(t)] = C$ by the combined inversion-and-thinning method.
If $C > 1$, then we take $G \sim$ hyperexponential distribution as given by Equation (3.17) and $G_e(x)$ is given by Equation (3.19).
If $C < 1$, then we take $G \sim$ hyper-Erlang distribution as given by Equation (3.21), and $G_e(x)$ is given by Equation (3.32).

[3] Set $n \leftarrow 1$, $j \leftarrow 0$, $S_0^\circ \leftarrow 0$, $\widetilde{S}_0 \leftarrow 0$, and $S_0 \leftarrow 0$. Generate $X_n^\circ \sim G_e$ and set $S_n^\circ \leftarrow S_{n-1}^\circ + X_n^\circ$. Set $\widetilde{S}_n \leftarrow \widetilde{\mu}^{-1}(S_n^\circ)$ and $\widetilde{X}_n \leftarrow \widetilde{S}_n - \widetilde{S}_{n-1}$.

[3a] **If** $\widetilde{S}_1 \leq S$, go to **[4]**.

[3b] **Otherwise stop, delivering** $j = 0$.

[4] Generate $U_n \sim$ Uniform[0,1].

[4a] **If** $U_n \leq \dfrac{\lambda(\widetilde{S}_n)}{\widetilde{\lambda}(\widetilde{S}_n)}$, **then** set $j \leftarrow j + 1$, $S_j \leftarrow \widetilde{S}_n$, set the interarrival time $X_j \leftarrow S_j - S_{j-1}$, and **goto [5]**.

[4b] **Otherwise**, **goto [5]**.

[5] Set $n \leftarrow n + 1$. Generate $X_n^\circ \sim G$. Set $S_n^\circ \leftarrow S_{n-1}^\circ + X_n^\circ$, $\widetilde{S}_n \leftarrow \widetilde{\mu}^{-1}(S_n^\circ)$, and $\widetilde{X}_n \leftarrow \widetilde{S}_n - \widetilde{S}_{n-1}$.

[5a] **If** $\widetilde{S}_n \leq S$, **goto [4]**.

[5b] **Otherwise stop**, **delivering** j and $\{S_i : i = 1, \ldots, j\}$ if $j > 0$.

Figure 3.2: Algorithmic statement of the combination of inversion and thinning method).

In Appendix A, we prove the following theorem establishing that the CIAT procedure delivers a point process with the desired mean-value function.

THEOREM 4. *If the point process* $\{N_Q(t) : 0 \leq t \leq S\}$ *is generated by the combined thinning-and-*

inversion technique (CIAT) detailed in Figure 3.2, then the process has mean-value function

$$\mathrm{E}[N_Q(t)] = \int_0^t \lambda(u)du \ \textit{for} \ 0 \le t \le S. \tag{3.33}$$

As in Section 3.2, we let $\widetilde{\lambda}_Q(t)$ and $\widetilde{\mu}_Q(t)$ respectively denote the majorizing rate and mean-value functions based on a subdivision of $[0, S]$ into Q nonoverlapping equal-length steps over which $\widetilde{\lambda}_Q(t)$ is constant. As $Q \to \infty$, the asymptotic property (3.7) of $\widetilde{\lambda}_Q(t)$ and the asymptotic property (3.10) of $\widetilde{\mu}_Q(t)$ will play critical roles in the following development. Let $\{\widetilde{N}_Q(t) : t \in [0, S]\}$ denote the point process that is obtained from the equilibrium renewal process $N^\circ(u)$ by inversion of $\widetilde{\mu}_Q(t)$ in the CIAT procedure and that is thinned in the CIAT procedure to yield the point process $\{N_Q(t) : t \in [0, S]\}$ with designated mean-value function

$$\mu_Q(t) \equiv \mathrm{E}[N_Q(t)] = \mu(t) = \int_0^t \lambda(u)du \text{ for } t \in [0, S] \tag{3.34}$$

as established in Theorem 4. Finally let

$$\begin{aligned} C_Q(t) &\equiv \mathrm{Var}[N_Q(t)]/\mathrm{E}[N_Q(t)] \\ &= \mathrm{Var}[N_Q(t)]/\mu(t) \text{ for } t \in [0, S] \end{aligned} \tag{3.35}$$

denote the dispersion ration for the thinned process $\{N_Q(t) : t \in [0, S]\}$ at a fixed time $t \in [0, S]$ as a function of Q. In Appendix B, we prove the following theorem.

THEOREM 5. *If $\{N_Q(t) : t \in [0, S]\}$ is generated by the CIAT procedure, then as $S \to \infty$ so that we can let $t \to \infty$, we have*

$$\lim_{Q\to\infty} C_Q(t) = C + \frac{o[\mu(t)]}{\mu(t)}. \tag{3.36}$$

Because the mean-value function $\mu(t)$ is a nondecreasing function of t, it approaches a (possibly infinite) value μ^* as $S \to \infty$,

$$\mu^* \equiv \lim_{S\to\infty} \mu(S) \ \in \ (0, \infty]. \tag{3.37}$$

If $\mu^* < \infty$, then Theorem 5 may not be a useful result, especially for small values of t. On the other hand if $\mu^* = \infty$, then Theorem 5 ensures that

$$\lim_{t\to\infty} \lim_{Q\to\infty} C_Q(t) = C; \tag{3.38}$$

and thus we have

$$C_Q(t) \approx C \text{ for } S,\ Q,\ t \text{ sufficiently large.} \tag{3.39}$$

In the next chapter we provide some experimental evidence supporting the asymptotic approximation (3.36).

3.6. CIATL: A CIAT Procedure with Lognormal Distribution for Interrenewal Times

In this section, we introduce the theoretical background and implementation of another approach of CIAT, a CIAT procedure with a lognormal distribution for the interarrival times $\{X_i : i = 2, 3, \ldots\}$. This procedure, called CIATL, has the potential advantage of requiring a single, unified approach for any designated dispersion ratio $C > 0$.

3.6.1 Lognormal Distribution Function for Interrenewal Times

If Z is a standard normal variable with $\mathrm{E}[Z] = 0$, and $\mathrm{Var}[Z] = 1$, then $X \equiv \exp(k + \beta Z)$ has a lognormal random distribution, the density function with shape parameter β and scale parameter k is given by

$$f_X(x; k, \beta) = \frac{1}{x\beta\sqrt{2\pi}} \exp\left\{-\frac{(\ln(x) - k)^2}{2\beta^2}\right\} \quad \text{for } x \geq 0, \tag{3.40}$$

and while the cumulative distribution function is given

$$F_X(x; k, \beta) = \Phi\left[\frac{\ln(x) - k}{\beta}\right] \quad \text{for } x \geq 0, \tag{3.41}$$

where $\Phi(z) = \int_{-\infty}^{z} \frac{1}{\sqrt{2\pi}} \exp(-\frac{1}{2}u^2)du$ is the CDF of the standard normal distribution. The mean and variance for the lognormal variable X are given by

$$\mathrm{E}[X] = \exp[k + (\beta^2/2)] \tag{3.42}$$

and

$$\mathrm{Var}[X] = [\exp(\beta^2) - 1]\exp(2k + \beta^2), \tag{3.43}$$

respectively, so that we have the squared coefficient of variation

$$(\mathrm{CV}[X])^2 = \frac{\mathrm{Var}(X)}{(\mathrm{E}[X])^2} = \exp(\beta^2) - 1. \tag{3.44}$$

For any designated $C > 0$, the interrenewal times $\{X_i^\circ, i = 2, 3, \ldots\}$ must follow the lognormal distribution with $\tau \equiv \mathrm{E}[X_i^\circ] = 1$ and $\sigma^2 \equiv \mathrm{Var}[X_i^\circ] = C$. For $i \geq 2$, we have

$$\mathrm{E}[X_i^\circ] = \exp[k + (\beta^2/2)] = 1,$$

so that we must have

$$k + \frac{\beta^2}{2} = 0. \tag{3.45}$$

Moreover for $i \geq 2$, we have

$$\begin{aligned} \mathrm{Var}[X_i^\circ] =& [\exp(\beta^2) - 1] \exp(2k + \beta^2) \\ =& \exp(\beta^2) - 1. \end{aligned} \tag{3.46}$$

To achieve

$$(\mathrm{CV}[X_i^\circ])^2 = C \quad \text{for } i \geq 2, \tag{3.47}$$

where $C > 0$ is given, Equations (3.46) and (3.47) imply that

$$\beta^2 = \ln(1 + C) \tag{3.48}$$

and combing (3.45) and (3.48), we finally obtain

$$k = -\frac{\ln(1 + C)}{2}. \tag{3.49}$$

For $i \geq 2$, the CDF for the lognormal interarrival times $\{X_i^\circ\}$ is

$$G(t) = \Phi\left[\frac{\ln(t) - k}{\beta}\right] \quad \text{for all } t \geq 0, \tag{3.50}$$

where $\phi(z) = (2\pi)^{-1/2} \exp(-z^2/2)$ is the PDF for standard normal distribution and $\Phi(z) = \int_{-\infty}^{z} \phi(u) du$ is the CDF of the standard normal distribution. It follows that for the CDF for the first interrenewal time X_1° is given by

$$
\begin{aligned}
G_e(t) = &\int_0^t [1 - G(x)]dx && (3.51)\\
= &\int_0^t \left\{1 - \Phi\left[\frac{\ln(x) - k}{\beta}\right]\right\} dx && (3.52)\\
= &\left\{1 - \Phi\left[\frac{\ln(x) - k}{\beta}\right]\right\} x\Big|_0^t + \int_0^t x\phi\left[\frac{\ln(x) - k}{\beta}\right]\frac{1}{\beta x}dx && (3.53)\\
= &\left\{1 - \Phi\left[\frac{\ln(t) - k}{\beta}\right]\right\} t + \frac{1}{\beta}\int_0^t \phi\left[\frac{\ln(x) - k}{\beta}\right]dx && (3.54)\\
= &\left\{1 - \Phi\left[\frac{\ln(t) - k}{\beta}\right]\right\} t + \frac{1}{\beta}\int_{-\infty}^{\frac{\ln(t)-k}{\beta}} \phi(w)\beta e^{\beta w + k}dw && (3.55)\\
= &\left\{1 - \Phi\left[\frac{\ln(t) - k}{\beta}\right]\right\} t + \exp(k + \beta^2/2)\int_{-\infty}^{\frac{\ln(t)-k}{\beta}} \frac{1}{\sqrt{2\pi}}e^{-(w-\beta)^2/2}dw && (3.56)\\
= &\left\{1 - \Phi\left[\frac{\ln(t) - k}{\beta}\right]\right\} t + \exp(k + \beta^2/2)\int_{-\infty}^{\frac{\ln(t)-k}{\beta}-\beta} \frac{1}{\sqrt{2\pi}}e^{-v^2/2}dv && (3.57)\\
= &\left\{1 - \Phi\left[\frac{\ln(t) - k}{\beta}\right]\right\} t + \exp(k + \beta^2/2)\Phi\left[\frac{\ln(t) - k - \beta^2}{\beta}\right] && (3.58)\\
= &t - t\Phi\left[\frac{\ln(t) + \beta^2/2}{\beta}\right] + \Phi\left[\frac{\ln(t) - \beta^2/2}{\beta}\right] \quad \text{for all } t \geq 0, && (3.59)
\end{aligned}
$$

where (3.55) is achieved by changing in variable $w = \dfrac{\ln x - k}{\beta}$ and (3.57) is achieved by changing in variable $v = w - \beta$.

3.6.2 Algorithm Statement of CIATL

Algorithm for CIATL has nearly the same design as the original CIAT algorithm given in Figure3.3, only Step **[2]** is slightly changed.

[1] Construct the majorizing rate function $\widetilde{\lambda}_Q(t)$ with easily invertible mean-value function $\widetilde{\mu}_Q(t) = \int_0^t \widetilde{\lambda}_Q(u)du$ using the algorithm in Figure 3.1;

[2*] Generate the point process $\{N_Q(t) : 0 \le t \le S\}$ with $\mathrm{E}[N_Q(t)] = \int_0^t \lambda(u)du$ for all $t \ge 0$ and $\lim_{t\to\infty} \lim_{Q\to\infty} \mathrm{Var}[N_Q(t)]/\mathrm{E}[N_Q(t)] = C$ by the combined inversion-and-thinning method.
For any designated $C > 0$, we take $G \sim$ lognormal distribution as given by Equation (3.50) and $G_e(x)$ is given by Equation (3.59).

[3] Set $n \leftarrow 1$, $j \leftarrow 0$, $S_0^\circ \leftarrow 0$, $\widetilde{S}_0 \leftarrow 0$, and $S_0 \leftarrow 0$. Generate $X_n^\circ \sim G_e$ and set $S_n^\circ \leftarrow S_{n-1}^\circ + X_n^\circ$. Set $\widetilde{S}_n \leftarrow \widetilde{\mu}^{-1}(S_n^\circ)$ and $\widetilde{X}_n \leftarrow \widetilde{S}_n - \widetilde{S}_{n-1}$.

[3a] **If** $\widetilde{S}_1 \le S$, go to **[4]**.

[3b] **Otherwise stop, delivering** $j = 0$.

[4] Generate $U_n \sim$ Uniform[0,1].

[4a] **If** $U_n \le \dfrac{\lambda(\widetilde{S}_n)}{\widetilde{\lambda}(\widetilde{S}_n)}$, **then** set $j \leftarrow j + 1$, $S_j \leftarrow \widetilde{S}_n$, set the interarrival time $X_j \leftarrow S_j - S_{j-1}$, and **goto [5]**.

[4b] **Otherwise**, **goto [5]**.

[5] Set $n \leftarrow n + 1$. Generate $X_n^\circ \sim G$. Set $S_n^\circ \leftarrow S_{n-1}^\circ + X_n^\circ$, $\widetilde{S}_n \leftarrow \widetilde{\mu}^{-1}(S_n^\circ)$, and $\widetilde{X}_n \leftarrow \widetilde{S}_n - \widetilde{S}_{n-1}$.

[5a] **If** $\widetilde{S}_n \le S$, **goto [4]**.

[5b] **Otherwise stop**, **delivering** j and $\{S_i : i = 1, \ldots, j\}$ if $j > 0$.

Figure 3.3: Algorithmic statement of the combination of inversion and thinning method with lognormal distribution.

Chapter 4

Performance Evaluation of CIAT Procedure

4.1. Experimental Setup

The minimum information required to define an NNPP process $\{N(t) : t \geq 0\}$ is a desired rate function $\lambda(t)$ and a variance-to-mean ratio C; the mean time τ between renewals for the base process $\{N^{\circ}(t) : t \geq 0\}$ is 1. For our test processes (experimental cases), we chose an exponential-polynomial-trigonometric rate function having multiple periodicities—that is, a rate function of the class we shall label **EPTMP** [21]. The use of an exponential rate function is a convenient means of ensuring that the instantaneous arrival rate is always positive. If the arrival rate includes a long-term evolutionary trend, then this trend is naturally represented in the exponent of the rate function by a polynomial component of appropriate degree. Finally if the arrival rate includes some periodic effects, then each of these effects is naturally represented in the exponent of the rate function by a trigonometric component with the appropriate oscillation frequency, oscillation amplitude, and phase delay.

An EPTMP-type rate function has the form

$$\lambda(t) = \exp\{h(t; m, p, \Theta)\} \quad \text{for } 0 \leq t \leq S, \tag{4.1}$$

with

$$h(t; m, p, \Theta) = \left[\sum_{i=0}^{m} \alpha_i t^i\right] + \left[\sum_{k=1}^{p} \gamma_k \sin(\omega_k t + \phi_k)\right], \tag{4.2}$$

where

$$\Theta = [\alpha_0, \alpha_1, \ldots, \alpha_m, \gamma_1, \ldots, \gamma_p, \omega_1, \ldots, \omega_p, \phi_1, \ldots, \phi_p,] \tag{4.3}$$

is the vector of continuous parameters of the designated rate function. The first $m + 1$ terms in (4.2) define a degree-m polynomial function representing the general trend over time. The next p terms in (4.3) are trigonometric functions representing cyclic effects exhibited by the process. The parameters we use for the rate function are shown in Table 4.1. Cases 1–3 consist of exponential rate functions with two periodic components. Case 1 does not contain a general trend over time. Cases 2 and 3 contain general trends that are represented by polynomials of degree 1 and 2, respectively. We then take $S = 8$, and the desired asymptotic variance-to-mean ratio is $C = 10$ in scenario 1, $C = 1.5$ in scenario 2, $C = 0.8$ in scenario 3 and $C = 0.2$ in scenario 4 for the rate function $\lambda(t)$ in Case 1, Case 2 and Case 3.

Table 4.1: Parameters of NNPPs used in the experimental evaluation

Parameter	Case		
	1	2	3
α_0	3.6269	3.6269	3.6269
α_1	–	0.1000	-0.1000
α_2	–	–	0.0200
γ_1	1.0592	1.0592	1.0592
ϕ_1	-0.6193	-0.6193	-0.6193
ω_1	6.2831	6.2831	6.2831
γ_2	0.5000	0.5000	0.5000
ϕ_2	0.5000	0.5000	0.5000
ω_2	12.5664	12.5664	12.5664

To evaluate the performance of the proposed CIAT procedure, we performed a *metaexperiment* consisting of $R = 100$ independent basic experiments; and in each basic experiment, we performed $K = 200$ independent replications of the CIAT procedure to generate 200 realizations of an NNPP $\{N(t) : t \in [0, S]\}$ that should have the rate function specified with parameters in Table 4.1 and that should have $C = 10$, $C = 1.5$, $C = 0.8$, and $C = 0.2$. Each basic experiment yielded estimates of the mean-value function $\mu(t) = \mathrm{E}[N_Q(t)]$ and the dispersion-ratio function

$$C_Q(t) \equiv \mathrm{Var}[N_Q(t)]/\mathrm{E}[N_Q(t)] \text{ for } t \in (0, S]. \tag{4.4}$$

From 100 replications of each basic experiment, we computed 95% confidence interval (CI) estimators of $\mu(t_i)$ and $C_Q(t_i)$ at the times $\{t_i : t_i = \psi i, \text{ for } i = 1, \ldots, M\}$, where ψ is the length of each subinterval and $M = S/\psi$. For all the experiments in this section, we set $\psi = 0.2$. To validate the proposed CIAT procedure, we examined the following:

(a) Graphs of the desired rate function $\lambda(t_i)$ and the desired mean-value functions $\mu(t_i)$ respectively superimposed on the majorizing rate function $\widetilde{\lambda}_Q(t_i)$ and on 95% CI estimators of the mean-value function $\mu_Q(t_i)$ for the CIAT-generated NNPP at the times $\{t_i : t_i = \psi i, \text{ for } i = 1, \ldots, M\}$;

(b) Graphs of the desired asymptotic dispersion ratios $C > 1$ (namely, $C = 1.5$ and $C = 10$) superimposed on simulation-based point and CI estimators of $C_Q(t_i)$ at the times $\{t_i : t_i = \psi i,\ \text{for}\ i = 1, \ldots, M\}$;

(c) Graphs of the desired asymptotic dispersion ratios $0 < C < 1$ (namely, $C = 0.2$ and $C = 0.8$) superimposed on simulation-based point and CI estimators of $C_Q(t_i)$ at the times $\{t_i : t_i = \psi i,\ \text{for}\ i = 1, \ldots, M\}$; and

(d) Tabular summaries of the same results depicted in (a), (b) and (c).

All of our algorithms have been implemented in Matlab, and all the experiments in this dissertation were carried out on a 2.66GHz Intel 2 Quad processor with 3.25 GB RAM, running Windows XP Professional.

4.2. Formulation of Performance Measures

On the kth realization of the CIAT-generated NNPP process in the rth basic experiment, let $N_Q(t; r, k)$ denote the number of accepted arrivals up to time $t \in [0, S]$, where $r = 1, \ldots, R$, and $k = 1, \ldots, K$. In the rth basic experiment, the estimator of the desired mean-value function $\mu(t)$ is the sample mean

$$\bar{N}_Q(t; r) = \frac{1}{K} \sum_{k=1}^{K} N_Q(t; r, k) \quad \text{for } t \in (0, S];$$

and the corresponding estimator of the variance of $N_Q(t; r, k)$ is the sample variance

$$\widehat{\text{Var}}\left[N_Q(t; r, 1)\right] = \frac{1}{K - 1} \sum_{k=1}^{K} \left[N_Q(t; r, k) - \bar{N}_Q(t; r)\right]^2 \quad \text{for } t \in (0, S].$$

The sample dispersion ratio at time t is

$$\widehat{C}_Q(t; r) = \frac{\widehat{\text{Var}}\left[N_Q(t; r, 1)\right]}{\bar{N}_Q(t; r)} \quad \text{for } t \in (0, S].$$

Based on the entire metaexperiment, the overall estimator of the desired mean-value function $\mu(t)$ is

$$\widehat{\mu}_Q(t) = \frac{1}{RK} \sum_{r=1}^{R} \sum_{k=1}^{K} N_Q(t; r, k) \quad \text{for } t \in (0, S];$$

and a pooled estimator of $\mathrm{Var}[N_Q(t)]$ is

$$\widehat{\mathrm{Var}}[N_Q(t)] = \frac{1}{R}\sum_{r=1}^{R} \widehat{\mathrm{Var}}\left[N_Q(t;r,1)\right] \quad \text{for } t \in (0,S].$$

The point estimator of $C_Q(t)$ is

$$\widehat{C}_Q(t) = \frac{1}{R}\sum_{r=1}^{R} \widehat{C}_Q(t;r) \quad \text{for } t \in (0,S],$$

and the overall estimator of $\mathrm{Var}[\widehat{C}_Q(t;1)]$ is

$$\widehat{\mathrm{Var}}[\widehat{C}_Q(t;1)] = \frac{1}{R-1}\sum_{r=1}^{R} \left\{\widehat{C}_Q(t;r) - \widehat{C}_Q(t)\right\}^2 \quad \text{for } t \in (0,S].$$

For a fixed time t, an approximate $100(1-\alpha)\%$ CI estimator for $C_Q(t)$ is

$$\widehat{C}_Q(t) \pm z_{1-\alpha/2}\sqrt{\widehat{\mathrm{Var}}[\widehat{C}_Q(t;1)]/R} \quad \text{for } t \in (0,S],$$

where $z_{1-\alpha/2}$ is the $1-\alpha/2$ quantile of the standard nomad distribution. For example, if $\alpha = 0.05$, then $z = 1.96$ and we will have an estimated 95% confidence interval for the variance-to-mean ratio. Similarly, confidence intervals are obtained for the mean-value function $\mu(t)$ at a fixed time t.

4.3. Presentation and Discussion of Results

4.3.1 Presentation and Discussion for CIAT-Generated NNPPs in Case 1

In Case 1, Figure 4.1 shows the desired rate function $\lambda(t)$ and the corresponding step rate function $\widetilde{\lambda}(t)$ for $t \in [0,8]$. For $C = 10$, 1.5, 0.8, and 0.2, we computed 95% CI estimators of $\mu(t)$ for $0 \le t \le 8$, and presented the results in Figures 4.2, 4.4, 4.6, and 4.8, as well as in Tables 4.2, 4.4, 4.6, and 4.8, respectively. In these figures, the red line represents the desired mean-value function $\mu(t)$ and the black line represents the estimated mean-value function $\widehat{\mu}(t)$. The 95% CI estimators of $C(t)$ for $0 \le t \le 8$ are presented in Figures 4.3, 4.5, 4.7, and 4.9, as well as in Tables 4.3, 4.5, 4.7, and 4.9, respectively.

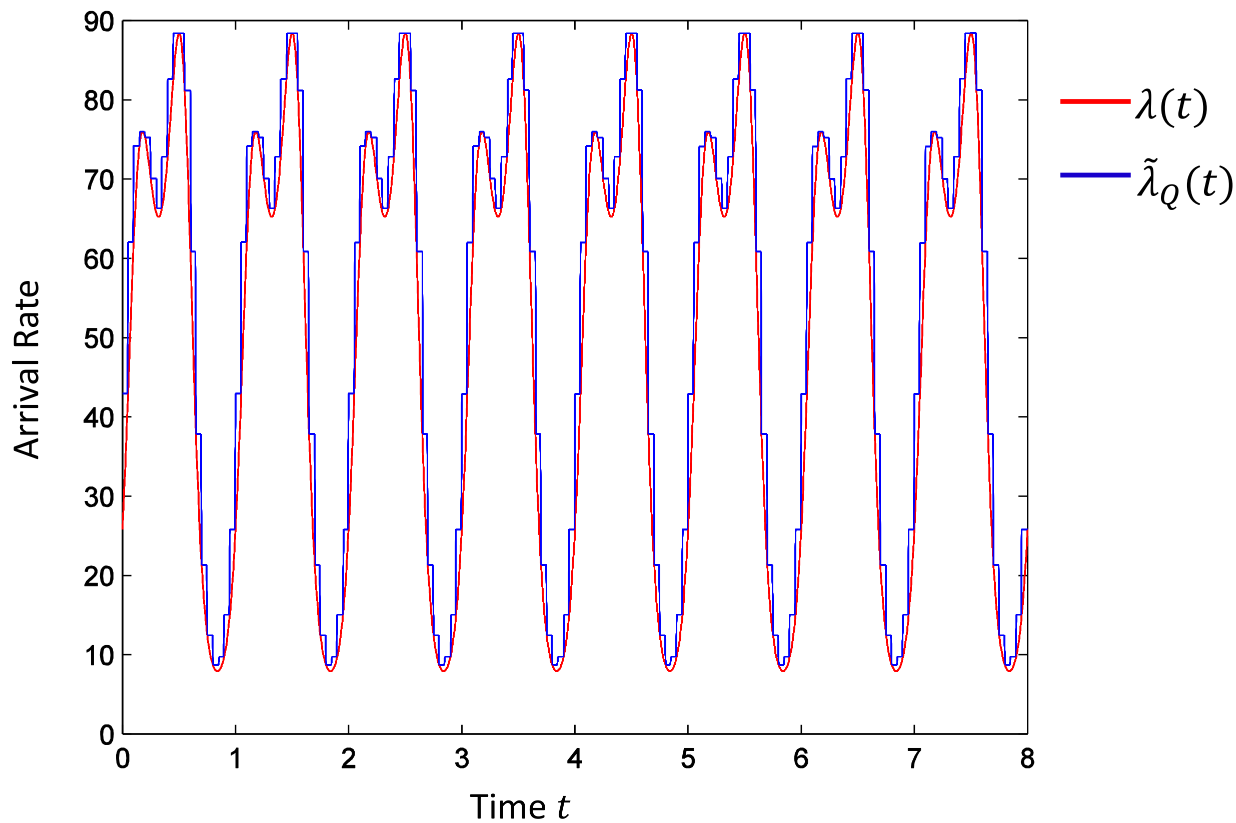

Figure 4.1: Step rate function $\widetilde{\lambda}_Q(t)$ that majorizes $\lambda(t)$ in Case 1.

Table 4.2: CIAT-generated 95% CI estimators for $\mu(t),\ t \in (0, 8]$, in Case 1 with $C = 10$.

time t	0.2	0.4	0.6	0.8	1.0	1.2	1.4	1.6	1.8	2.0
$\widehat{\mu}(t)_{0.975}$	16.742	34.274	53.370	59.306	61.967	74.963	90.254	108.034	113.689	116.347
$\widehat{\mu}(t)$	11.540	25.523	41.651	46.859	49.217	60.809	74.392	90.463	95.581	98.029
$\widehat{\mu}(t)_{0.025}$	6.338	16.771	29.931	34.411	36.467	46.655	58.531	72.893	77.474	79.710
time t	2.2	2.4	2.6	2.8	3.0	3.2	3.4	3.6	3.8	4.0
$\widehat{\mu}(t)_{0.975}$	128.869	143.641	161.349	166.940	169.507	181.801	196.687	213.740	219.328	221.927
$\widehat{\mu}(t)$	109.474	123.070	139.351	144.500	146.913	158.356	172.151	188.003	193.284	195.755
$\widehat{\mu}(t)_{0.025}$	90.079	102.499	117.352	122.061	124.318	134.911	147.616	162.266	167.239	169.583
time t	4.2	4.4	4.6	4.8	5.0	5.2	5.4	5.6	5.8	6.0
$\widehat{\mu}(t)_{0.975}$	234.089	249.029	266.300	271.935	274.556	286.737	301.248	318.131	323.590	326.110
$\widehat{\mu}(t)$	207.279	221.231	237.412	242.727	245.228	256.730	270.446	286.436	291.652	294.062
$\widehat{\mu}(t)_{0.025}$	180.469	193.433	208.523	213.518	215.900	226.724	239.644	254.742	259.714	262.013
time t	6.2	6.4	6.6	6.8	7.0	7.2	7.4	7.6	7.8	8.0
$\widehat{\mu}(t)_{0.975}$	338.220	352.666	369.392	374.985	377.526	389.655	404.081	420.898	426.302	428.442
$\widehat{\mu}(t)$	305.601	319.323	335.172	340.440	342.869	354.390	368.169	384.157	389.383	391.422
$\widehat{\mu}(t)_{0.025}$	272.982	285.981	300.953	305.895	308.211	319.125	332.256	347.415	352.463	354.403

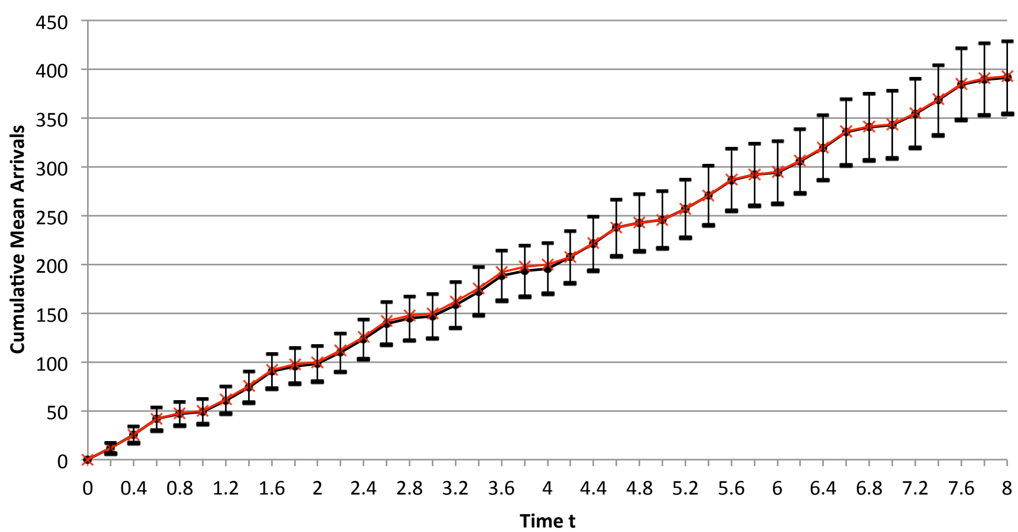

Figure 4.2: CIAT-generated 95% CIs for $\mu(t),\ t \in (0, 8]$, in Case 1 with $C = 10$.

Table 4.3: CIAT-generated 95% CI estimators for $C_Q(t)$, $t \in (0, 8]$, in Case 1 with $C = 10$.

time t	0.2	0.4	0.6	0.8	1.0	1.2	1.4	1.6	1.8	2.0
$\widehat{C}(t)_{0.975}$	7.144	8.827	9.675	9.834	9.883	10.063	10.225	10.267	10.391	10.402
$\widehat{C}(t)$	6.630	8.202	8.989	9.130	9.165	9.281	9.434	9.467	9.560	9.575
$\widehat{C}(t)_{0.025}$	6.116	7.577	8.304	8.426	8.446	8.499	8.643	8.666	8.729	8.748
time t	2.2	2.4	2.6	2.8	3.0	3.2	3.4	3.6	3.8	4.0
$\widehat{C}(t)_{0.975}$	10.504	10.382	10.514	10.619	10.573	10.671	10.795	10.786	10.754	10.713
$\widehat{C}(t)$	9.688	9.660	9.721	9.796	9.775	9.813	9.871	9.907	9.887	9.867
$\widehat{C}(t)_{0.025}$	8.871	8.938	8.928	8.972	8.977	8.954	8.947	9.029	9.020	9.020
time t	4.2	4.4	4.6	4.8	5.0	5.2	5.4	5.6	5.8	6.0
$\widehat{C}(t)_{0.975}$	10.679	10.727	10.806	10.785	10.778	10.809	10.819	10.844	10.835	10.830
$\widehat{C}(t)$	9.821	9.876	9.934	9.935	9.929	9.951	9.932	9.908	9.893	9.885
$\widehat{C}(t)_{0.025}$	8.963	9.025	9.062	9.084	9.080	9.093	9.045	8.972	8.951	8.940
time t	6.2	6.4	6.6	6.8	7.0	7.2	7.4	7.6	7.8	8.0
$\widehat{C}(t)_{0.975}$	10.823	10.802	10.777	10.815	10.813	10.830	10.797	10.829	10.835	10.841
$\widehat{C}(t)$	9.881	9.871	9.874	9.915	9.912	9.953	9.921	9.936	9.904	9.908
$\widehat{C}(t)_{0.025}$	8.939	8.940	8.970	9.014	9.010	9.076	9.045	9.044	8.973	8.974

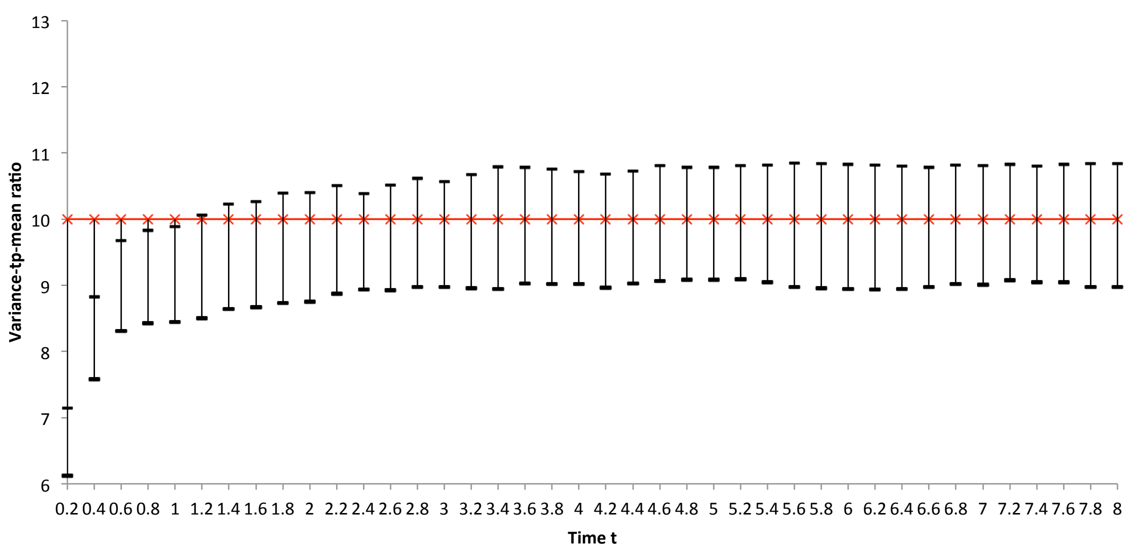

Figure 4.3: CIAT-generated 95% CIs for $C_Q(t)$, $t \in (0, 8]$, in Case 1 with $C = 10$.

Table 4.4: CIAT-generated 95% CI estimators for $\mu(t),\ t \in (0, 8]$, in Case 1 with $C = 1.5$.

time t	0.2	0.4	0.6	0.8	1.0	1.2	1.4	1.6	1.8	2.0
$\widehat{\mu}(t)_{0.975}$	14.074	28.956	46.220	51.764	54.327	66.425	80.827	97.565	103.036	105.600
$\widehat{\mu}(t)$	11.590	25.283	41.401	46.650	49.106	60.646	74.440	90.594	95.875	98.342
$\widehat{\mu}(t)_{0.025}$	9.106	21.609	36.582	41.536	43.886	54.867	68.053	83.622	88.714	91.084
time t	2.2	2.4	2.6	2.8	3.0	3.2	3.4	3.6	3.8	4.0
$\widehat{\mu}(t)_{0.975}$	117.647	131.843	148.543	153.964	156.475	168.426	182.593	199.091	204.415	206.884
$\widehat{\mu}(t)$	109.956	123.735	139.866	145.108	147.557	159.098	172.802	188.866	194.052	196.474
$\widehat{\mu}(t)_{0.025}$	102.265	115.627	131.189	136.253	138.639	149.770	163.011	178.642	183.689	186.064
time t	4.2	4.4	4.6	4.8	5.0	5.2	5.4	5.6	5.8	6.0
$\widehat{\mu}(t)_{0.975}$	218.770	232.872	249.373	254.744	257.222	269.255	283.286	299.629	304.969	307.465
$\widehat{\mu}(t)$	208.070	221.814	237.885	243.111	245.537	257.240	270.976	286.966	292.247	294.680
$\widehat{\mu}(t)_{0.025}$	197.370	210.756	226.397	231.478	233.853	245.226	258.665	274.303	279.524	281.894
time t	6.2	6.4	6.6	6.8	7.0	7.2	7.4	7.6	7.8	8.0
$\widehat{\mu}(t)_{0.975}$	319.273	333.213	349.590	354.833	357.283	369.026	382.999	399.478	404.861	406.866
$\widehat{\mu}(t)$	306.213	319.865	335.862	341.046	343.448	354.966	368.723	384.874	390.152	392.134
$\widehat{\mu}(t)_{0.025}$	293.152	306.517	322.134	327.258	329.612	340.906	354.448	370.270	375.443	377.401

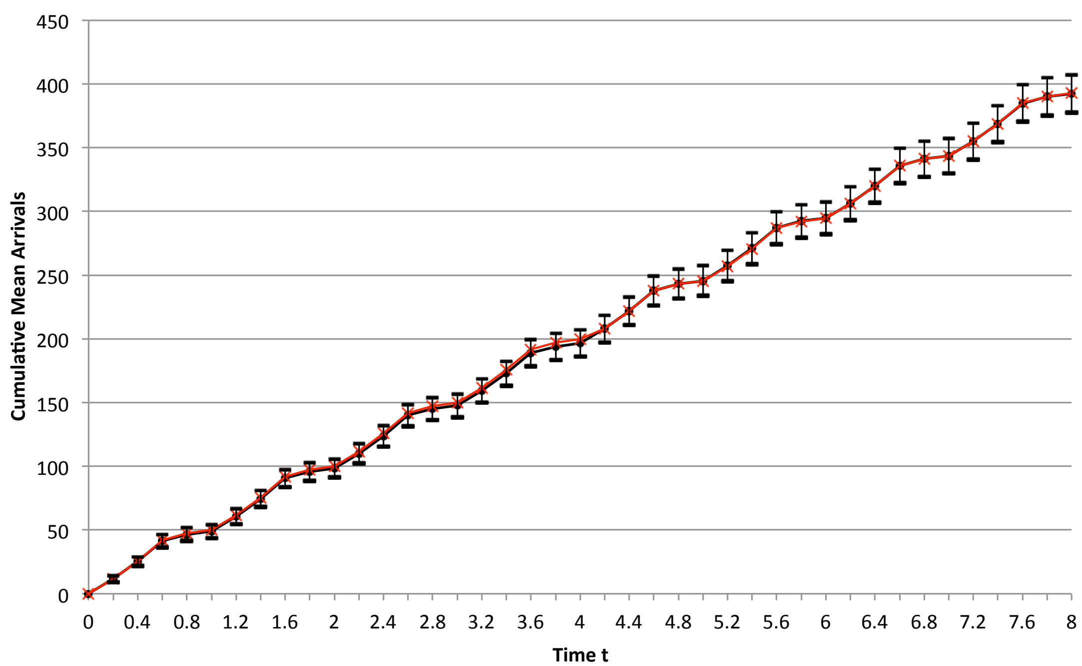

Figure 4.4: CIAT-generated 95% CIs for $\mu(t),\ t \in (0, 8]$, in Case 1 with $C = 1.5$.

Table 4.5: CIAT-generated 95% CI estimators for $C_Q(t)$, $t \in (0, 8]$, in Case 1 with $C = 1.5$.

time t	0.2	0.4	0.6	0.8	1.0	1.2	1.4	1.6	1.8	2.0
$\widehat{C}(t)_{0.975}$	1.565	1.557	1.613	1.613	1.598	1.576	1.573	1.532	1.527	1.530
$\widehat{C}(t)$	1.422	1.422	1.486	1.490	1.480	1.472	1.459	1.424	1.423	1.426
$\widehat{C}(t)_{0.025}$	1.278	1.288	1.360	1.367	1.363	1.368	1.345	1.316	1.319	1.322
time t	2.2	2.4	2.6	2.8	3.0	3.2	3.4	3.6	3.8	4.0
$\widehat{C}(t)_{0.975}$	1.563	1.555	1.574	1.573	1.568	1.595	1.610	1.606	1.614	1.608
$\widehat{C}(t)$	1.442	1.423	1.443	1.452	1.448	1.470	1.486	1.485	1.488	1.483
$\widehat{C}(t)_{0.025}$	1.320	1.291	1.312	1.331	1.328	1.345	1.363	1.363	1.362	1.358
time t	4.2	4.4	4.6	4.8	5.0	5.2	5.4	5.6	5.8	6.0
$\widehat{C}(t)_{0.975}$	1.610	1.618	1.631	1.629	1.625	1.635	1.634	1.616	1.603	1.605
$\widehat{C}(t)$	1.477	1.477	1.486	1.489	1.487	1.500	1.491	1.489	1.478	1.480
$\widehat{C}(t)_{0.025}$	1.344	1.336	1.340	1.349	1.350	1.365	1.348	1.361	1.353	1.355
time t	6.2	6.4	6.6	6.8	7.0	7.2	7.4	7.6	7.8	8.0
$\widehat{C}(t)_{0.975}$	1.618	1.610	1.621	1.614	1.618	1.628	1.616	1.609	1.610	1.603
$\widehat{C}(t)$	1.489	1.488	1.498	1.488	1.488	1.493	1.483	1.484	1.486	1.483
$\widehat{C}(t)_{0.025}$	1.361	1.366	1.376	1.362	1.359	1.358	1.350	1.359	1.363	1.363

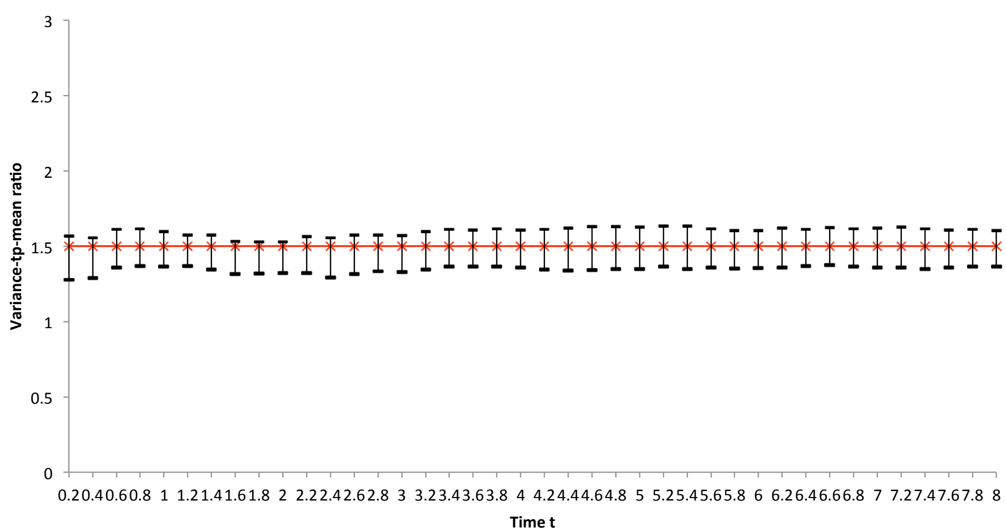

Figure 4.5: CIAT-generated 95% CIs for $C_Q(t)$, $t \in (0, 8]$, in Case 1 with $C = 1.5$.

Table 4.6: CIAT-generated 95% CI estimators for $\mu(t),\ t \in (0, 8]$, in Case 1 with $C = 0.8$.

time t	0.2	0.4	0.6	0.8	1.0	1.2	1.4	1.6	1.8	2.0
$\widehat{\mu}(t)_{0.975}$	13.451	28.144	44.930	50.367	52.925	64.913	79.161	95.773	101.138	103.637
$\widehat{\mu}(t)$	11.571	25.348	41.363	46.581	49.028	60.575	74.348	90.404	95.624	98.048
$\widehat{\mu}(t)_{0.025}$	9.690	22.551	37.796	42.796	45.132	56.237	69.535	85.034	90.109	92.459
time t	2.2	2.4	2.6	2.8	3.0	3.2	3.4	3.6	3.8	4.0
$\widehat{\mu}(t)_{0.975}$	115.521	129.546	146.039	151.345	153.853	165.720	179.811	196.199	201.497	203.987
$\widehat{\mu}(t)$	109.582	123.269	139.373	144.578	147.028	158.625	172.425	188.531	193.750	196.191
$\widehat{\mu}(t)_{0.025}$	103.642	116.993	132.707	137.811	140.204	151.531	165.038	180.863	186.002	188.394
time t	4.2	4.4	4.6	4.8	5.0	5.2	5.4	5.6	5.8	6.0
$\widehat{\mu}(t)_{0.975}$	215.783	229.746	246.255	251.557	254.033	265.844	279.870	296.293	301.521	304.001
$\widehat{\mu}(t)$	207.717	221.478	237.683	242.886	245.322	256.952	270.765	286.890	292.047	294.494
$\widehat{\mu}(t)_{0.025}$	199.650	213.210	229.111	234.215	236.611	248.059	261.660	277.488	282.573	284.988
time t	6.2	6.4	6.6	6.8	7.0	7.2	7.4	7.6	7.8	8.0
$\widehat{\mu}(t)_{0.975}$	315.674	329.669	345.980	351.276	353.723	365.430	379.404	395.863	401.191	403.169
$\widehat{\mu}(t)$	306.024	319.809	335.895	341.086	343.518	355.025	368.764	384.978	390.213	392.176
$\widehat{\mu}(t)_{0.025}$	296.374	309.949	325.810	330.895	333.314	344.620	358.123	374.092	379.234	381.184

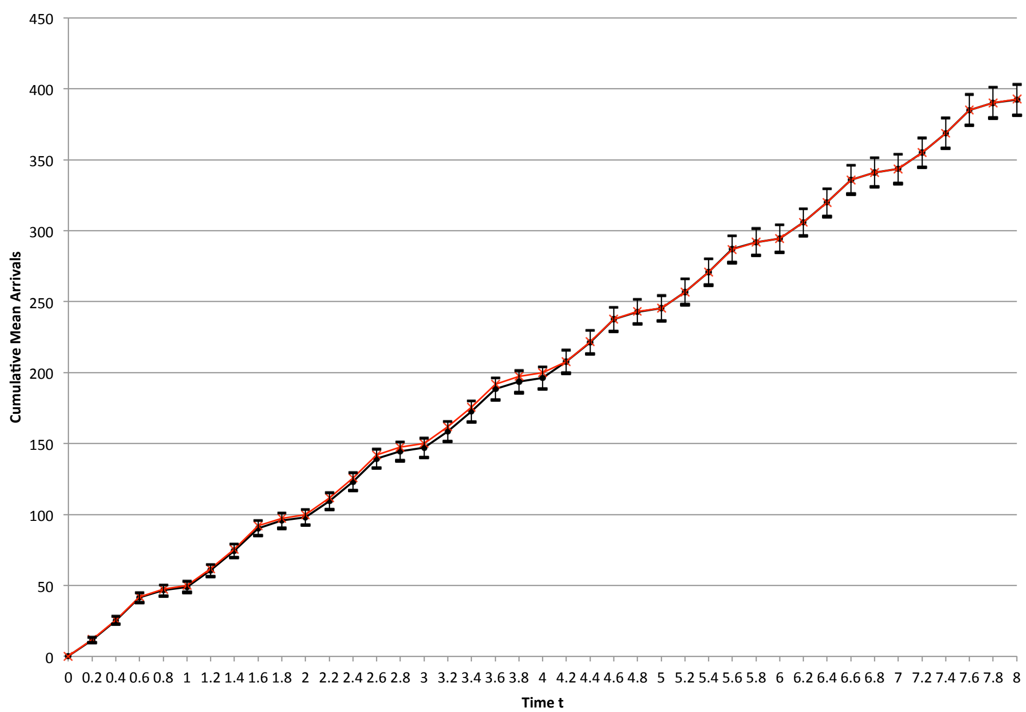

Figure 4.6: CIAT-generated 95% CIs for $\mu(t),\ t \in (0, 8]$, in Case 1 with $C = 0.8$.

Table 4.7: CIAT-generated 95% CI estimators for $C_Q(t)$, $t \in (0, 8]$, in Case 1 with $C = 0.8$.

time t	0.2	0.4	0.6	0.8	1.0	1.2	1.4	1.6	1.8	2.0
$\widehat{C}(t)_{0.975}$	0.860	0.865	0.864	0.866	0.867	0.863	0.871	0.892	0.893	0.891
$\widehat{C}(t)$	0.798	0.806	0.804	0.804	0.809	0.811	0.814	0.833	0.831	0.832
$\widehat{C}(t)_{0.025}$	0.736	0.747	0.743	0.742	0.750	0.759	0.757	0.774	0.769	0.773
time t	2.2	2.4	2.6	2.8	3.0	3.2	3.4	3.6	3.8	4.0
$\widehat{C}(t)_{0.975}$	0.908	0.906	0.910	0.903	0.904	0.904	0.899	0.893	0.882	0.880
$\widehat{C}(t)$	0.841	0.836	0.834	0.829	0.829	0.830	0.828	0.816	0.811	0.810
$\widehat{C}(t)_{0.025}$	0.774	0.765	0.758	0.754	0.753	0.756	0.756	0.739	0.739	0.740
time t	4.2	4.4	4.6	4.8	5.0	5.2	5.4	5.6	5.8	6.0
$\widehat{C}(t)_{0.975}$	0.893	0.879	0.881	0.879	0.881	0.878	0.877	0.879	0.879	0.879
$\widehat{C}(t)$	0.820	0.808	0.809	0.810	0.809	0.805	0.801	0.806	0.804	0.803
$\widehat{C}(t)_{0.025}$	0.746	0.736	0.737	0.740	0.738	0.732	0.726	0.734	0.730	0.728
time t	6.2	6.4	6.6	6.8	7.0	7.2	7.4	7.6	7.8	8.0
$\widehat{C}(t)_{0.975}$	0.871	0.867	0.860	0.864	0.859	0.866	0.871	0.868	0.874	0.873
$\widehat{C}(t)$	0.797	0.795	0.792	0.796	0.793	0.798	0.803	0.804	0.808	0.806
$\widehat{C}(t)_{0.025}$	0.722	0.724	0.724	0.728	0.726	0.729	0.734	0.741	0.741	0.738

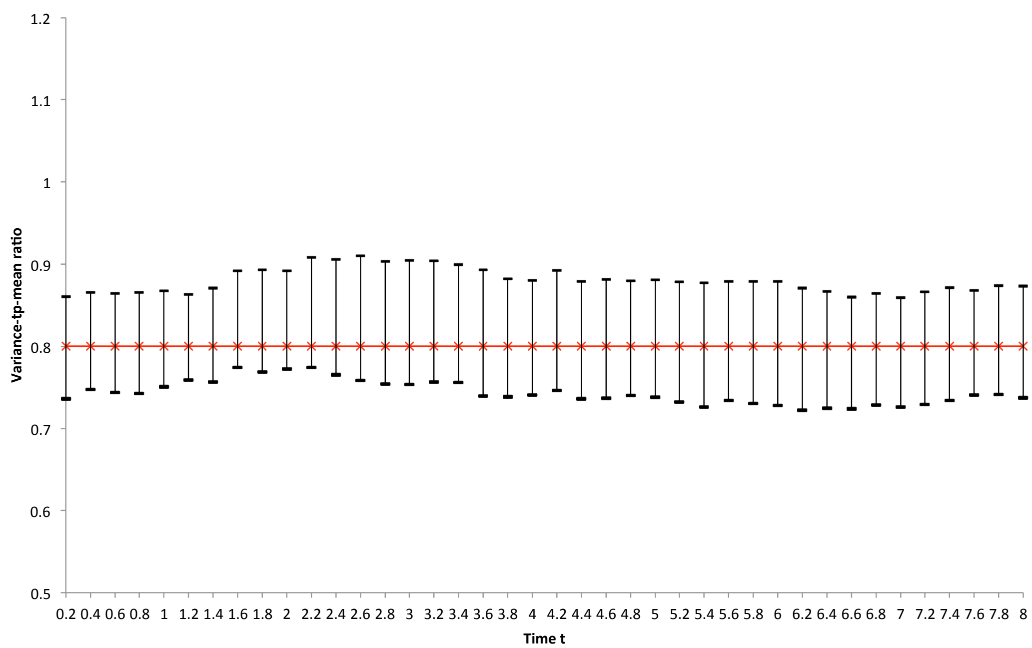

Figure 4.7: CIAT-generated 95% CIs for $C_Q(t)$, $t \in (0, 8]$, in Case 1 with $C = 0.8$.

Table 4.8: CIAT-generated 95% CI estimators for $\mu(t),\ t \in (0, 8]$, in Case 1 with $C = 0.2$.

time t	0.2	0.4	0.6	0.8	1.0	1.2	1.4	1.6	1.8	2.0
$\widehat{\mu}(t)_{0.975}$	12.610	26.796	43.354	48.762	51.261	63.089	77.061	93.411	98.769	101.283
$\widehat{\mu}(t)$	11.510	25.264	41.392	46.613	49.043	60.599	74.349	90.446	95.697	98.144
$\widehat{\mu}(t)_{0.025}$	10.410	23.732	39.430	44.465	46.824	58.109	71.636	87.482	92.626	95.005

time t	2.2	2.4	2.6	2.8	3.0	3.2	3.4	3.6	3.8	4.0
$\widehat{\mu}(t)_{0.975}$	113.036	126.961	143.265	148.599	151.064	162.725	176.625	192.917	198.223	200.694
$\widehat{\mu}(t)$	109.701	123.437	139.516	144.748	147.175	158.701	172.476	188.573	193.800	196.228
$\widehat{\mu}(t)_{0.025}$	106.366	119.913	135.767	140.898	143.285	154.676	168.327	184.228	189.376	191.762

time t	4.2	4.4	4.6	4.8	5.0	5.2	5.4	5.6	5.8	6.0
$\widehat{\mu}(t)_{0.975}$	212.414	226.332	242.557	247.898	250.346	262.045	275.904	292.088	297.388	299.842
$\widehat{\mu}(t)$	207.828	221.595	237.678	242.924	245.346	256.909	270.670	286.688	291.902	294.334
$\widehat{\mu}(t)_{0.025}$	203.243	216.859	232.800	237.950	240.345	251.772	265.436	281.287	286.417	288.826

time t	6.2	6.4	6.6	6.8	7.0	7.2	7.4	7.6	7.8	8.0
$\widehat{\mu}(t)_{0.975}$	311.467	325.351	341.506	346.754	349.218	360.853	374.720	390.906	396.178	398.154
$\widehat{\mu}(t)$	305.856	319.660	335.694	340.882	343.321	354.870	368.614	384.709	389.957	391.902
$\widehat{\mu}(t)_{0.025}$	300.244	313.969	329.882	335.010	337.425	348.886	362.507	378.511	383.736	385.649

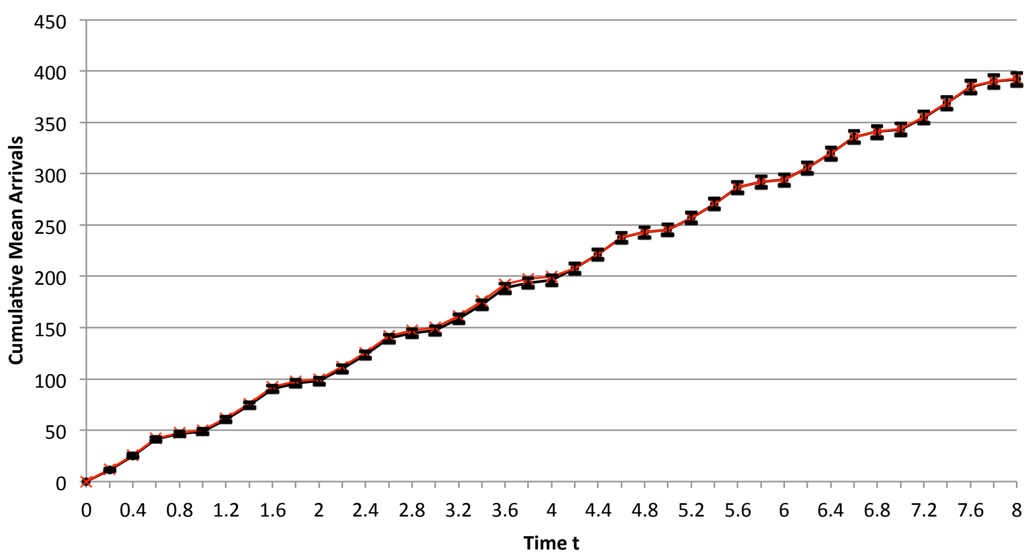

Figure 4.8: CIAT-generated 95% CIs for $\mu(t),\ t \in (0, 8]$, in Case 1 with $C = 0.2$.

Table 4.9: CIAT-generated 95% CI estimators for $C_Q(t)$, $t \in (0, 8]$, in Case 1 with $C = 0.2$.

time t	0.2	0.4	0.6	0.8	1.0	1.2	1.4	1.6	1.8	2.0
$\widehat{C}(t)_{0.975}$	0.229	0.221	0.217	0.219	0.217	0.221	0.219	0.218	0.220	0.222
$\widehat{C}(t)$	0.209	0.202	0.202	0.204	0.203	0.206	0.206	0.205	0.205	0.207
$\widehat{C}(t)_{0.025}$	0.189	0.184	0.187	0.189	0.188	0.191	0.192	0.191	0.190	0.192
time t	2.2	2.4	2.6	2.8	3.0	3.2	3.4	3.6	3.8	4.0
$\widehat{C}(t)_{0.975}$	0.222	0.224	0.228	0.229	0.231	0.228	0.226	0.227	0.227	0.228
$\widehat{C}(t)$	0.208	0.208	0.210	0.211	0.212	0.209	0.207	0.209	0.209	0.210
$\widehat{C}(t)_{0.025}$	0.193	0.192	0.192	0.193	0.194	0.191	0.188	0.191	0.191	0.191
time t	4.2	4.4	4.6	4.8	5.0	5.2	5.4	5.6	5.8	6.0
$\widehat{C}(t)_{0.975}$	0.227	0.227	0.224	0.225	0.226	0.228	0.226	0.228	0.228	0.228
$\widehat{C}(t)$	0.208	0.209	0.207	0.208	0.208	0.209	0.207	0.209	0.210	0.209
$\widehat{C}(t)_{0.025}$	0.189	0.191	0.189	0.190	0.190	0.190	0.188	0.190	0.192	0.191
time t	6.2	6.4	6.6	6.8	7.0	7.2	7.4	7.6	7.8	8.0
$\widehat{C}(t)_{0.975}$	0.226	0.221	0.222	0.222	0.223	0.223	0.226	0.226	0.224	0.224
$\widehat{C}(t)$	0.208	0.204	0.204	0.205	0.205	0.206	0.208	0.208	0.206	0.206
$\widehat{C}(t)_{0.025}$	0.190	0.187	0.186	0.187	0.187	0.189	0.190	0.189	0.188	0.187

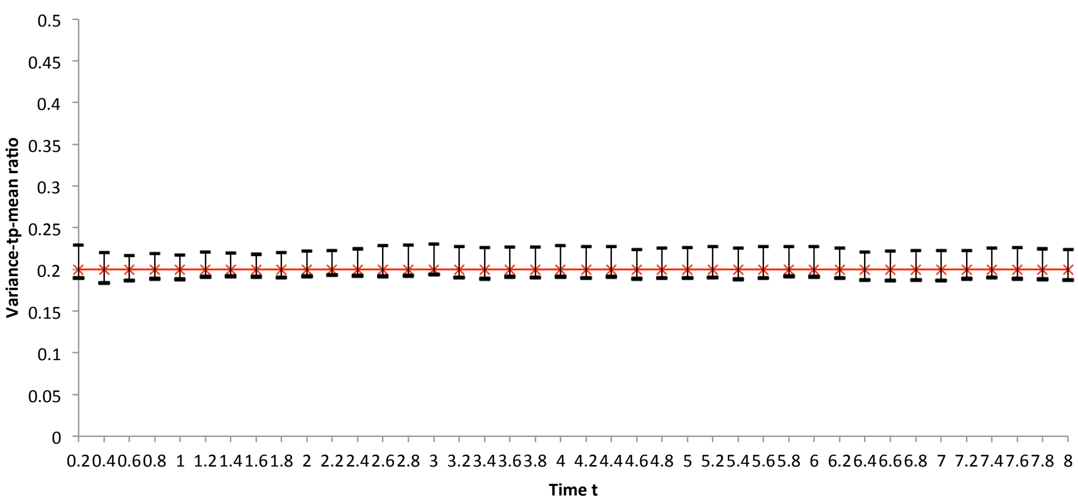

Figure 4.9: CIAT-generated 95% CIs for $C_Q(t)$, $t \in (0, 8]$, in Case 1 with $C = 0.2$.

Figure 4.1 indicates that the algorithm in Figure 3.1 is able to generate a step function $\widetilde{\lambda}_Q(t)$ that satisfies $\widetilde{\lambda}_Q(t) > 0$ and $\widetilde{\lambda}_Q(t)$ majorizes and closely approximates the designated rate function $\lambda(t)$ of Case 1, and that also has an invertible piecewise linear mean-value function $\widetilde{\mu}_Q(t) = \int_0^t \widetilde{\lambda}_Q(u)du$ for all $t \in [0, 8]$.

Table 4.2 and Figure 4.2 show that the mean-value function of the CIAT-generated arrival process mimics the trend and numerical values of the desired mean-value function closely for Case 1 with $C = 10$. Similar results were obtained for the $C = 1.5$, 0.8, and 0.2.

Table 4.3 and Figure 4.3 indicate that CIAT can generate an NNPP with the desired asymptotic dispersion ratio $C = 10$; and for $t \geq 1.2$, the 95% CIs for $C_Q(t)$ include the desired value 10. In other words, it takes 1.2 seconds to converge, suggesting a fast convergence of CIAT procedure. Table 4.5 and Figure 4.5 indicate that CIAT can generate an NNPP with the desired asymptotic dispersion ratio $C = 1.5$; and for $t \geq 0.2$, the 95% CIs for $C_Q(t)$ include the desired value 1.5. Equivalently, it takes less than 0.2 seconds to converge, suggesting a significantly fast convergence of CIAT procedure. Table 4.7 and Figure 4.7 indicate that CIAT can generate an NNPP with the desired asymptotic dispersion ratio $C = 0.8$; and for $t \geq 0.2$, the 95% CIs for $C_Q(t)$ include the desired value 0.8, suggesting a significantly fast convergence of CIAT as well. Table 4.9 and Figure 4.9 indicate that CIAT can generate an NNPP with the desired asymptotic dispersion ratio $C = 0.2$; and for $t \geq 0.2$, the 95% CIs for $C_Q(t)$ include the desired value 0.2, which also suggests a significantly convergence of CIAT procedure.

The numerical results and plots also indicate that the estimated dispersion ratio $\widehat{C}_Q(t)$ approaches the desired value C from blew for scenarios in which $C > 1$; and $\widehat{C}_Q(t)$ approaches the desired value C from above for scenarios in which $0 < C < 1$.

4.3.2 Presentation and Discussion for CIAT-Generated NNPPs in Case 2

In Case 2, Figure 4.10 shows the desired rate function $\lambda(t)$ and the corresponding step rate function $\widetilde{\lambda}_Q(t)$ for $t \in [0, 8]$. For Case 2 and for $C = 10$, 1.5, 0.8, and 0.2, we also computed 95% CI estimators of $\mu(t)$ and 95% CI estimators of $C_Q(t)$ for $0 \leq t \leq 8$. The results of Case 2 are similar to those of Case 1. We presented the results for $C = 10$ and $C = 0.8$ in Figures 4.11–4.14, and Tables 4.10–4.13. The 95% CI estimators of $\mu(t)$ and $C_Q(t)$ for $C = 1.5$ and $C = 0.2$ are listed in Figures C.1–C.4 and Tables C.1–C.4 of Appendix C.

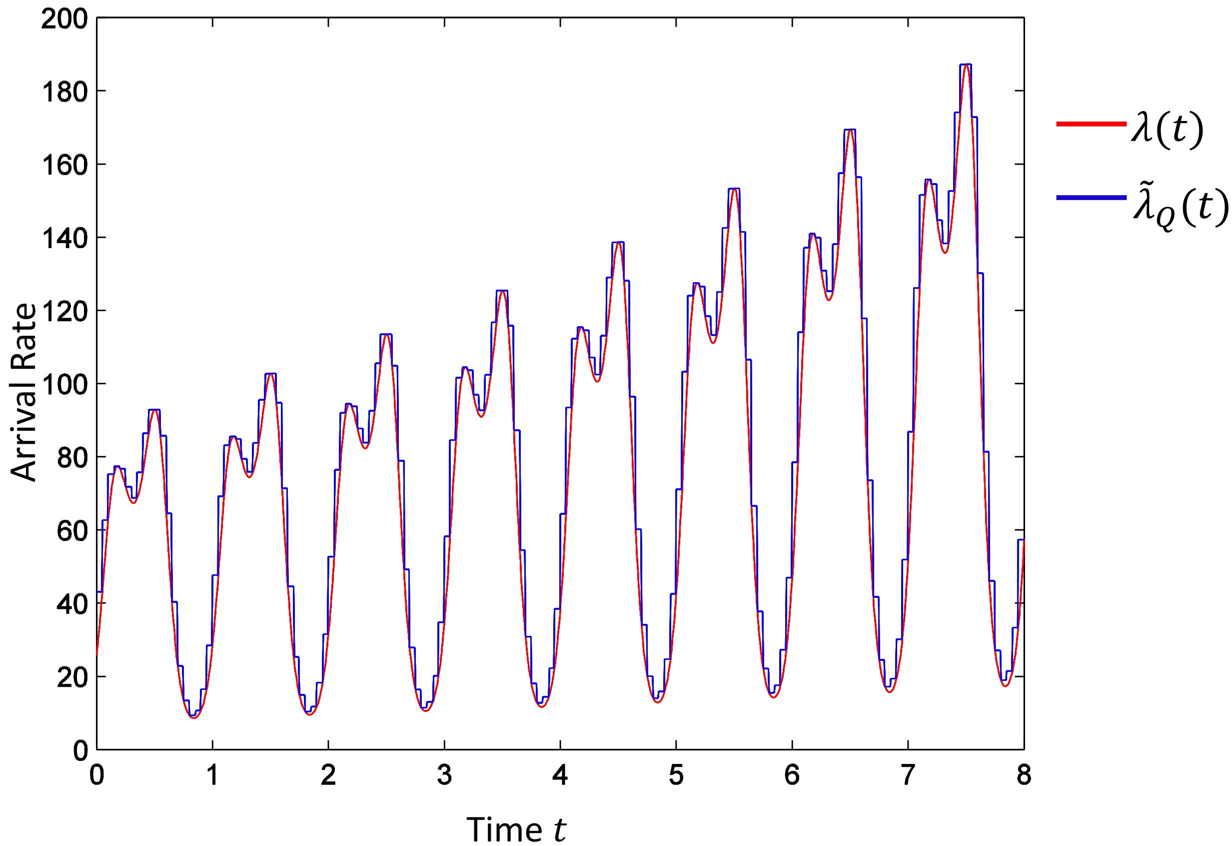

Figure 4.10: Step rate function $\widetilde{\lambda}_Q(t)$ that majorizes $\lambda(t)$ in Case 2.

Table 4.10: CIAT-generated 95% CI estimators for $\mu(t),\ t \in (0, 8]$, in Case 2 with $C = 10$.

time t	0.2	0.4	0.6	0.8	1.0	1.2	1.4	1.6	1.8	2.0
$\widehat{\mu}(t)_{0.975}$	16.774	34.543	54.466	60.680	63.673	78.023	95.741	116.452	123.099	126.226
$\widehat{\mu}(t)$	11.614	25.687	42.631	48.134	50.805	63.562	79.209	97.940	104.053	106.975
$\widehat{\mu}(t)_{0.025}$	6.455	16.831	30.795	35.588	37.937	49.101	62.678	79.429	85.007	87.724
time t	2.2	2.4	2.6	2.8	3.0	3.2	3.4	3.6	3.8	4.0
$\widehat{\mu}(t)_{0.975}$	141.529	160.126	182.400	189.662	193.171	210.278	230.740	254.956	262.718	266.373
$\widehat{\mu}(t)$	121.149	138.263	158.993	165.751	169.033	185.039	204.315	227.030	234.460	237.964
$\widehat{\mu}(t)_{0.025}$	100.770	116.401	135.586	141.839	144.894	159.800	177.890	199.104	206.203	209.555
time t	4.2	4.4	4.6	4.8	5.0	5.2	5.4	5.6	5.8	6.0
$\widehat{\mu}(t)_{0.975}$	284.510	306.780	333.435	342.138	346.299	366.549	391.077	420.224	430.060	434.650
$\widehat{\mu}(t)$	255.126	276.103	301.232	309.495	313.484	332.816	356.206	384.117	393.492	397.929
$\widehat{\mu}(t)_{0.025}$	225.743	245.426	269.029	276.853	280.668	299.084	321.335	348.009	356.923	361.207
time t	6.2	6.4	6.6	6.8	7.0	7.2	7.4	7.6	7.8	8.0
$\widehat{\mu}(t)_{0.975}$	456.797	483.805	515.955	526.569	531.658	556.192	585.622	620.728	632.373	637.009
$\widehat{\mu}(t)$	419.214	445.004	475.750	485.990	490.870	514.392	542.852	576.531	587.714	592.164
$\widehat{\mu}(t)_{0.025}$	381.631	406.203	435.545	445.410	450.082	472.592	500.082	532.335	543.056	547.319

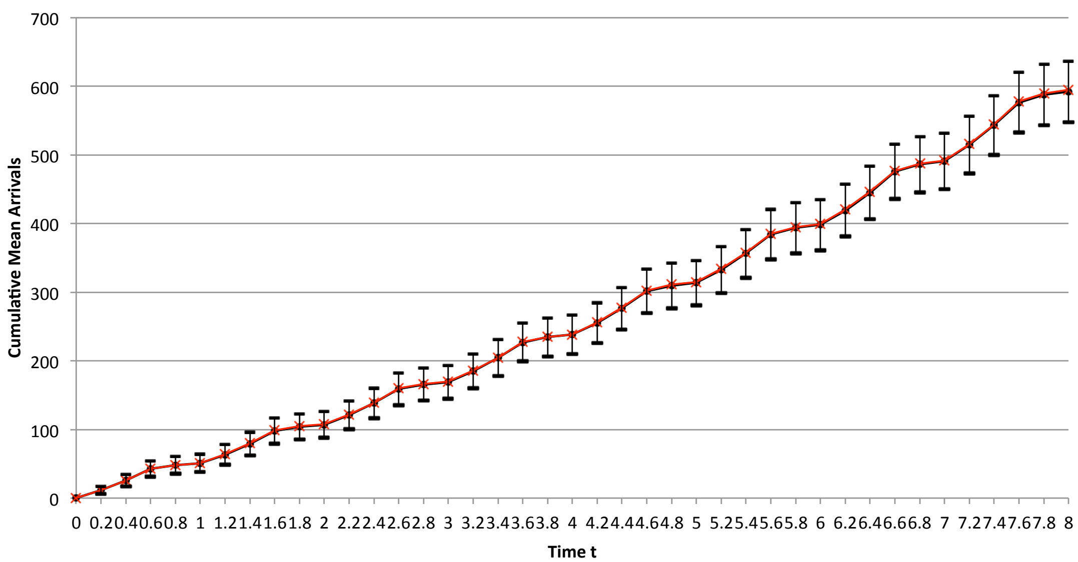

Figure 4.11: CIAT-generated 95% CIs for $\mu(t),\ t \in (0, 8]$, in Case 2 with $C = 10$.

Table 4.11: CIAT-generated 95% CI estimators for $C_Q(t)$, $t \in (0, 8]$, in Case 2 with $C = 10$.

time t	0.2	0.4	0.6	0.8	1.0	1.2	1.4	1.6	1.8	2.0
$\widehat{C}(t)_{0.975}$	6.890	8.953	9.616	9.682	9.739	10.053	10.404	10.469	10.452	10.404
$\widehat{C}(t)$	6.470	8.317	8.919	9.001	9.046	9.305	9.646	9.715	9.719	9.689
$\widehat{C}(t)_{0.025}$	6.049	7.681	8.223	8.320	8.353	8.557	8.888	8.960	8.985	8.975
time t	2.2	2.4	2.6	2.8	3.0	3.2	3.4	3.6	3.8	4.0
$\widehat{C}(t)_{0.975}$	10.351	10.451	10.551	10.622	10.619	10.706	10.590	10.604	10.495	10.480
$\widehat{C}(t)$	9.654	9.694	9.648	9.687	9.694	9.736	9.632	9.638	9.581	9.563
$\widehat{C}(t)_{0.025}$	8.957	8.936	8.744	8.752	8.770	8.766	8.674	8.673	8.667	8.646
time t	4.2	4.4	4.6	4.8	5.0	5.2	5.4	5.6	5.8	6.0
$\widehat{C}(t)_{0.975}$	10.453	10.483	10.646	10.679	10.683	10.606	10.527	10.534	10.508	10.497
$\widehat{C}(t)$	9.586	9.622	9.699	9.728	9.719	9.703	9.649	9.585	9.605	9.599
$\widehat{C}(t)_{0.025}$	8.718	8.761	8.751	8.777	8.754	8.801	8.772	8.637	8.701	8.701
time t	6.2	6.4	6.6	6.8	7.0	7.2	7.4	7.6	7.8	8.0
$\widehat{C}(t)_{0.975}$	10.414	10.411	10.427	10.381	10.379	10.394	10.365	10.389	10.471	10.488
$\widehat{C}(t)$	9.561	9.567	9.585	9.569	9.577	9.606	9.515	9.530	9.566	9.586
$\widehat{C}(t)_{0.025}$	8.707	8.722	8.744	8.756	8.776	8.818	8.665	8.671	8.661	8.684

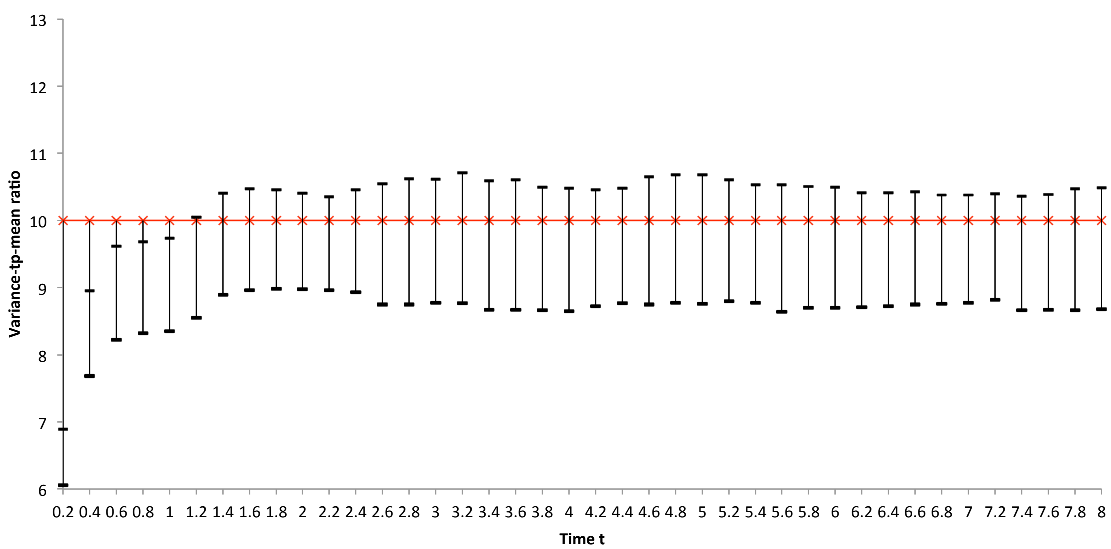

Figure 4.12: CIAT-generated 95% CIs for $C_Q(t)$, $t \in (0, 8]$, in Case 2 with $C = 10$.

Table 4.12: CIAT-generated 95% CI estimators for $\mu(t),\ t \in (0, 8]$, in Case 2 with $C = 0.8$.

time t	0.2	0.4	0.6	0.8	1.0	1.2	1.4	1.6	1.8	2.0
$\widehat{\mu}(t)_{0.975}$	13.612	28.736	46.507	52.331	55.117	68.620	84.697	103.873	110.296	113.323
$\widehat{\mu}(t)$	11.687	25.886	42.868	48.443	51.101	64.051	79.643	98.279	104.514	107.466
$\widehat{\mu}(t)_{0.025}$	9.761	23.035	39.229	44.554	47.084	59.481	74.588	92.685	98.732	101.609
time t	2.2	2.4	2.6	2.8	3.0	3.2	3.4	3.6	3.8	4.0
$\widehat{\mu}(t)_{0.975}$	128.056	145.854	166.983	173.961	177.365	193.473	213.128	236.303	243.958	247.608
$\widehat{\mu}(t)$	121.795	139.135	159.801	166.614	169.925	185.722	204.985	227.742	235.262	238.842
$\widehat{\mu}(t)_{0.025}$	115.533	132.417	152.619	159.267	162.485	177.970	196.841	219.180	226.566	230.076
time t	4.2	4.4	4.6	4.8	5.0	5.2	5.4	5.6	5.8	6.0
$\widehat{\mu}(t)_{0.975}$	265.388	286.819	312.343	320.781	324.815	344.547	368.303	396.509	405.946	410.409
$\widehat{\mu}(t)$	256.256	277.365	302.546	310.880	314.864	334.218	357.592	385.403	394.746	399.142
$\widehat{\mu}(t)_{0.025}$	247.124	267.910	292.748	300.979	304.914	323.889	346.882	374.297	383.545	387.874
time t	6.2	6.4	6.6	6.8	7.0	7.2	7.4	7.6	7.8	8.0
$\widehat{\mu}(t)_{0.975}$	431.996	458.289	489.655	499.994	504.947	528.769	557.613	592.279	603.721	608.019
$\widehat{\mu}(t)$	420.472	446.403	477.305	487.573	492.471	516.024	544.609	578.864	590.180	594.447
$\widehat{\mu}(t)_{0.025}$	408.947	434.516	464.954	475.152	479.996	503.278	531.605	565.449	576.638	580.875

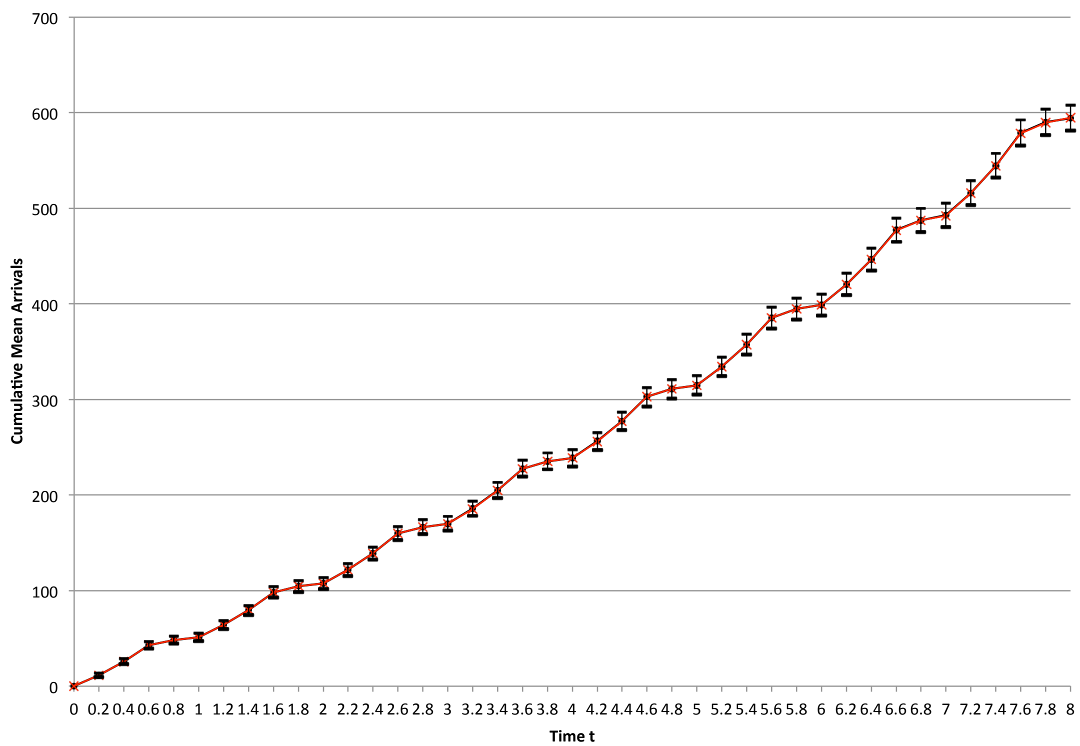

Figure 4.13: CIAT-generated 95% CIs for $\mu(t),\ t \in (0, 8]$, in Case 2 with $C = 0.8$.

Table 4.13: CIAT-generated 95% CI estimators for $C_Q(t)$, $t \in (0, 8]$, in Case 2 with $C = 0.8$.

time t	0.2	0.4	0.6	0.8	1.0	1.2	1.4	1.6	1.8	2.0
$\widehat{C}(t)_{0.025}$	0.863	0.838	0.854	0.866	0.891	0.878	0.890	0.891	0.879	0.882
$\widehat{C}(t)$	0.806	0.775	0.793	0.807	0.828	0.814	0.826	0.818	0.813	0.813
$\widehat{C}(t)_{0.975}$	0.749	0.713	0.732	0.747	0.765	0.750	0.763	0.744	0.747	0.744
time t	2.2	2.4	2.6	2.8	3.0	3.2	3.4	3.6	3.8	4.0
$\widehat{C}(t)_{0.025}$	0.885	0.886	0.878	0.881	0.882	0.892	0.895	0.894	0.901	0.905
$\widehat{C}(t)$	0.822	0.822	0.816	0.817	0.819	0.822	0.821	0.819	0.822	0.822
$\widehat{C}(t)_{0.975}$	0.758	0.758	0.754	0.753	0.755	0.753	0.748	0.745	0.742	0.739
time t	4.2	4.4	4.6	4.8	5.0	5.2	5.4	5.6	5.8	6.0
$\widehat{C}(t)_{0.025}$	0.908	0.903	0.889	0.893	0.891	0.893	0.898	0.895	0.891	0.892
$\widehat{C}(t)$	0.824	0.818	0.812	0.816	0.815	0.818	0.820	0.821	0.818	0.818
$\widehat{C}(t)_{0.975}$	0.739	0.732	0.735	0.738	0.740	0.742	0.743	0.747	0.745	0.744
time t	6.2	6.4	6.6	6.8	7.0	7.2	7.4	7.6	7.8	8.0
$\widehat{C}(t)_{0.025}$	0.886	0.882	0.875	0.876	0.880	0.874	0.876	0.879	0.880	0.886
$\widehat{C}(t)$	0.815	0.812	0.807	0.811	0.812	0.807	0.805	0.803	0.804	0.808
$\widehat{C}(t)_{0.975}$	0.745	0.742	0.739	0.745	0.744	0.739	0.733	0.727	0.727	0.730

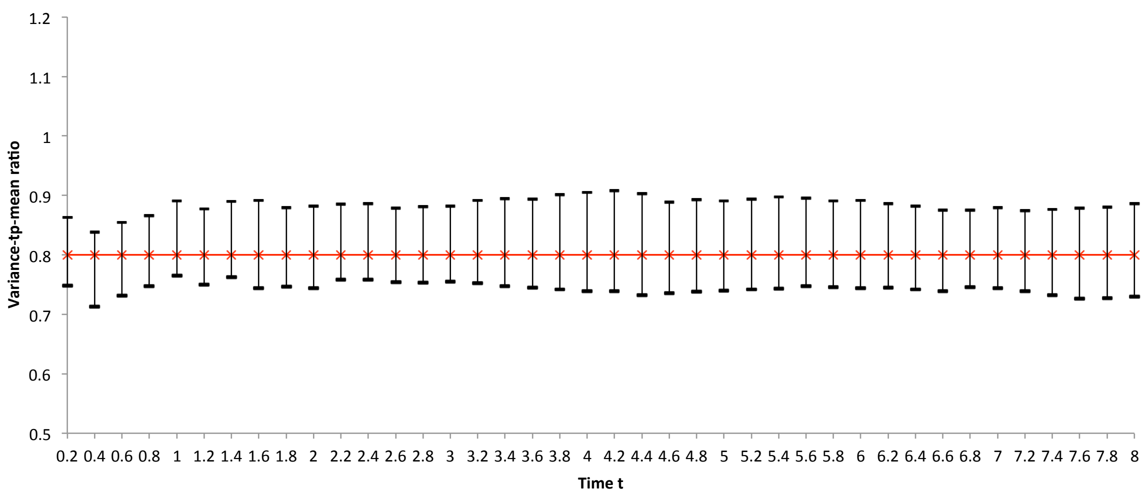

Figure 4.14: CIAT-generated 95% CIs for $C_Q(t)$, $t \in (0, 8]$, in Case 2 with $C = 0.8$.

Figure 4.10 indicates that the algorithm in Figure 3.1 is able to generate a step function $\widetilde{\lambda}_Q(t)$ that satisfies $\widetilde{\lambda}_Q(t) > 0$ and $\widetilde{\lambda}_Q(t)$ majorizes and closely approximates the designated rate function $\lambda(t)$ of Case 2, and that also has an invertible piecewise linear mean-value function $\widetilde{\mu}_Q(t) = \int_0^t \widetilde{\lambda}_Q(u)du$ for all $t \in [0, 8]$.

Table 4.10 and Figure 4.11 show that the mean-value function of the CIAT-generated arrival process mimics the trend and numerical values of the desired mean-value function closely for Case 2 with $C = 10$. Similar results were obtained for $C = 1.5$, 0.8, and 0.2.

Table 4.11 and Figure 4.12 indicate that CIAT can generate an NNPP with the desired asymptotic dispersion ratio $C = 10$; and for $t \geq 1.2$, the 95% CIs for $C_Q(t)$ include the desired value 10. In other words, it takes 1.2 seconds to converge, suggesting a fast convergence of CIAT. Table C.2 and Figure 4.14 indicate that CIAT can generate an NNPP with the desired asymptotic dispersion ratio $C = 0.8$; and for $t \geq 0.2$, the 95% CIs for $C_Q(t)$ include the desired value 0.8, suggesting a significantly fast convergence of CIAT. For scenarios $C = 1.5$ and $C = 0.2$, we also saw that CIAT can generate an NNPP with the desired asymptotic dispersion ratio; and under both scenarios, for $t \geq 0.2$, the 95% CIs for $C_Q(t)$ include the corresponding desired value. It indicates that it takes less than 0.2 seconds to converge for both scenarios. Please see Figures C.1–C.4 and Tables C.1–C.4 for details.

Similarly to Case 1, the numerical results and plots of Case 2 indicate that for Case 2 the estimated dispersion ratio $\widehat{C}_Q(t)$ approaches the desired value C from below for scenarios in which $C > 1$; and $\widehat{C}(t)$ approaches the desired value C from above for scenarios in which $0 < C < 1$.

4.3.3 Presentation and Discussion for CIAT-Generated NNPPs in Case 3

In Case 3, Figure 4.15 shows the desired rate function $\lambda(t)$ and the corresponding step rate function $\widetilde{\lambda}_Q(t)$ for $t \in [0, 8]$. For Case 3 and for $C = 10$, 1.5, 0.8, and 0.2, we also computed 95% CI estimators of $\mu(t)$ and 95% CI estimators of $C_Q(t)$ for $0 \leq t \leq 8$. The results of Case 3 are similar to those of Cases 1 and 2. We presented the results for $C = 10$ and $C = 0.8$ in Figures 4.16–4.19 and Tables 4.14–4.17. The 95% CI estimators of $\mu(t)$ and $C_Q(t)$ for $C = 1.5$ and $C = 0.2$ are listed in Figures C.5-C.8 and Tables C.5-C.8 of Appendix C.

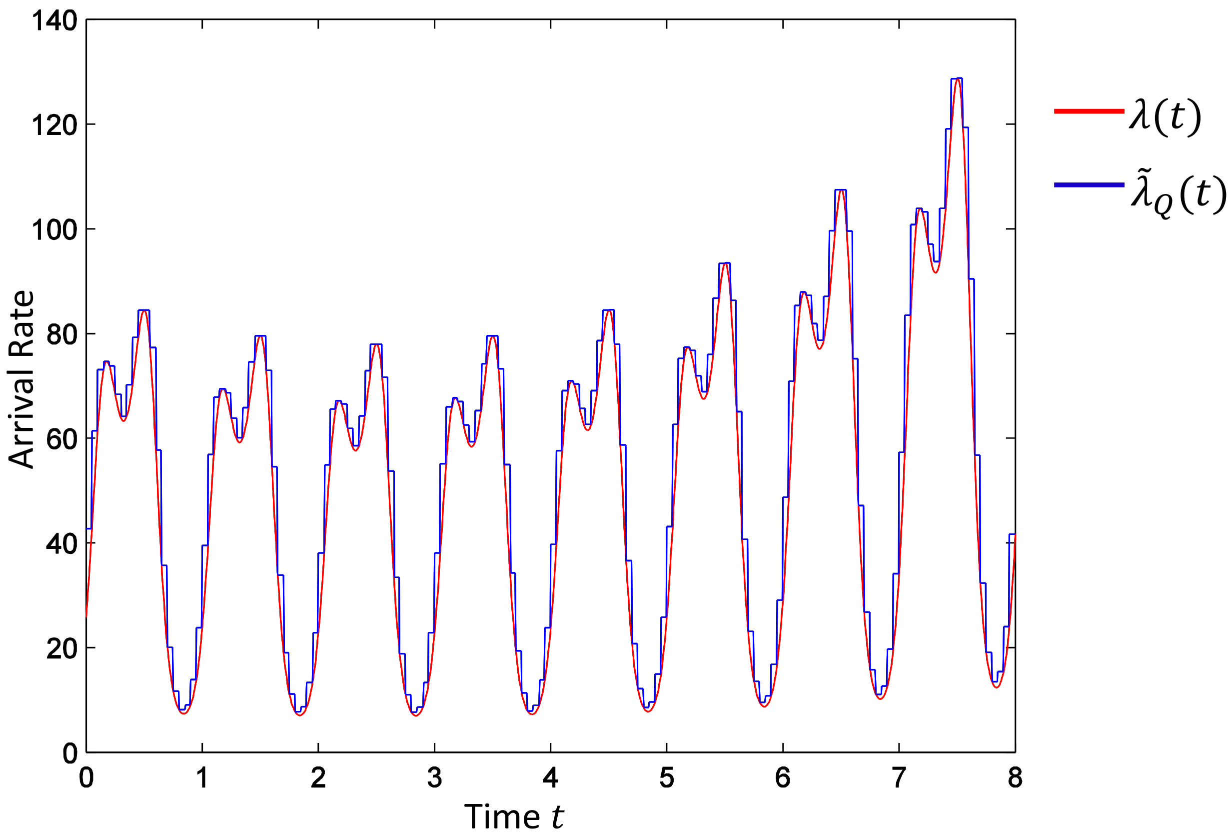

Figure 4.15: Step rate function $\tilde{\lambda}_Q(t)$ that majorizes $\lambda(t)$ in Case 3.

Table 4.14: CIAT-generated 95% CI estimators for $\mu(t),\ t \in (0, 8]$, in Case 3 with $C = 10$.

time t	0.2	0.4	0.6	0.8	1.0	1.2	1.4	1.6	1.8	2.0
$\widehat{\mu}(t)_{0.975}$	16.742	33.611	51.555	57.124	59.674	71.595	85.644	101.964	107.358	109.846
$\widehat{\mu}(t)$	11.279	24.595	39.670	44.507	46.720	57.243	69.675	84.558	89.256	91.440
$\widehat{\mu}(t)_{0.025}$	5.815	15.578	27.785	31.889	33.765	42.891	53.706	67.153	71.154	73.033
time t	2.2	2.4	2.6	2.8	3.0	3.2	3.4	3.6	3.8	4.0
$\widehat{\mu}(t)_{0.975}$	120.387	133.420	148.545	153.777	156.256	168.313	181.433	196.789	202.011	204.366
$\widehat{\mu}(t)$	101.592	113.845	128.194	132.788	134.958	145.209	157.481	171.947	176.765	178.989
$\widehat{\mu}(t)_{0.025}$	82.796	94.269	107.843	111.799	113.660	122.106	133.528	147.106	151.518	153.612
time t	4.2	4.4	4.6	4.8	5.0	5.2	5.4	5.6	5.8	6.0
$\widehat{\mu}(t)_{0.975}$	215.982	230.177	246.692	252.120	254.655	267.142	282.185	299.866	306.254	309.527
$\widehat{\mu}(t)$	189.783	202.800	218.146	223.171	225.609	237.247	251.298	268.380	274.151	276.966
$\widehat{\mu}(t)_{0.025}$	163.583	175.422	189.600	194.221	196.562	207.353	220.410	236.893	242.048	244.405
time t	6.2	6.4	6.6	6.8	7.0	7.2	7.4	7.6	7.8	8.0
$\widehat{\mu}(t)_{0.975}$	323.819	340.153	360.654	367.542	371.069	388.371	409.483	432.988	440.947	444.309
$\widehat{\mu}(t)$	290.228	306.139	325.246	331.701	334.800	350.446	369.664	392.680	400.474	403.784
$\widehat{\mu}(t)_{0.025}$	256.637	272.125	289.838	295.859	298.531	312.520	329.846	352.372	360.000	363.258

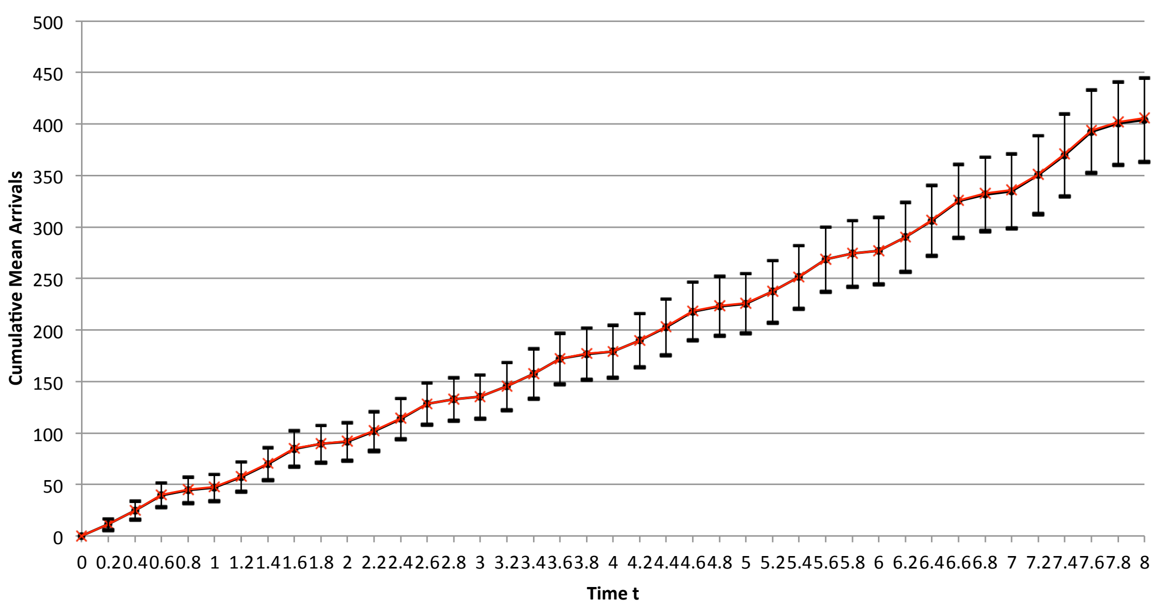

Figure 4.16: CIAT-generated 95% CIs for $\mu(t),\ t \in (0, 8]$, in Case 3 with $C = 10$.

Table 4.15: CIAT-generated 95% CI estimators for $C_Q(t)$, $t \in (0, 8]$, in Case 3 with $C = 10$.

time t	0.2	0.4	0.6	0.8	1.0	1.2	1.4	1.6	1.8	2.0
$\widehat{C}(t)_{0.975}$	6.799	8.759	9.462	9.652	9.680	9.719	9.787	9.995	10.064	10.089
$\widehat{C}(t)$	6.4741	8.311	9.017	9.193	9.217	9.292	9.328	9.386	9.409	9.422
$\widehat{C}(t)_{0.025}$	6.148	7.862	8.572	8.734	8.753	8.864	8.868	8.778	8.754	8.754
time t	2.2	2.4	2.6	2.8	3.0	3.2	3.4	3.6	3.8	4.0
$\widehat{C}(t)_{0.975}$	10.134	10.178	10.173	10.180	10.195	10.213	10.266	10.391	10.441	10.461
$\widehat{C}(t)$	9.435	9.492	9.511	9.551	9.580	9.609	9.646	9.769	9.816	9.829
$\widehat{C}(t)_{0.025}$	8.735	8.806	8.850	8.922	8.965	9.006	9.027	9.146	9.191	9.197
time t	4.2	4.4	4.6	4.8	5.0	5.2	5.4	5.6	5.8	6.0
$\widehat{C}(t)_{0.975}$	10.597	10.658	10.829	10.822	10.793	10.830	10.902	10.916	10.958	10.937
$\widehat{C}(t)$	9.910	9.979	10.087	10.049	10.023	10.043	10.189	10.149	10.196	10.194
$\widehat{C}(t)_{0.025}$	9.223	9.300	9.344	9.276	9.253	9.256	9.477	9.382	9.433	9.451
time t	6.2	6.4	6.6	6.8	7.0	7.2	7.4	7.6	7.8	8.0
$\widehat{C}(t)_{0.975}$	10.913	10.966	11.008	11.034	11.072	11.100	11.009	11.039	10.989	10.944
$\widehat{C}(t)$	10.199	10.229	10.288	10.324	10.366	10.431	10.405	10.399	10.362	10.319
$\widehat{C}(t)_{0.025}$	9.485	9.493	9.567	9.615	9.660	9.762	9.800	9.760	9.7345	9.694

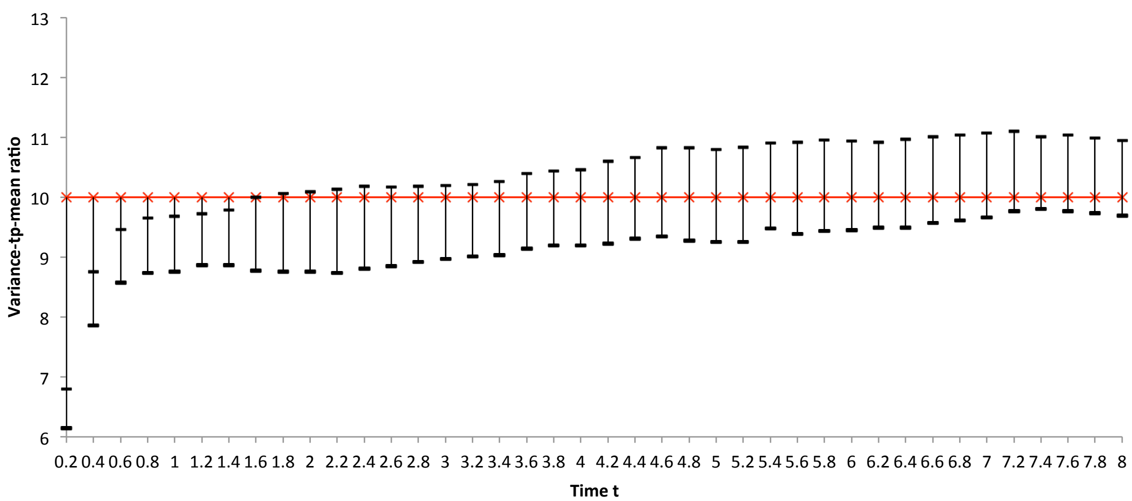

Figure 4.17: CIAT-generated 95% CIs for $C_Q(t)$, $t \in (0, 8]$, in Case 3 with $C = 10$.

Table 4.16: CIAT-generated 95% CI estimators for $\mu(t),\ t \in (0, 8]$, in Case 3 with $C = 0.8$.

time t	0.2	0.4	0.6	0.8	1.0	1.2	1.4	1.6	1.8	2.0
$\widehat{\mu}(t)_{0.975}$	13.382	27.596	43.798	48.980	51.324	62.382	75.319	90.299	95.175	97.433
$\widehat{\mu}(t)$	11.465	24.831	40.285	45.227	47.496	58.177	70.688	85.163	89.896	92.073
$\widehat{\mu}(t)_{0.025}$	9.548	22.067	36.771	41.473	43.668	53.971	66.056	80.027	84.617	86.713

time t	2.2	2.4	2.6	2.8	3.0	3.2	3.4	3.6	3.8	4.0
$\widehat{\mu}(t)_{0.975}$	107.903	120.415	134.969	139.702	141.922	152.421	164.972	179.887	184.780	187.043
$\widehat{\mu}(t)$	102.252	114.393	128.598	133.224	135.401	145.684	157.957	172.496	177.278	179.498
$\widehat{\mu}(t)_{0.025}$	96.602	108.371	122.226	126.746	128.880	138.946	150.941	165.106	169.776	171.953

time t	4.2	4.4	4.6	4.8	5.0	5.2	5.4	5.6	5.8	6.0
$\widehat{\mu}(t)_{0.975}$	197.999	211.286	226.949	232.075	234.527	246.526	260.970	278.334	284.132	286.948
$\widehat{\mu}(t)$	190.253	203.212	218.541	223.585	225.975	237.748	251.987	269.046	274.710	277.451
$\widehat{\mu}(t)_{0.025}$	182.507	195.137	210.133	215.095	217.423	228.970	243.004	259.758	265.287	267.955

time t	6.2	6.4	6.6	6.8	7.0	7.2	7.4	7.6	7.8	8.0
$\widehat{\mu}(t)_{0.975}$	300.346	316.836	336.510	343.170	346.378	362.275	381.775	405.567	413.574	416.688
$\widehat{\mu}(t)$	290.616	306.884	326.292	332.868	336.018	351.696	370.943	394.422	402.279	405.345
$\widehat{\mu}(t)_{0.025}$	280.887	296.932	316.073	322.566	325.659	341.117	360.111	383.277	390.985	394.002

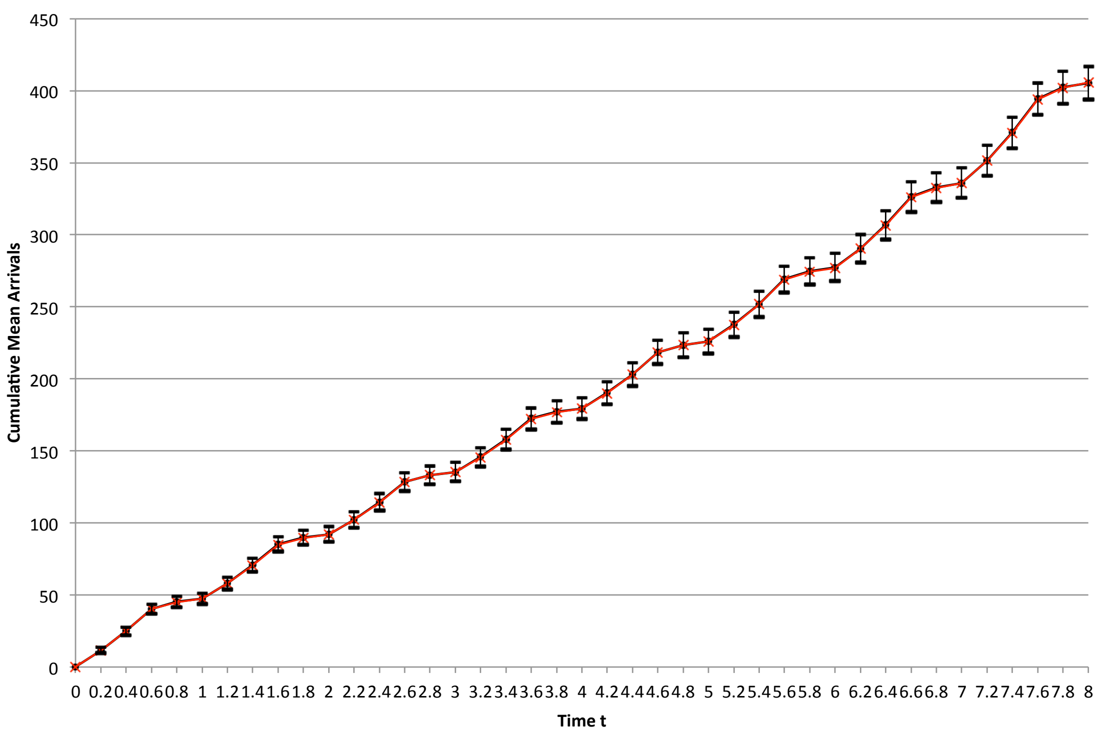

Figure 4.18: CIAT-generated 95% CIs for $\mu(t),\ t \in (0, 8]$, in Case 3 with $C = 0.8$.

Table 4.17: CIAT-generated 95% CI estimators for $C_Q(t)$, $t \in (0, 8]$, in Case 3 with $C = 0.8$.

time t	0.2	0.4	0.6	0.8	1.0	1.2	1.4	1.6	1.8	2.0
$\widehat{C}(t)_{0.975}$	0.872	0.870	0.859	0.866	0.879	0.899	0.882	0.874	0.880	0.874
$\widehat{C}(t)$	0.827	0.819	0.806	0.815	0.824	0.850	0.837	0.830	0.834	0.832
$\widehat{C}(t)_{0.025}$	0.783	0.768	0.753	0.764	0.769	0.801	0.791	0.786	0.789	0.791
time t	2.2	2.4	2.6	2.8	3.0	3.2	3.4	3.6	3.8	4.0
$\widehat{C}(t)_{0.975}$	0.879	0.886	0.887	0.884	0.887	0.884	0.890	0.885	0.886	0.890
$\widehat{C}(t)$	0.839	0.846	0.842	0.845	0.849	0.843	0.844	0.839	0.838	0.839
$\widehat{C}(t)_{0.025}$	0.800	0.806	0.797	0.805	0.811	0.802	0.797	0.794	0.790	0.789
time t	4.2	4.4	4.6	4.8	5.0	5.2	5.4	5.6	5.8	6.0
$\widehat{C}(t)_{0.975}$	0.894	0.884	0.875	0.868	0.866	0.882	0.884	0.884	0.878	0.879
$\widehat{C}(t)$	0.849	0.840	0.828	0.822	0.820	0.833	0.837	0.835	0.829	0.830
$\widehat{C}(t)_{0.025}$	0.803	0.797	0.780	0.777	0.774	0.784	0.789	0.785	0.780	0.781
time t	6.2	6.4	6.6	6.8	7.0	7.2	7.4	7.6	7.8	8.0
$\widehat{C}(t)_{0.975}$	0.872	0.871	0.880	0.873	0.873	0.864	0.847	0.844	0.846	0.842
$\widehat{C}(t)$	0.824	0.825	0.833	0.825	0.824	0.821	0.809	0.810	0.810	0.808
$\widehat{C}(t)_{0.025}$	0.775	0.779	0.787	0.778	0.775	0.778	0.771	0.776	0.774	0.773

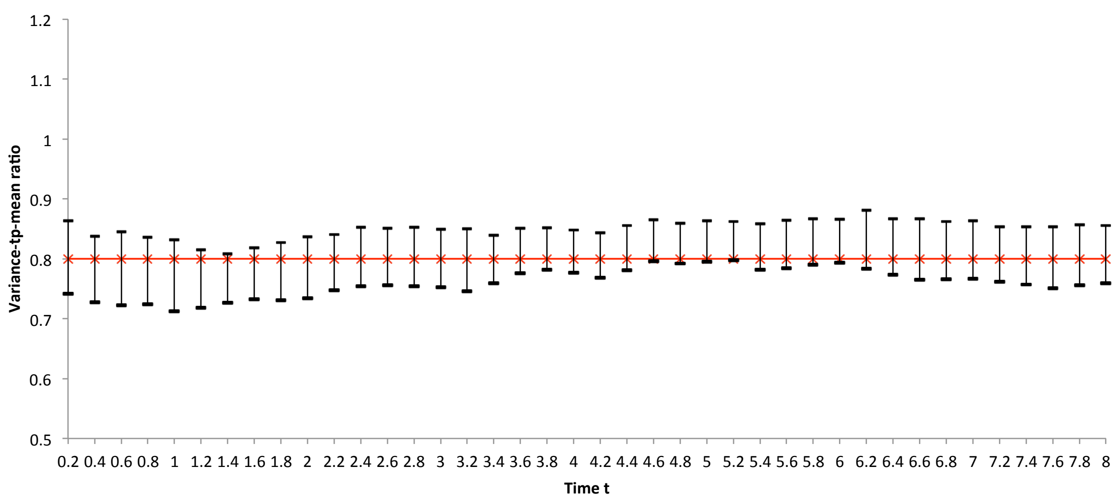

Figure 4.19: CIAT-generated 95% CIs for $C_Q(t)$, $t \in (0, 8]$, in Case 3 with $C = 0.8$.

Figure 4.15 indicates that the algorithm in Figure 3.1 is able to generate a step function $\widetilde{\lambda}_Q(t)$ that satisfies $\widetilde{\lambda}_Q(t) > 0$ and $\widetilde{\lambda}_Q(t)$ majorizes and closely approximates the designated rate function $\lambda(t)$ of Case 3, and that also has an invertible piecewise linear mean-value function $\widetilde{\mu}_Q(t) = \int_0^t \widetilde{\lambda}_Q(u)du$ for all $t \in [0, 8]$.

Table 4.14 and Figure 4.16 show that the mean-value function of the CIAT-generated arrival process mimics the trend and numerical values of the desired mean-value function closely for Case 3 with $C = 10$. Similar results were obtained for $C = 1.5$, 0.8, and 0.2.

Table 4.15 and Figure 4.17 indicate that CIAT can generate an NNPP with the desired asymptotic dispersion ratio $C = 10$; and for $t \geq 1.8$, the 95% CIs for $C_Q(t)$ include the desired value 10, or equivalently, it takes 1.8 seconds to converge. Table 4.17 and Figure 4.19 indicate that CIAT can generate an NNPP with the desired asymptotic dispersion ratio $C = 0.8$; and for $t \geq 0.2$, the 95% CIs for $C_Q(t)$ include the desired value 0.8, suggesting it takes less than 0.2 seconds to converge. For scenarios $C = 1.5$ and $C = 0.2$, we also saw that CIAT can generate an NNPP with the desired asymptotic dispersion ratio; and under both scenarios, for $t \geq 0.2$, the 95% CIs for $C_Q(t)$ include the corresponding desired value. In other words, it takes less than 0.2 seconds to converge for each scenario, which suggests a significantly fast convergence of CIAT procedure. Please see Figures C.5-C.8 and Tables C.5-C.8 for details.

Similarly to Cases 1 and 2, the numerical results and plots of Case 3 indicate that for Case 3 the estimated dispersion ratio $\widehat{C}_Q(t)$ approaches the desired value C from below for scenarios in which $C > 1$; and $\widehat{C}_Q(t)$ approaches the desired value from above for scenarios in which $0 < C < 1$.

4.4. Performance Evaluation of CIAT

In this section we evaluate the performance of CIAT by examining (i) the speed of convergence of CIAT and (ii) the closeness of the estimated values $\widehat{\mu}_Q(t)$ and $\widehat{C}_Q(t)$ to their respective theoretical counterparts $\mu(t)$ and C for various cases and for various scenarios. The experimental results show that both the speed of convergence and the quality of the estimated values varies among the instances of each test process (case) and across the test processes. The speed of convergence depends on the properties of the rate function $\lambda(t)$ and on the dispersion ratio C, while the quality of estimated values depends on Q, the number of subintervals used to construct the step rate function $\widetilde{\lambda}_Q(t)$ that majorizes and closely approximates $\lambda(t)$.

To evaluate the speed of convergence of CIAT, we define the "warm-up time" t_w of a test process as the minimum time value such that C lies in the associated confidence interval when $t \geq t_w$. The warm-up time indicates the speed of convergence of CIAT for each test process. We compare the warm-up time t_w of all the three cases and all the four scenarios in Table 4.18.

As shown in Table 4.18, for every case and for every scenario the associated CI includes the corresponding value of C when $t \geq 1.8$. This indicates a fast convergence of CIAT for all the cases and for

Table 4.18: Warm-up time of all the cases and all the scenarios generated by CIAT algorithm.

case number	$C = 10$	$C = 1.5$	$C = 0.8$	$C = 0.2$
Case 1	1.2	0.2	0.2	0.2
Case 2	1.2	0.2	0.2	0.2
Case 3	1.8	0.2	0.2	0.2

all the scenarios. The estimated dispersion ratio for the CIAT-generated NNPP in Case 3 takes longer to converge because the desired mean-value function in Case 3 is smaller than that in Case 1 and 2, as we can observe from Figure 4.1, Figure 4.10, and Figure 4.15. This is consistent to the conclusion of Theorem 5 in Section 3.5. In all the three cases, when the desired asymptotic dispersion ratio $C = 1.5$, 0.8, or 0.2, the value of C falls in the corresponding confidence interval when $t \geq 0.2$. It follows that the speed of convergence of CIAT is relatively faster when $C = 1.5$, 0.8, and 0.2.

To examine the closeness of the estimated values $\widehat{\mu}_Q(t)$ and $\widehat{C}_Q(t)$ to the respective values $\mu(t)$ and C, we first define the "percentage discrepancy" $D_i(\cdot)$, where $D_i(\widehat{\mu}_Q)$ is the percentage difference of $\widehat{\mu}_Q(t_i)$ from $\mu(t_i)$ and, $D_i(\widehat{C}_Q)$ is the percentage difference of $\widehat{C}_Q(t_i)$ from C:

$$D_i(\widehat{\mu}_Q) = \left| \frac{\widehat{\mu}_Q(t_i) - \mu(t_i)}{\mu(t_i)} \right| \times 100\%, \tag{4.5}$$

and

$$D_i(\widehat{C}_Q) = \left| \frac{\widehat{C}_Q(t_i) - C}{C} \right| \times 100\% \quad \text{for } i = 1, \ldots, M. \tag{4.6}$$

We then define the "average percentage discrepancy" and the "maximum percentage discrepancy" as two measures of closeness of a parameter estimate from its corresponding desired value as follows:

$$\Delta_M(\widehat{\mu}_Q) = \frac{1}{M} \sum_{i=1}^{M} D_i(\widehat{\mu}_Q), \tag{4.7}$$

$$\Delta_M^*(\widehat{\mu}_Q) = \max_{1 \leq i \leq M} \left\{ D_i(\widehat{\mu}_Q) \right\}, \tag{4.8}$$

$$\Delta_M(\widehat{C}_Q) = \frac{1}{M} \sum_{i=1}^{M} D_i(\widehat{C}_Q), \tag{4.9}$$

$$\Delta_M^*(\widehat{C}_Q) = \max_{1 \leq i \leq M} \left\{ D_i(\widehat{C}_Q) \right\}, \tag{4.10}$$

and the as a measure of the variability of the $\{D_i(\widetilde{\mu}_Q) : 1 \leq i \leq M\}$, we compute the associated standard deviation

$$S_\Delta(\widehat{\mu}_Q) = \sqrt{\frac{1}{M-1} \sum_{i=1}^{M} \left[D_i(\widehat{\mu}_Q) - \Delta_M(\widehat{\mu}_Q) \right]^2}. \tag{4.11}$$

It follows that an approximate 95% CI estimator for the expected value of $\Delta_M(\widehat{\mu}_Q)$ is

$$\Delta_M(\widehat{\mu}_Q) \pm z_{1-\alpha/2}\frac{S_\Delta(\widehat{\mu}_Q)}{\sqrt{M}}, \tag{4.12}$$

where $z_{1-\alpha/2}$ is the $1-\alpha/2$ quantile of the standard nomad distribution, and $\alpha = 0.05$. For the average-percentage-discrepancy estimator $\Delta_M(\widehat{C}_Q)$, the standard-deviation estimator $S_\Delta(\widehat{C}_Q)$, and the CI estimator of $\mathrm{E}[\Delta_M(\widehat{C}_Q)]$ are defined similarly.

We computed $\Delta_M(\widehat{\mu}_Q)$, $\Delta^*_M(\widehat{\mu}_Q)$, $\Delta_M(\widehat{C}_Q)$, and $\Delta^*_M(\widehat{C}_Q)$ and the approximate 95% CIs for $\mathrm{E}[\Delta_M(\widehat{\mu}_Q)]$ and $\mathrm{E}[\Delta_M(\widehat{C}_Q)]$ for every case and for every scenario. The results for each scenario in Case 1 are reported in Table 4.19. We obtained similar results for Cases 2 and 3.

Table 4.19: Closeness measures for Case 1, generated by CIAT algorithm.

Scenario	$\Delta_M(\widehat{\mu}_Q)$	$\Delta^*_M(\widehat{\mu}_Q)$	$\Delta_M(\widehat{C}_Q)$	$\Delta^*_M(\widehat{C}_Q)$
$C = 20$	1.164%± 0.133%	2.499%	14.082%± 2.108%	58.960%
$C = 15$	1.409% ± 0.261%	2.966%	11.536%± 1.694%	50.735%
$C = 10$	0.957% ± 0.19%	2.287%	10.324% ± 1.146%	38.490%
$C = 1.5$	0.819% ± 0.176%	2.463%	1.901%± 0.35%	5.233%
$C = 0.8$	0.915%±0.200%	2.028%	1.669%±0.323%	5.163%
$C = 0.2$	0.918%±0.197%	2.538%	3.530% ±0.266%	6.150%

As observed in Table 4.19, for all the scenarios the average percentage discrepancy of $\widehat{\mu}_Q$ is less than 1.5% while the maximum percentage discrepancy of $\widehat{\mu}_Q$ is less than 3%. This indicates that the estimated value of $\mu(t)$ is relatively close to the true value for all the scenarios.

When $C \le 1$, we obtained significantly smaller values of the measures $\Delta_M(\widehat{C}_Q)$ and $\Delta^*_M(\widehat{C}_Q)$ for the scenario $C = 0.8$ than those for $C = 0.2$. When $C \ge 1$, the values of these two measures for the scenario $C = 1.5$ are much smaller than those for the scenarios $C = 10$, 15, and 20. In general when C is close to 1, CIAT can generate NNPPs with estimated values of C relatively close to the corresponding true values.

The magnitudes of the four measures $\Delta_M(\widehat{\mu}_Q)$, $\Delta^*_M(\widehat{\mu}_Q)$, $\Delta_M(\widehat{C}_Q)$, and $\Delta^*_M(\widehat{C}_Q)$ vary significantly among the test processes. This variation indicates that the adequacy of a CIAT-generated NNPP depends on the characteristics of the given rate and mean-value functions as well as the given dispersion ratio. The adequacy of a CIAT-generated NNPP can also be impacted by Q, the number of subintervals that are used to generate the majorizing rate function $\widetilde{\lambda}_Q(t)$. To evaluate the impact of Q on the adequacy of CIAT-generated NNPPs, we compare the values of the four discrepancy measures and the 95% CIs for $\mathrm{E}[\Delta_M(\widehat{\mu}_Q)]$ and $\mathrm{E}[\Delta_M(\widehat{C}_Q)]$ on the first test process with $C = 10$ and with different values of Q. More specifically, we conducted experiments for Case 1, Scenario 1 by partitioning the time interval

$(0, 8]$ into $Q = 160$, 320, and 640 subintervals to generate a majorizing rate function $\widetilde{\lambda}_Q(t)$ that is a progressively more refined estimate of the desired rate function $\lambda(t)$ for $t \in (0, 8]$. The detailed results are in Table 4.20.

Table 4.20: Closeness measures and 95% CI estimators in terms of Q, for Case 1, Scenario 1, using the CIAT algorithm.

Scenario	$\Delta_M(\widehat{\mu}_Q)$	$\Delta^*_M(\widehat{\mu}_Q)$	$\Delta_M(\widehat{C}_Q)$	$\Delta^*_M(\widehat{C}_Q)$
$Q = 640$	$0.674\% \pm 0.103\%$	1.373%	$7.459\% \pm 1.366\%$	39.714%
$Q = 320$	$0.895\% \pm 0.148\%$	1.861%	$8.463\% \pm 1.249\%$	37.857%
$Q = 160$	$0.957\% \pm 0.19\%$	2.287%	$10.324\% \pm 1.146\%$	38.490%

As shown in Table 4.20, we observe that for all three scenarios the values of $\Delta_M(\widehat{\mu}_Q)$ and $\Delta^*_M(\widehat{\mu}_Q)$ are less than 1% and 2.3%, respectively. It follows that CIAT is able to deliver an NNPP with an empirical mean-value function that is relatively close to the desired mean-value function for cases when $Q = 160$, 320, and 640. (Of course we know by Theorem 4 that the CIAT-generated NNPP has a theoretical mean-value function that coincides exactly with the desired mean-value function.) When we compare the closeness of $\widehat{C}_Q(t)$ for the cases when $Q = 320$ and $Q = 640$, we find that there is no significant statistical difference. However, it is also observed that the closeness for the estimated dispersion ratio $\widehat{C}_Q(t)$ is significantly improved as Q jumps from 160 to 320. The impact of the number of subintervals Q on the closeness of $\widehat{C}_Q(t)$ is due to the fact that the closeness and accuracy of the step rate function $\widetilde{\lambda}_Q(t)$ which majorizes and approximates the desired rate function $\lambda(t)$ depends on the number of subintervals Q.

To evaluate the computation time, we used CIAT to generated 50 NNPPs on $(0, 4]$ and we recorded the execution time for $Q = 8, 16, 24, \ldots, 200, 300, \ldots, 1000$, for Case 1, $C = 1.5$. The result is presented in Figure 4.20. Figure 4.20 indicates that the computation time for small Q ($Q = 8, 16, 24$) is long since the acceptance probability for the thinning procedure is low, and Figure 4.20 also indicates that the computation time is increasing approximately linear in terms of Q with an slope approximately equal to 0.025.

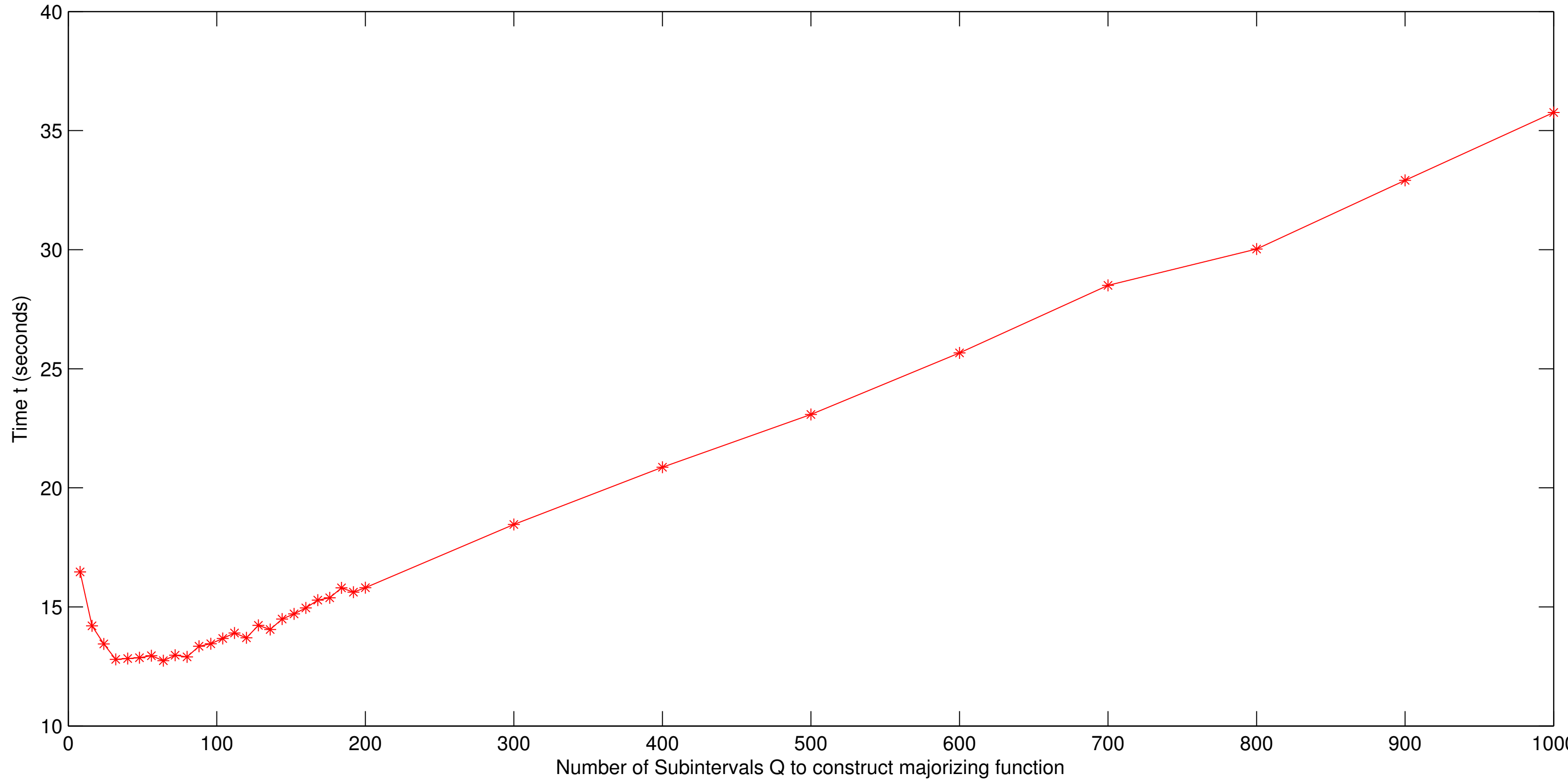

Figure 4.20: Computation time (in seconds) for CIAT in Case 1 with $C = 1.5$.

4.5. Presentation and Discussion of Results for CIATL-Generated NNPPs in Case 1

In this section we conduct experiments and present the results of evaluating the effectiveness of the CIATL procedure. As we observed in Sections 4.3.1–4.3.3, there is no significant difference between the various performance measures for CIAT-generated NNPPs across the selected test processes. We only apply CIATL to generate NNPPs on the given time interval for Case 1 with scenarios $C = 10$, $C = 1.5$ and $C = 0.2$, and the parameters for the desired rate function $\lambda(t)$ are presented in Table 4.1 of Section 4.1. For $C = 1.5$ and $C = 0.2$, we performed a metaexperiment which is similar to that for the CIAT procedure. It consists of $R = 100$ independent basic experiments; and in each basic experiment, we performed $K = 200$ independent replications of the CIATL procedure to generate 200 realizations of an NNPP process $\{N_Q(t) : t \in [0, S]\}$ with $S = 8$. For $C = 10$, we performed the same experiments to generate NNPPs on time horizon [0, 16], the reason is detailed in Section 4.6. We calculate the overall estimates of the mean-value function $\mu(t)$ and the dispersion-ratio function $C_Q(t)$. For $C = 10$, we performed the same experiments to generate NNPPs on time horizon [0, 16], the reason is detailed in Section 4.6.

The CIATL procedure adopts the same algorithm as the CIAT procedure to construct the majorizing rate function $\widetilde{\lambda}_Q(t)$ from the desired rate function $\lambda(t)$, as shown in Figure 4.1 of Section 4.3.1. For $C = 10$, 1.5, and 0.2, we computed 95% CI estimators of $\mu(t)$ for $0 \le t \le 8$, and we present the results for $C = 10$ and $C = 0.2$ in Figures 4.21 and 4.23, as well as in Tables 4.21 and 4.23, respectively. In these figures, the red line represents the desired mean-value $\mu(t)$ and the black line represents the estimated mean-value function $\widehat{\mu}_Q(t)$. For $C = 10$, the 95% CI estimators of $C_Q(t)$ over $0 \le t \le 16$ are presented in Figure 4.22 as well as in Table 4.22. For $C = 0.2$ the 95% CI estimators of $C_Q(t)$ over $0 \le t \le 8$ are presented in Figure 4.24, as well as in Table 4.24. The results for $C = 1.5$ are listed in Figures C.9 and C.10, as well as in Tables C.9 and C.10 of Appendix C.

Table 4.21: CIATL-generated 95% CI estimators for $\mu(t),\ t \in (0, 8]$, in Case 1 with $C = 10$.

time t	0.2	0.4	0.6	0.8	1.0	1.2	1.4	1.6	1.8	2.0
$\widehat{\mu}(t)_{0.025}$	16.169	33.004	52.136	58.239	61.011	74.077	89.470	107.338	112.932	115.588
$\widehat{\mu}(t)$	11.660	25.512	41.843	47.168	49.626	61.170	74.894	90.967	96.101	98.515
$\widehat{\mu}(t)_{0.975}$	7.151	18.019	31.550	36.096	38.241	48.263	60.317	74.595	79.269	81.442
time t	2.2	2.4	2.6	2.8	3.0	3.2	3.4	3.6	3.8	4.0
$\widehat{\mu}(t)_{0.025}$	128.202	143.332	160.730	166.469	169.125	181.630	196.413	213.848	219.291	221.869
$\widehat{\mu}(t)$	110.050	123.949	140.034	145.312	147.776	159.399	173.002	189.168	194.279	196.700
$\widehat{\mu}(t)_{0.975}$	91.897	104.567	119.338	124.155	126.427	137.167	149.590	164.488	169.267	171.531
time t	4.2	4.4	4.6	4.8	5.0	5.2	5.4	5.6	5.8	6.0
$\widehat{\mu}(t)_{0.025}$	234.379	249.085	266.343	271.867	274.403	286.577	301.006	318.041	323.650	326.210
$\widehat{\mu}(t)$	208.429	222.106	238.191	243.412	245.810	257.314	270.855	286.882	292.125	294.542
$\widehat{\mu}(t)_{0.975}$	182.479	195.127	210.038	214.956	217.218	228.052	240.703	255.724	260.599	262.874
time t	6.2	6.4	6.6	6.8	7.0	7.2	7.4	7.6	7.8	8.0
$\widehat{\mu}(t)_{0.025}$	338.350	352.951	369.946	375.463	378.026	390.117	404.444	421.314	426.889	429.504
$\widehat{\mu}(t)$	306.041	319.918	336.008	341.252	343.709	355.261	368.882	385.033	390.372	392.844
$\widehat{\mu}(t)_{0.975}$	273.732	286.886	302.069	307.041	309.391	320.404	333.319	348.751	353.855	356.184

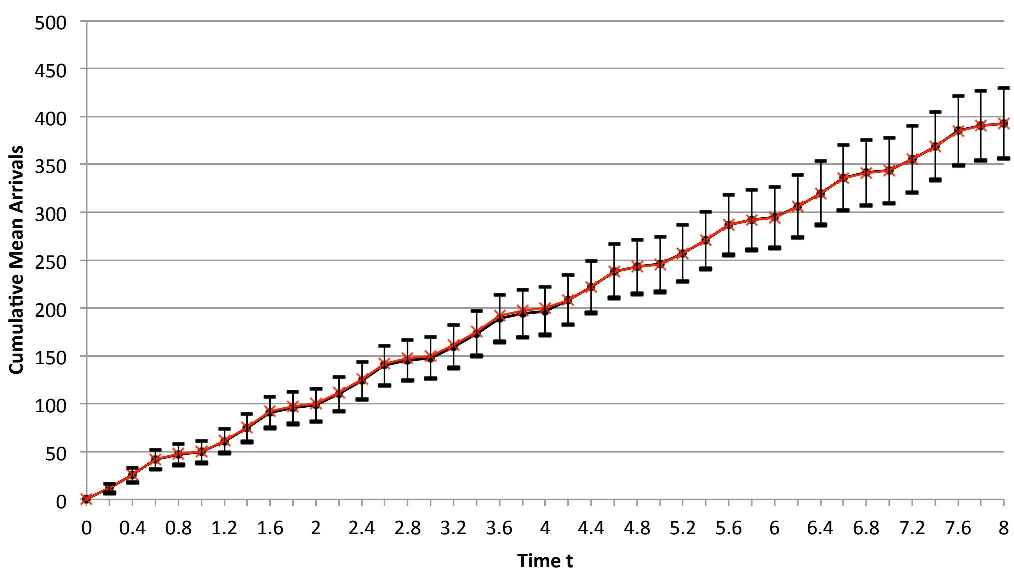

Figure 4.21: CIATL-generated 95% CIs for $\mu(t),\ t \in (0, 8]$, in Case 1 with $C = 10$.

Table 4.22: CIATL-generated 95% CI estimators for $C_Q(t)$, $t \in (0, 16]$, in Case 1 with $C = 10$.

time t	0.2	0.4	0.6	0.8	1.0	1.2	1.4	1.6	1.8	2.0
$\widehat{C}(t)_{0.025}$	4.854	6.189	7.059	7.176	7.229	7.447	7.788	8.114	8.183	8.184
$\widehat{C}(t)$	4.618	5.864	6.629	6.722	6.754	6.918	7.191	7.483	7.544	7.548
$\widehat{C}(t)_{0.975}$	4.382	5.539	6.198	6.268	6.279	6.389	6.593	6.853	6.905	6.913
time t	2.2	2.4	2.6	2.8	3.0	3.2	3.4	3.6	3.8	4.0
$\widehat{C}(t)_{0.025}$	8.303	8.435	8.565	8.593	8.593	8.649	8.733	8.911	8.906	8.906
$\widehat{C}(t)$	7.634	7.728	7.860	7.871	7.870	7.905	7.975	8.136	8.139	8.142
$\widehat{C}(t)_{0.975}$	6.965	7.020	7.156	7.149	7.147	7.160	7.217	7.361	7.371	7.378
time t	4.2	4.4	4.6	4.8	5.0	5.2	5.4	5.6	5.8	6.0
$\widehat{C}(t)_{0.025}$	8.978	9.049	9.121	9.114	9.110	9.143	9.199	9.238	9.250	9.257
$\widehat{C}(t)$	8.213	8.292	8.360	8.362	8.356	8.371	8.441	8.480	8.482	8.492
$\widehat{C}(t)_{0.975}$	7.447	7.534	7.600	7.611	7.603	7.599	7.682	7.722	7.715	7.727
time t	6.2	6.4	6.6	6.8	7.0	7.2	7.4	7.6	7.8	8.0
$\widehat{C}(t)_{0.025}$	9.210	9.239	9.225	9.211	9.199	9.185	9.178	9.221	9.222	9.210
$\widehat{C}(t)$	8.477	8.506	8.519	8.508	8.507	8.525	8.530	8.563	8.564	8.559
$\widehat{C}(t)_{0.975}$	7.745	7.773	7.813	7.806	7.814	7.864	7.881	7.906	7.906	7.908
time t	8.2	8.4	8.6	8.8	9.0	9.2	9.4	9.6	9.8	10.0
$\widehat{C}(t)_{0.025}$	9.210	9.260	9.342	9.349	9.356	9.384	9.433	9.499	9.505	9.510
$\widehat{C}(t)$	8.594	8.616	8.665	8.675	8.678	8.691	8.713	8.768	8.778	8.784
$\widehat{C}(t)_{0.975}$	7.977	7.972	7.987	8.000	8.000	7.997	7.994	8.037	8.051	8.058
time t	10.2	10.4	10.6	10.8	11.0	11.2	11.4	11.6	11.8	12.0
$\widehat{C}(t)_{0.025}$	9.521	9.498	9.525	9.544	9.550	9.589	9.625	9.673	9.694	9.697
$\widehat{C}(t)$	8.780	8.760	8.771	8.781	8.781	8.794	8.815	8.837	8.855	8.851
$\widehat{C}(t)_{0.975}$	8.040	8.023	8.016	8.018	8.013	8.000	8.005	8.001	8.016	8.006
time t	12.2	12.4	12.6	12.8	13.0	13.2	13.4	13.6	13.8	14.0
$\widehat{C}(t)_{0.025}$	9.734	9.738	9.740	9.730	9.719	9.710	9.734	9.743	9.757	9.760
$\widehat{C}(t)$	8.880	8.886	8.896	8.889	8.881	8.877	8.893	8.911	8.923	8.924
$\widehat{C}(t)_{0.975}$	8.027	8.033	8.051	8.049	8.043	8.045	8.052	8.080	8.089	8.088
time t	14.2	14.4	14.6	14.8	15.0	15.2	15.4	15.6	15.8	16.0
$\widehat{C}(t)_{0.025}$	9.777	9.829	9.877	9.888	9.884	9.871	9.877	9.898	9.905	9.903
$\widehat{C}(t)$	8.924	8.949	8.961	8.966	8.958	8.945	8.957	8.971	8.982	8.978
$\widehat{C}(t)_{0.975}$	8.070	8.068	8.044	8.044	8.033	8.019	8.037	8.044	8.059	8.053

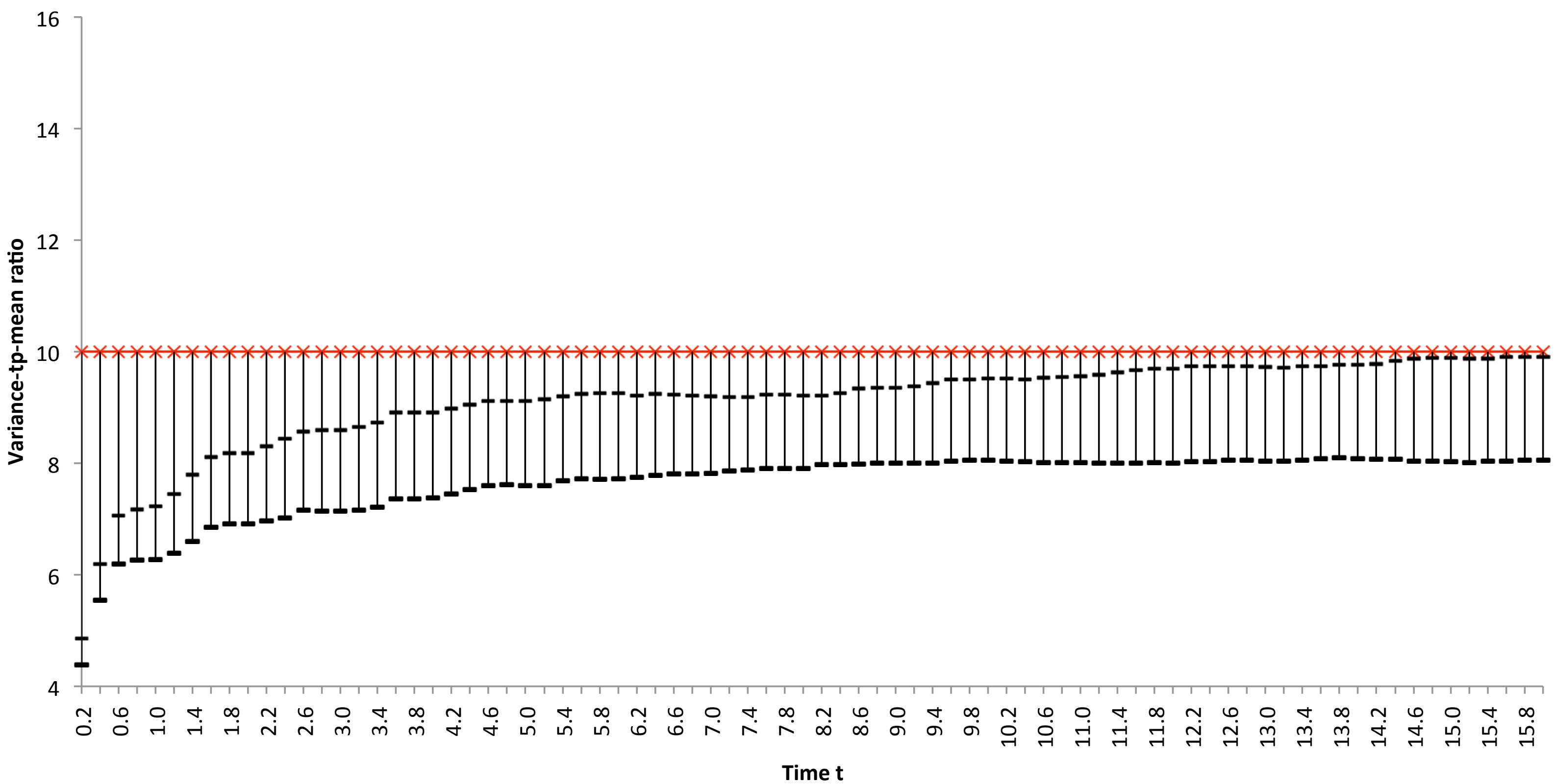

Figure 4.22: CIATL-generated 95% CIs for $C_Q(t)$, $t \in (0, 16]$, in Case 1 with $C = 10$.

Table 4.23: CIATL-generated 95% CI estimators for $\mu(t),\ t \in (0, 8]$, in Case 1 with $C = 0.2$.

time t	0.2	0.4	0.6	0.8	1.0	1.2	1.4	1.6	1.8	2.0
$\widehat{\mu}(t)_{0.025}$	12.672	26.883	43.374	48.768	51.262	63.090	77.118	93.468	98.842	101.318
$\widehat{\mu}(t)$	11.576	25.327	41.403	46.614	49.056	60.617	74.395	90.490	95.744	98.173
$\widehat{\mu}(t)_{0.975}$	10.479	23.771	39.431	44.460	46.850	58.145	71.673	87.512	92.645	95.027
time t	2.2	2.4	2.6	2.8	3.0	3.2	3.4	3.6	3.8	4.0
$\widehat{\mu}(t)_{0.025}$	112.977	126.940	143.212	148.530	151.006	162.690	176.660	192.929	198.265	200.704
$\widehat{\mu}(t)$	109.684	123.457	139.527	144.767	147.199	158.730	172.501	188.603	193.851	196.268
$\widehat{\mu}(t)_{0.975}$	106.391	119.974	135.842	141.004	143.391	154.769	168.342	184.276	189.436	191.832
time t	4.2	4.4	4.6	4.8	5.0	5.2	5.4	5.6	5.8	6.0
$\widehat{\mu}(t)_{0.025}$	212.395	226.277	242.497	247.803	250.267	261.942	275.807	292.041	297.335	299.835
$\widehat{\mu}(t)$	207.828	221.592	237.673	242.913	245.345	256.917	270.683	286.761	291.965	294.419
$\widehat{\mu}(t)_{0.975}$	203.262	216.906	232.848	238.023	240.422	251.891	265.559	281.481	286.594	289.002
time t	6.2	6.4	6.6	6.8	7.0	7.2	7.4	7.6	7.8	8.0
$\widehat{\mu}(t)_{0.025}$	311.585	325.430	341.619	346.885	349.344	360.944	374.841	391.068	396.379	398.314
$\widehat{\mu}(t)$	306.055	319.803	335.879	341.094	343.519	355.040	368.840	384.944	390.201	392.112
$\widehat{\mu}(t)_{0.975}$	300.525	314.175	330.138	335.303	337.694	349.136	362.838	378.819	384.022	385.910

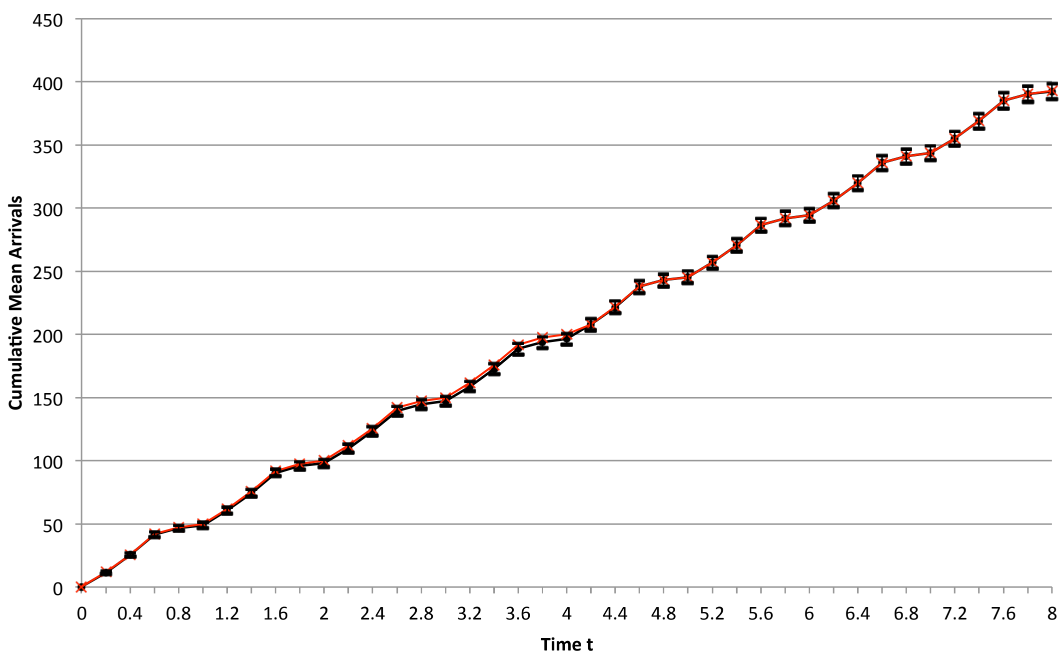

Figure 4.23: CIATL-generated 95% CIs for $\mu(t),\ t \in (0, 8]$, in Case 1 with $C = 0.2$.

Table 4.24: CIATL-generated 95% CI estimators for $C_Q(t)$, $t \in (0, 8]$, in Case 1 with $C = 0.2$.

time t	0.2	0.4	0.6	0.8	1.0	1.2	1.4	1.6	1.8	2.0
$\widehat{C}(t)_{0.025}$	0.227	0.225	0.221	0.216	0.213	0.210	0.209	0.212	0.211	0.213
$\widehat{C}(t)$	0.213	0.211	0.206	0.204	0.202	0.199	0.200	0.202	0.202	0.204
$\widehat{C}(t)_{0.975}$	0.198	0.196	0.192	0.192	0.191	0.189	0.191	0.193	0.194	0.195
time t	2.2	2.4	2.6	2.8	3.0	3.2	3.4	3.6	3.8	4.0
$\widehat{C}(t)_{0.025}$	0.208	0.209	0.213	0.214	0.213	0.215	0.217	0.214	0.213	0.212
$\widehat{C}(t)$	0.200	0.201	0.203	0.205	0.204	0.206	0.208	0.205	0.204	0.203
$\widehat{C}(t)_{0.975}$	0.193	0.193	0.193	0.196	0.196	0.198	0.200	0.196	0.195	0.194
time t	4.2	4.4	4.6	4.8	5.0	5.2	5.4	5.6	5.8	6.0
$\widehat{C}(t)_{0.025}$	0.215	0.215	0.214	0.212	0.213	0.211	0.211	0.212	0.212	0.213
$\widehat{C}(t)$	0.205	0.203	0.202	0.201	0.202	0.199	0.198	0.198	0.199	0.200
$\widehat{C}(t)_{0.975}$	0.195	0.192	0.191	0.191	0.191	0.187	0.185	0.185	0.186	0.187
time t	6.2	6.4	6.6	6.8	7.0	7.2	7.4	7.6	7.8	8.0
$\widehat{C}(t)_{0.025}$	0.213	0.212	0.209	0.209	0.210	0.210	0.209	0.211	0.211	0.211
$\widehat{C}(t)$	0.199	0.198	0.198	0.198	0.199	0.198	0.198	0.199	0.199	0.199
$\widehat{C}(t)_{0.975}$	0.185	0.184	0.187	0.188	0.189	0.187	0.187	0.186	0.186	0.186

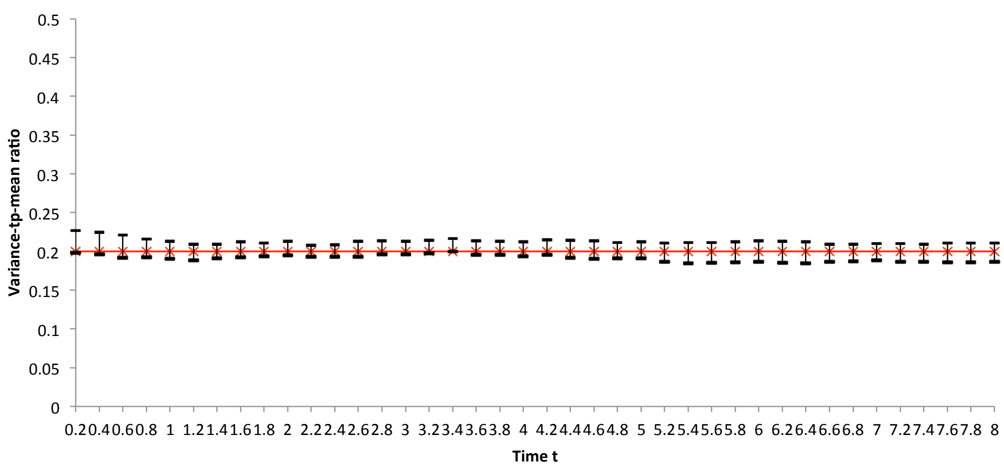

Figure 4.24: CIATL-generated 95% CIs for $C_Q(t)$, $t \in (0, 8]$, in Case 1 with $C = 0.2$.

Table 4.21 and Figure 4.21 show that the mean-value function of the CIATL-generated arrival process mimics the trend and numerical values of the desired mean-value function closely for $C = 10$. Similar results were obtained for $C = 1.5$, and 0.2.

Table 4.24 and Figure 4.24 indicate that CIATL can generate an NNPP with the desired asymptotic dispersion ratio $C = 0.2$; and for $t \geq 0.2$, the 95% CIs for $C_Q(t)$ include the desired value 0.2.

This indicates that it takes less than 0.2 time units to converge for this scenario. For $C = 1.5$ we also observed that CIATL can generate an NNPP converging relatively fast to the desired asymptotic dispersion ratio: for $t \geq 1.6$, the 95% CIs for $C_Q(t)$ include the corresponding desired value. Please see Figure C.10 and Table C.10 for details. However, when $C = 10$, all the 95% CIs for $C_Q(t)$ for $t \in (0, 16]$ obtained by CIATL fail to include the desired value 10, though the estimated dispersion ratio $\widehat{C}_Q(t)$ is asymptotically approaching the desired value from below. Table 4.22 and Figure 4.22 indicate that the estimated asymptotic dispersion ratio of CIATL-generated NNPP takes a long time to coverage to the desired value $C = 10$.

Similarly to the NNPPs generated by the CIAT procedure, in general, the numerical results and plots CIATL-generated NNPPs indicate that the estimated dispersion ratio $\widehat{C}_Q(t)$ approaches the desired value C from below for scenarios in which $C > 1$; and $\widehat{C}_Q(t)$ approaches the desired value C from above for scenarios in which $0 < C < 1$.

4.6. Performance Evaluation for CIATL

For Case 1 and for $C = 10$, 1.5 and 0.2, we compute 95% CI estimators of $\mu(t)$ for $0 \leq t \leq 8$, and we present the results in Figures 4.21, C.9 and 4.23 as well as in Tables 4.21, C.9 and 4.23, respectively. In these figures, the red line represents the desired mean-value function $\mu(t)$ and the black line represents the estimated mean-value function $\widehat{\mu}_Q(t)$. The 95% CI estimators of $C_Q(t)$ for $0 \leq t \leq 8$ are presented in Figures 4.22, C.10 and 4.24 as well as in Tables 4.22, C.10 and 4.24, respectively. For these three test processes, we set $Q = 160$.

In the experiments with large values of C for the CIATL procedure, we use a larger right endpoint S than that for CIAT procedure based on the properties of the lognormal distribution. The lognormal distribution possesses a heavy right tail that gets heavier ("fatter") as the value of the parameter β in Equation (3.41) increases. In Section 3.6.1 we showed that $\beta = \sqrt{\ln(1 + C)}$. Thus, if C is relatively large, the corresponding lognormal distribution possesses a relatively heavy right tail. As a result, a relatively large time horizon $[0, S]$ is required to enable us to randomly generate a lognormally distributed interrenewal time within this interval. Thus, even though our target interval is relatively small, we need to set a large value of S to perform the CIATL procedure so as to ensure that on every realization of a CIATL-generated NNPP, the first arrival epoch S_1 occurs prior to the end of the given time horizon. In the experiment of this section, we set S as the smallest integer such that $1 - G_e[\widetilde{\mu}_Q(S)] < 10^{-6}$ and S is at least as large as the originally specified time horizon, where $G_e(\cdot)$ is the CDF of the first renewal X_1, and is defined in Equation (3.59). For the three test processes of Case 1, we set $S = 16$ when $C = 10$, while we use the original time interval $(0, 8]$ to perform CIATL procedure when $C = 1.5$ and $C = 0.2$.

Tables 4.21 and C.9, and Figures 4.21 and C.9 show that the mean-value function of the CIATL-generated arrival process mimics the trend and numerical values of the desired mean-value function closely; the red line represents the desired mean-value function $\mu(t)$ and the black line represents the estimated mean-value function $\widehat{\mu}_Q(t)$. Table 4.22 and Figure 4.22 indicate that CIATL can generate an NNPP that has an asymptotic dispersion ratio approaching to the designated asymptotic dispersion ratio $C = 10$. Table C.10 and Figure C.10 indicate that CIATL can generate an NNPP with designated asymptotic dispersion ratio $C = 1.5$; and for $t \geq 0.6$, the 95% CIs for $C_Q(t)$ include the desired value 1.5. The numerical results and plots also indicate that the estimated dispersion ratio $\widehat{C}_Q(t)$ may have a negative bias. However, the numerical measures and plots do show that the CIATL procedure can generate a NNPP with designated mean-value function $\mu(t)$ and asymptotic dispersion ratio C, provided the time horizon is sufficiently large.

We compare the performance of methods CIAT and CIATL by comparing (i) the warm-up time t_w; (ii) the discrepancy measures (4.7)–(4.10) and the 95% CIs for $\mathrm{E}[\Delta_M(\widehat{\mu}_Q)]$ and $\mathrm{E}[\Delta_M(\widehat{C}_Q)]$; and (iii) the execution times for the two procedures.

First, we compare the warm-up time of CIAT and CIATL for Case 1, and we present the results in Table 4.25. We observe that when C is relatively large, the warm-up time of CIATL procedure is longer than that of CIAT, especially when $C = 10$. This is due to the fact that when C is large, the corresponding lognormal distributions possess heavy right tails. However, there is no significant difference in warm-up time between the two procedures when C is relatively small.

Table 4.25: Comparison of warm-up time Case 1, using CIAT and CIATL

Procedure	$C = 10$	$C = 1.5$	$C = 0.2$
CIAT	1.2	0.2	0.2
CIATL	> 8	1.6	0.2

In Tables 4.26–4.28, we compare the values of the four discrepancy measures between CIAT and CIATL for Case 1 and for $C = 10$, 1.5, and 0.2. When $C = 1.5$ or 10, we observe that the values of the measures $\Delta_M(\widehat{C}_Q)$ and $\Delta^*_M(\widehat{C}_Q)$ achieved by CIATL are significantly larger than those achieved by the CIAT, while all the values of the measures $\Delta_M(\widehat{\mu}_Q)$ and $\Delta^*_M(\widehat{\mu}_Q)$ are below 3%. This indicates that when C is relatively large, there is no significant difference between CIAT and CIATL in the resulting estimated mean-value functions, and these estimates are close to the value of the corresponding true mean-value functions. However, when C is relatively larger, CIAT outperforms CIATL in the closeness of the resulting estimated asymptotic dispersion ratio to its desired value. We had different observations on the four measures when $C = 0.2$. As observed in Table 4.28, the value of the average percentage discrepancy $\Delta_M(\widehat{C}_Q)$ obtained by CIATL is less than half of that obtained by CIAT, while the maximum percentage discrepancy $\Delta^*_M(\widehat{C}_Q)$ achieved by CIATL is only 2% more than that achieved by CIAT. We also observe that all the values of the measures $\Delta_M(\widehat{\mu}_Q)$ and $\Delta^*_M(\widehat{\mu}_Q)$ are below 3%. This indicates that when C is relatively small, the estimated mean-value functions obtained by both procedures are relatively close to the corresponding desired mean-value functions, and CIATL outperforms CIAT in the closeness of the resulting estimated asymptotic dispersion ratio to its desired value.

Table 4.26: Comparison of discrepancy measures, for Case 1 with $C = 10$, using CIAT and CIATL.

Procedure	$\Delta_M(\hat{\mu}_Q)$	$\Delta^*_M(\hat{\mu}_Q)$	$\Delta_M(\widehat{C}_Q)$	$\Delta^*_M(\widehat{C}_Q)$
CIAT	0.957% ± 0.190%	2.287%	10.324% ± 1.146%	38.490%
CIATL	0.639%± 0.135%	1.609%	18.399% ± 2.140%	54.475%

Table 4.27: Comparison of discrepancy measures, for Case 1 with $C = 1.5$ using CIAT and CIATL.

Procedure	$\Delta_M(\hat{\mu}_Q)$	$\Delta^*_M(\hat{\mu}_Q)$	$\Delta_M(\widehat{C}_Q)$	$\Delta^*_M(\widehat{C}_Q)$
CIAT	0.819% ± 0.176%	2.463%	1.901%± 0.35%	5.233%
CIATL	0.845% ± 0.139%	2.037%	3.684%±0.355%	10.433%

Table 4.28: Comparison of discrepancy measures, for Case 1 with $C = 0.2$ using CIAT and CIATL.

Procedure	$\Delta_M(\hat{\mu}_Q)$	$\Delta^*_M(\hat{\mu}_Q)$	$\Delta_M(\widehat{C}_Q)$	$\Delta^*_M(\widehat{C}_Q)$
CIAT	0.918%±0.197%	2.538%	3.530% ±0.266%	6.150%
CIATL	0.874%±0.192%	1.986%	1.493%±0.300%	6.35%

To compare the execution time of CIAT and CIATL, we generated 50 NNPPs using each procedure on time interval $[0, 4]$ for Case 1, $C = 1.5$ and for different values of Q. The results are shown in Table 4.29. We observed that for all the instances in Table 4.29 the execution time of CIATL is more than that of CIAT, but the difference is not significant.

Table 4.29: Comparison of Execution Time (in seconds), for Case 1 with $C = 1.5$, using CIAT and CIATL.

Q	500	600	700	800	900	1000
CIAT	23.08	25.67	28.50	30.03	32.91	35.76
CIATL	29.17	31.29	33.73	35.48	37.77	40.68

Chapter 5

Concluding remarks and future work

5.1. Conclusion

In this dissertation we designed two effective procedures for modeling and simulation of nonstationary non-Poisson processes. More specifically, our contributions are as follows:

- We developed the Combined Inversion-and-Thinning (CIAT) method for modeling and simulation of a nonstationary non-Poisson process (NNPP) with given rate and mean-value function and with a given asymptotic variance-to-mean ratio. We provided detailed proofs that our method overcomes the disadvantages of the inversion and thinning methods of [12] while retaining the attractive features of those methods. More specifically, the key advantages of CIAT can be summarized as follows:
  - CIAT can be applied to generate a wider range of NNPPs than other methods, especially for NNPPs whose given rate function $\lambda(t)$ corresponds to a mean-value function that can not be inverted either analytically or numerically with sufficient accuracy and speed for large-scale simulation applications. CIAT achieves this capability by constructing a step rate function $\widetilde{\lambda}_Q(t)$ which majorizes and closely approximates $\lambda(t)$.
  - CIAT generates NNPPs whose theoretical mean-value function exactly equals the given mean-value function $\mu(t)$ over the given time horizon $[0, S]$; and CIAT's execution speed increases linearly with the length S of the time horizon.
  - CIAT generates NNPPs whose time-dependent dispersion ratio $C_Q(t)$ converges to the desired asymptotic dispersion ratio C with bias of the form $o[\mu(t)]/\mu(t)$, provided the majorizing step rate function $\widetilde{\lambda}_Q(t)$ is based on a sufficiently fine subdivision of the time horizon $[0, S]$ into Q equal-length subintervals. Thus if $\mu(t)$ grows without bound as t increases, then

$$C_Q(t) \approx C \quad \text{for sufficiently large } S, Q, t. \tag{5.1}$$

In our numerical experiments, we often found that taking $200 \le Q \le 300$ was sufficient to ensure the validity of the approximation (5.1) for values of $t \ge t_w$, the so-called warm-up time; in many test processes, we found that t_w was between 2.5% and 15% of length S of the time horizon.

  - CIAT is computationally efficient in generating NNPPs by utilizing a step rate function which approximates the given rate function closely.

- We also developed the CIATL procedure for modeling and simulation of NNPP processes. CIATL is similar to CIAT except that we use a lognormal distribution for interrenewal times for both scenarios $0 < C < 1$ and $C > 1$ instead of using two different distributions as in CIAT.

- We conducted several computational experiments with different designated mean-value functions and asymptotic dispersion ratios. We showed that both CIAT and CIATL can generate NNPPs with a given mean-value function and asymptotic dispersion ratio. The performance of both methods, expressed by the speed of convergence of our methods and by the closeness of the estimated values $\hat{\mu}_Q(t)$ and $\hat{C}_Q(t)$ to their theoretical counterparts $\mu(t)$ and C, varies among test processes. The performance of CIAT and CIATL depends on the properties of the rate function $\lambda(t)$, on the value of asymptotic dispersion ratio C, and on the value of Q , the number of subintervals that is used to generate the majorizing rate function $\tilde{\lambda}_Q(t)$. In comparing the performance of CIAT and CIATL, we found that CIAT outperforms CIATL on the speed of convergence of $\hat{C}_Q(t)$ to C. When C is relatively large, CIAT outperforms CIATL on the closeness of $\hat{C}_Q(t)$ to the asymptotic dispersion ratio C; but when C is relatively small, CIATL performs better than CIAT. There is no significant difference between the two procedures on the closeness of the estimated mean-value function or on the execution time.

5.2. Directions of Future Work

Several future research paths can be followed based on the results of this dissertation:

- It would be desirable to establish the theoretical computational complexity of CIAT in terms of Q so that a theoretically optimal Q can be identified.

- It would be desirable to seek a dynamic algorithm in partitioning the time interval $[0, S]$ into Q subintervals: the length of the subintervals are not necessarily identical, and we should have more subintervals where the rate function $\lambda(t)$ has a rapid change. Similarly in regions of time where $\lambda(t)$ is nearly constant or zero, it would be advantageous to merge subintervals so as to speed up the scheme for inverting the majorizing mean-value function in those time regions. In this way, the computational cost of CIAT can be further reduced while retaining the accuracy and convergence rate of CIAT.

- Explore other distribution functions to generate the interarrival times $\{X_j^\circ : j = 1, 2, \ldots\}$, where $X_1^\circ \sim G_e$ and $X_j^\circ \sim G$ for $j \geq 2$. It is clear from our computational experience with the lognormal distribution that lighter-tailed alternatives may be more attractive.

- The experimental performance evaluation of CIAT and its extensions should be expanded to cover a greater diversity of types of NNPPs.

- CIAT should be extended to cover NNPPs with time-varying dispersion ratios. Such an extension would seem to require a fundamentally new approach.

REFERENCES

[1] T. M. Apostol. *Calculus: Calculus of Several Variables with Applications to Probability and Vector Analysis*, volume 2. Blaisdell Pub. Co., 1962.

[2] T. M. Apostol. *Mathematical Analysis*. Addison Wesley Publishing Company, 1974.

[3] B. L. Arkin and L. M. Leemis. Nonparametric Estimation of the Cumulative Intensity Function for a Nonhomogeneous Poisson Process from Overlapping Realizations. *Management Science*, 46(7):989–998, July 2000.

[4] Peter J. Bickel and Kjell A. Doksum. *Mathematical Statistics: Basic Ideas and Selected Topics*. Prentice-Hall, Inc., 2007.

[5] Patrick Billingsley. *Probability and measure*. Wiley, 2nd ed. edition, 1986.

[6] H. Chen and B. W. Schmeiser. Simulation of Poisson Processes with Trigonometric Rates. In *Proceedings of the 1992 Winter Simulation Conference*, pages 609–617. ACM, 1992.

[7] H. Chen and B. W. Schmeiser. I-SMOOTH: Iteratively Smoothing Mean-Constrained and Non-negative Piecewise-Constant Functions. *INFORMS Journal on Computing*, 2012.

[8] G. Chryssolouris. *Manufacturing Systems: Theory and Practice*. Springer Verlag, 2006.

[9] E. Çinlar. *Introduction to Stochastic Processes.* Prentice-Hall, Englewood Cliffs, New Jersey, 1975.

[10] D. R. Cox and P. A. W. Lewis. *The Statistical Analysis of Series of Events*. Chapman and Hall, Londa, 1966.

[11] D. R. Cox and W. L. Smith. On the Superposition of Renewal Processes. *Biometrika*, 41(1-2):91–99, 1954.

[12] I. Gerhardt and B. L. Nelson. Transforming Renewal Processes for Simulation of Nonstationary Arrival Processes. *INFORMS Journal on Computing*, 21(4):630–640, November 2009.

[13] A. M. Harper, S. E. Taranto, E. B. Edwards, and O. P. Daily. Organ transplantation policies: an update on a successful simulation project: the Unos Liver Allocation Model. In J. A. Joines, R. R. Barton, K. Kang, and P. A. Fishwick, editors, *Proceedings of the 2000 Winter simulation Conference*, pages 1955–1962, Piscataway, New Jersey, 2000. Institute of Electrical and Electroics Engineers.

[14] S. Harrod and W. D. Kelton. Numerical Methods for Realizing Nonstationary Poisson Processes with Piecewise-Constant Instantaneous-Rate Functions. *Simulation*, 82(3):147–157, 2006.

[15] Samuel Karlin and Howard M. Taylor. *A First Course in Stochastic Processes*. Acedemic Press, Inc, New York, 1975.

[16] R. W. Klein and S. D. Roberts. A Time-Varying Poisson Arrival Process Generator. *SIMULATION*, 43(4):193–195, October 1984.

[17] A.N. Kolmogorov and S.V. Fomin. *Introduction to Real Analysis Rev. English Ed.* Dover, 1970.

[18] M. E. Kuhl, S. C. Deo, and J. R. Wilson. Smooth Flexible Models of Nonhomogeneous Poisson Processes Using One or More Process Realizations. In S. J. Mason, R. R. Hill, L. Mönch, O. Rose, T. Jefferson, and J. W. Fowler, editors, *Proceedings of the 2008 Winter Simulation Conference*, pages 353–361, Piscataway, New Jersey, 2008. Winter Simulation Conference.

[19] M. E. Kuhl, S. G. Sumant, and J. R. Wilson. An Automated Multiresolution Procedure for Modeling Complex Arrival Processes. *INFORMS Journal on Computing*, 18(1):3, 2006.

[20] M. E. Kuhl and J. R. Wilson. Least Squares Estimation of Nonhomogeneous Poisson Processes. *Journal of Statistical Computation and Simulation*, 67(1):699–712, 2000.

[21] M. E. Kuhl, J. R. Wilson, and M. A. Johnson. Estimating and simulating Poisson processes having trends or multiple periodicities. *IIE Transactions*, 29(3):201–211, 1997.

[22] M.E. Kuhl and J.R. Wilson. Modeling and Simulating Poisson Processes Having Trends or Nontrigonometric Cyclic Effects. *European Journal of Operational Research*, 133(3):566–582, 2001.

[23] S. Lee, J. R. Wilson, and M. M. Crawford. Modeling and Simulation of a Nonhomogeneous Poisson Process Having Cyclic Behavior. *Communications in Statistics-Simulation and Computation*, 20(2-3):777–809, 1991.

[24] L. M. Leemis. Nonparametric Estimation of the Cumulative Intensity Function for a Nonhomogeneous Poisson Process. *Management Science*, pages 886–900, 1991.

[25] L.M. Leemis. Nonparametric Estimation and Variate Generation for a Nonhomogeneous Poisson Process from Event Count Data. *IIE Transactions*, 36(12):1155–1160, 2004.

[26] P. A. W. Lewis. Recent Results in the Statistical Analysis of Univariate Point Processes. *Stochastic Point Processes: Statistical Analysis, Theory, and Applications*, 51:1, 1972.

[27] P. A. W. Lewis and G. S. Shedler. Statistical Analysis of Non-stationary Series of Events in a Data Base System. *IBM Journal of Research and Development*, 20(5):465–482, 1976.

[28] P. A. W. Lewis and G. S. Shedler. Simulation of Nonhomogeneous Poisson Processes by Thinning. *Naval Research Logistics Quarterly*, 26(3):403–413, 1979.

[29] C. J. MacLean. Estimation and Testing of an Exponential Polynomial Rate Function Within the Nonstationary Poisson Process. *Biometrika*, pages 81–85, 1974.

[30] V. Paxson and S. Floyd. Wide-area traffic: The failure of poisson modeling. *IEEE/ACM Transactions on Networking (ToN)*, 3(3):226–244, 1995.

[31] A. A. B. Pritsker, D. L. Martin, J. S. Reust, M. A. Wagner, O. P. Daily, A. M. Harper, E. B. Edwards, L. E. Bennett, J. R. Wilson, M. E. Kuhl, J. P. Roberts, M. D. Allen, and J. F. Brudick. Organ Transplantation Policy Evaluation. In C. Alexopoulos, K. Kang, W. R. Lilegdon, and D. Goldsman, editors, *Proceedings of the 1995 Winter Simulation Conference*, pages 1314–1323, Piscataway, New Jersey, 1995. Institute of Electrical and Electroics Engineers.

[32] W. L. Smith. On the Cumulants of Renewal Processes. *Biometrika*, 46(1/2):1–29, 1959.

[33] C. Wu and H.L. Chen. A Consumer Purchasing Model with Learning and Departure Behaviour. *Journal of the Operational Research Society*, 51(5):583–591, 2000.

APPENDICES

Appendix A

Proof of Theorem 4

Proof. Define the binary sequence $\{B_n : n = 0, 1, \dots\}$, such that $B_0 \equiv 0$ and for $n = 1, 2, \dots,\ B_n = 1$ if the nth renewal epoch $\widetilde{S}_n$ sampled by inversion is accepted as a nonstationary arrival, and $B_n = 0$ if $\widetilde{S}_n$ is rejected. Then

$$N_Q(t) = \sum_{n=0}^{\infty} \mathbb{I}_{[\widetilde{S}_n \leq t]} B_n,$$

where the indicator random variable

$$\mathbb{I}_{[\widetilde{S}_n \leq t]} = \begin{cases} 1, & \text{if } \widetilde{S}_n \leq t, \\ \\ 0, & \text{otherwise.} \end{cases}$$

It follows that

$$\begin{aligned} \mathrm{E}[N_Q(t)] &= \mathrm{E}\left[\sum_{n=0}^{\infty} \mathbb{I}_{[\widetilde{S}_n \leq t]} B_n\right] \\ &= \sum_{n=0}^{\infty} \mathrm{E}[\mathbb{I}_{[\widetilde{S}_n \leq t]} B_n] \end{aligned}$$

by the monotone convergence theorem (page 305 of [17]). Conditioning on S_n and applying the law of total probability for expectations, we have

$$
\begin{aligned}
\mathrm{E}[N_Q(t)] &= \sum_{n=0}^{\infty} \mathrm{E}\{\mathrm{E}[\mathbb{I}_{[\widetilde{S}_n \le t]} B_n | \widetilde{S}_n]\} \\
&= \sum_{n=1}^{\infty} \mathrm{E}\{[\mathbb{I}_{[\widetilde{S}_n \le t]} \mathrm{E}[B_n | \widetilde{S}_n]\}
\end{aligned}
$$

by the substitution theorem for conditional expectations of [4] and because $B_0 \equiv 0$. We observe that for $n \ge 1$,

$$
\mathrm{E}[B_n | \widetilde{S}_n] = 1 \cdot \Pr\{B_n = 1 | \widetilde{S}_n\} + 0 \cdot \Pr\{B_n = 0 | \widetilde{S}_n\} = \Pr\{B_n = 1 | \widetilde{S}_n\} = \frac{\lambda(\widetilde{S}_n)}{\widetilde{\lambda}_Q(\widetilde{S}_n)},
$$

because the nth event in the NNPP $\{\widetilde{N}(t) : t \ge 0\}$ that occurs at time $\widetilde{S}_n$ is accepted with probability $\lambda(\widetilde{S}_n)/\widetilde{\lambda}_Q(\widetilde{S}_n)$. Then

$$
\begin{aligned}
\mathrm{E}[N_Q(t)] &= \sum_{n=1}^{\infty} \mathrm{E}\left\{ \mathbb{I}_{[\widetilde{S}_n \le t]} \frac{\lambda(\widetilde{S}_n)}{\widetilde{\lambda}_Q(\widetilde{S}_n)} \right\} \\
&= \mathrm{E}\left\{ \sum_{n=1}^{\infty} \mathbb{I}_{[\widetilde{S}_n \le t]} \frac{\lambda(\widetilde{S}_n)}{\widetilde{\lambda}_Q(\widetilde{S}_n)} \right\}
\end{aligned} \tag{A.1}
$$

by the monotone convergence theorem.

In terms of the desired rate function $\lambda(t)$, we see that the desired mean-value function

$$
\mu(t) \equiv \int_0^t \lambda(u) du \text{ for } t \ge 0 \tag{A.2}
$$

must be absolutely continuous (Theorem 5 on p. 338 of [17]). It follows from the Lebesgue differentiation theorem (Theorem 6 on p. 340 of [17]) that $\mu(t)$ is differentiable almost everywhere on the nonnegative real numbers and

$$
\frac{d}{dt}\mu(t) = \lambda(t) \text{ for almost all } t \ge 0. \tag{A.3}
$$

For an ordinary renewal process $\{N^{\#}(t) : t \ge 0\}$ whose interoccurence times $\{X_n^{\#} : n = 1, 2, \ldots\}$ are all sampled from the c.d.f. $G(\cdot)$, the mean-value function

$$
\mu^{\#}(t) = \mathrm{E}[N^{\#}(t)] \text{ for all } t \ge 0 \tag{A.4}
$$

is finite and differentiable for almost all $t \geq 0$; and by Equation (7.1) on p. 198 of [15], we have

$$\widetilde{\mu}_Q(t) = G_e(t) + \int_0^t G_e(t-u)d\mu^{\#}(u) \text{ for all } t \geq 0. \tag{A.5}$$

Because $G_e(t) \leq 1$ for all $t \geq 0$, it follows immediately from (A.5) that

$$0 \leq \widetilde{\mu}_Q(t) \leq 1 + \mu^{\#}(t) < \infty \text{ for all } t \geq 0. \tag{A.6}$$

To complete the proof of Theorem 4, we establish the following auxiliary result.

LEMMA 1. *If $f(u)$ is a nonnegative, bounded, Lebesgue-integrable function that vanishes outside a finite interval, then*

$$\mathrm{E}\left\{\sum_{n=1}^{\infty} f(\widetilde{S}_n)\right\} = \int_0^{\infty} f(u)\widetilde{\lambda}_Q(u)du < \infty. \tag{A.7}$$

Proof. If $0 \leq f(u) \leq f^* < \infty$ for all $u \geq 0$ and for some $u^* \in (0,\infty)$, we have $f(u) = 0$ for $u > u^*$, then we have

$$0 \leq \sum_{n=1}^{\infty} f(\widetilde{S}_n) \leq f^*\widetilde{N}_Q(u^*) \tag{A.8}$$

so that

$$\mathrm{E}\left[\sum_{n=1}^{\infty} f(\widetilde{S}_n)\right] \leq f^*\widetilde{\mu}_Q(u^*) < \infty; \tag{A.9}$$

therefore the expectation on the left-hand side of (A.9) is well defined.

If we take $\varphi(u) \equiv \mathbb{I}_{[t_* < u \leq t^*]}$, where $0 \leq t_* \leq t^* < \infty$, then we see that

$$\begin{aligned}\mathrm{E}\left[\sum_{n=1}^{\infty} \varphi(\widetilde{S}_n)\right] &= \mathrm{E}\left[\widetilde{N}_Q(t^*) - \widetilde{N}_Q(t_*)\right] \\ &= \widetilde{\mu}_Q(t^*) - \widetilde{\mu}_Q(t_*) \\ &= \int_0^{\infty} \varphi(u)\widetilde{\lambda}_Q(u)du. \end{aligned} \tag{A.10}$$

It follows that (A.10) also holds if $\varphi(u)$ is a simple function, that is, a finite linear combination of indicator functions of pairwise disjoint (measurable) sets. Now $f(u)$ can be expressed as the limit of a uniformly convergent sequences of simple functions $\{\varphi_k(u) : k = 1, 2, \cdots\}$ increasing to $f(u)$,

$$\left.\begin{aligned} &\varphi_k(u) \leq \varphi_{k+1}(u) \text{ for } k = 1, 2, \ldots, \\ &\lim_{k\to\infty} \varphi_k(u) = f(u) \end{aligned}\right\} \text{ for all } u \geq 0; \tag{A.11}$$

see, for example, Theorem 5 in Chapter 8 of [17], p. 286. Equation (A.11) and the monotone convergence theorem imply that

$$\lim_{k\to\infty}\int_0^\infty \varphi_k(u)\widetilde{\lambda}_Q(u)du = \int_0^\infty f(u)\widetilde{\lambda}_Q(u)du < \infty. \tag{A.12}$$

To complete the proof of the Lemma 1, we observe from Equation (A.10) that

$$\begin{aligned}\lim_{k\to\infty}\int_0^\infty \varphi_k(u)\widetilde{\lambda}_Q(u)du &= \lim_{k\to\infty} \mathrm{E}\left[\sum_{n=1}^{\infty}\varphi_k(\widetilde{S}_n)\right]\\ &= \mathrm{E}\left[\lim_{k\to\infty}\sum_{n=1}^{\infty}\varphi_k(\widetilde{S}_n)\right],\end{aligned} \tag{A.13}$$

again by invoking the monotone convergence theorem. In view of (A.9), we see that

$$\sum_{n=1}^{\infty} f(\widetilde{S}_n) < \infty \quad \text{with probability 1;} \tag{A.14}$$

and because $\varphi_k(u) \to f(u)$ uniformly in u as $k \to \infty$, Equation (A.14) implies that

$$\begin{aligned}\lim_{k\to\infty}\sum_{n=1}^{\infty}\varphi_k(\widetilde{S}_n) &= \sum_{n=1}^{\infty}[\lim_{k\to\infty}\varphi_k(\widetilde{S}_n)]\\ &= \sum_{n=1}^{\infty} f(\widetilde{S}_n) \text{ with probability 1,}\end{aligned} \tag{A.15}$$

by Theorem 9.16 of [2]. Combining (A.15), (A.12), and (A.13), we have the conclusion (A.7) of Lemma 1.

To complete the proof that $\mathrm{E}[N_Q(t)] = \mu(t)$ for all $t \ge 0$ when $\{N_Q(t) : t \ge 0\}$ is generated by the CIAT method, we must verify that the function

$$f(u) \equiv \mathbb{I}_{[u\le t]}\lambda(u)/\widetilde{\lambda}_Q(u) \text{ for all } u \ge 0 \tag{A.16}$$

satisfies the hypotheses of the Lemma 1. Because $0 \le \lambda(u) \le \widetilde{\lambda}_Q(u)$ and $\widetilde{\lambda}_Q(u) > 0$ for all $u \ge 0$, we see that

$$\left.\begin{array}{ll} 0 \le f(u) \le 1 & \text{for all } u \ge 0,\\ f(u) = 0 & \text{for } u > t.\end{array}\right\} \tag{A.17}$$

Moreover, because $\mathbb{I}_{[u\le t]}$, $\lambda(u)$, and $\widetilde{\lambda}_Q(u)$ are all Lebesgue-integrable functions, we see that $f(u)$ is measurable and bounded and hence Lebesgue-integrable on the interval $(0, \infty)$ (see Corollary to Theorem 3 on p. 298 of [17]). In this situation we see that

$$\begin{aligned}\int_0^\infty f(u)\widetilde{\lambda}_Q(u)du &= \int_0^\infty \mathbb{I}_{[u\le t]}\left[\frac{\lambda(u)}{\widetilde{\lambda}_Q(u)}\right]\widetilde{\lambda}_Q(u)du \\ &= \int_0^t \lambda(u)du \\ &= \mu(t). \end{aligned} \tag{A.18}$$

Combining Equation (A.1), the definition (A.16) , the conclusion of Lemma 1, and Equation (A.18), we finally obtain the desired result,

$$\begin{aligned}\mathrm{E}[N_Q(t)] &= \mathrm{E}\left[\sum_{n=1}^{\infty} f(\widetilde{S}_n)\right] \\ &= \int_0^\infty f(u)\widetilde{\lambda}_Q(u)du \\ &= \mu(t) \text{ for } t \ge 0. \end{aligned} \tag{A.19}$$

Appendix B

Proof of Theorem 5

Proof. The properties (3.7) and (3.10) follow from Property FD that $\lambda(t)$ is continuous except at a finite number of points in $[0, S]$ and by the construction of $\widetilde{\lambda}_Q(t)$ and $\widetilde{\mu}_Q(t)$. We define the auxiliary point process $\{\ddot{N}(t) : 0 \leq t \leq S\}$ that is obtained from the stationary renewal process $\{N^\circ(t) : 0 \leq t \leq S\}$ (with interrenewal times $\{X_j^\circ : j = 1, 2, \ldots\}$, where $X_1^\circ \sim G_e$ and $X_j^\circ \sim G$ for $j \geq 2$) by inversion of the desired mean-value function $\mu(t)$ so that the arrival epochs of the NNPP $\{\ddot{N}(t) : 0 \leq t \leq S\}$ are given by

$$\ddot{S}_j = \mu^{-1}(S_j^\circ) \text{ for } j = 0, 1, \ldots, \tag{B.1}$$

and we have

$$\ddot{N}(t) \equiv \max\{n : \ddot{S}_n \leq t\} \text{ for all } t \in [0, S]. \tag{B.2}$$

First we observe that with probability 1, we have

$$\left.\begin{array}{l} \widetilde{N}_Q(t) = N^\circ[\widetilde{\mu}_Q(t)] \\ \ddot{N}(t) = N^\circ[\mu(t)] \end{array}\right\} \text{ for all } t \in [0, S] \text{ and for all } Q = 1, 2, \ldots. \tag{B.3}$$

In view of (3.10) and (B.3), we see that with probability 1,

$$\begin{aligned} \lim_{Q\to\infty} \widetilde{N}_Q(t) &= \lim_{Q\to\infty} N^\circ[\widetilde{\mu}_Q(t)] \\ &= N^\circ[\mu(t)] \\ &= \ddot{N}(t) \text{ for each } t \in [0, S]. \end{aligned} \tag{B.4}$$

Since convergence with probability 1 (denoted $\xrightarrow{wp1}$) implies convergence in distribution (denoted $\xrightarrow{D}$) (see Theorem 20.5 of [5]), by (B.4) we have

$$\widetilde{N}_Q(t) \xrightarrow{D} \ddot{N}(t) \text{ as } Q \to \infty \text{ for each } t \in [0, S]. \tag{B.5}$$

Recall that to emphasize its dependence on Q, we let $\{N_Q(t) : 0 \le t \le S\}$ denote the CIAT-generated process that has the desired mean-value function as established in Theorem 4. Next we prove that as $Q \to \infty$, the difference $N_Q(t) - \widetilde{N}_Q(t)$ converges in probability (denoted $\xrightarrow{P}$) to zero. Choose $\delta > 0$ arbitrarily, where without loss of generality we may assume that $\delta < 1$. We need to prove that

$$\lim_{Q\to\infty} \Pr\{|N_Q(t) - \ddot{N}_Q(t)| > \delta\} = 0 \text{ for each } t \in [0, S]. \tag{B.6}$$

For simplicity in the rest of the proof in Theorem 5, we fix $t \in [0, S]$ arbitrarily. Pick $\varepsilon > 0$ arbitrarily small. We need to prove (B.6) by finding $Q(\varepsilon)$ such that

$$\Pr\{|N_Q(t) - \widetilde{N}_Q(t)| > \delta\} < \varepsilon \text{ for every } Q \ge Q(\varepsilon). \tag{B.7}$$

First we make a brief digression on probability generating functions. Let

$$\ddot{\mathcal{P}}(z) \equiv \sum_{n=0}^{\infty} \Pr\{\ddot{N}(t) = n\} z^n \text{ for } -1 \le z \le 1 \tag{B.8}$$

denote the probability generating function of the limiting random variable $\ddot{N}(t)$. Now since $\ddot{\mathcal{P}}(1) = 1$ and $\ddot{\mathcal{P}}(z)$ is continuous on $[-1, 1]$, we can find $\eta \in (0, 1)$ sufficiently small so that

$$\ddot{\mathcal{P}}(1 - \eta) > 1 - \varepsilon \tag{B.9}$$

Now back to the proof of (B.6). Given the following event in the underlying probability space

$$\mathcal{G}_n \equiv \{\, \ddot{N}(t) = n \,\} \text{ for } n = 0, 1, \ldots, \tag{B.10}$$

we see by Property FD of the given rate function $\lambda(\cdot)$, the continuity of the CDFs $G_e(\cdot)$ and $G(\cdot)$, and the uniform convergence properties (3.7) and (3.10) that for each sample point $\omega \in \mathcal{G}_n$, there exits a positive integer-valued random variable $Q_1 = Q_1(\omega)$ such that

$$\widetilde{N}_Q(t) = N^\circ[\widetilde{\mu}_Q(t)] = N^\circ[\mu(t)] = \ddot{N}(t) = n \text{ for } Q \ge Q_1. \tag{B.11}$$

To avoid trivialities in the rest of the proof, we assume $n > 0$. We observe that in the time horizon $[0, S]$, the isolated zeros of the given rate function $\lambda(\cdot)$ and the intervals over which $\lambda(\cdot)$ is zero are countable; and because the interrenewal-time distributions $G_e(\cdot)$ and $G(\cdot)$ are continuous, it follows that the arrival epochs

$$\ddot{S}_j = \widetilde{\mu}^{-1}(S_j^\circ) \text{ for } j = 1, \ldots, n \tag{B.12}$$

satisfy the relation

$$\text{Given } \mathcal{G}_n, \lambda(\ddot{S}_j) > 0 \text{ for } j = 1, \ldots, n \text{ with probability 1.} \tag{B.13}$$

By construction of the majorizing rate function $\widetilde{\lambda}_Q(\cdot)$ as detailed in Figure 3.1, we see that the majorizing arrival epochs

$$\widetilde{S}_{j,Q} = \widetilde{\mu}_Q^{-1}(S_j^\circ) \text{ for } j = 1, \ldots, n \tag{B.14}$$

satisfy the relation

$$\text{Given } \mathcal{G}_n, \widetilde{S}_{j,Q} \xrightarrow{wp1} \ddot{S}_j \text{ for } j = 1, \ldots, n. \tag{B.15}$$

Since the given rate function $\lambda(\cdot)$ has at most a finite set of discontinuities by Property FD, we have by (B.13) and (B.15) that

$$\left.\begin{array}{l} \text{Given } \mathcal{G}_n, \text{ with probability 1} \\ \lim_{Q\to\infty} \dfrac{\lambda(\widetilde{S}_{j,Q})}{\widetilde{\lambda}_Q(\widetilde{S}_{j,Q})} = \dfrac{\lambda(\ddot{S}_j)}{\lambda(\ddot{S}_j)} = 1 \text{ for } j = 1, \ldots, n. \end{array}\right\} \tag{B.16}$$

Let $\mathcal{G}_n' \subset \mathcal{G}_n$ denote the subevent defined by (B.16) so that we have

$$\Pr\{\mathcal{G}_n' \big| \mathcal{G}_n\} = 1 \text{ for } n = 0, 1, \ldots, \tag{B.17}$$

where we take $\mathcal{G}_0' \equiv \mathcal{G}_0$. For each sample point $\omega \in \mathcal{G}_n'$, it follows from (B.16) that we can find an integer-valued random variable $Q_2 = Q_2(\omega) \geq Q_1$ such that the following key property holds:

$$\left.\begin{array}{l} \text{Given } \mathcal{G}_n, \text{ with probability 1} \\ \dfrac{\lambda(\widetilde{S}_{j,Q})}{\widetilde{\lambda}_Q(\widetilde{S}_{j,Q})} \geq 1 - \eta \text{ for } j = 1, \ldots, n, \text{ provided } Q > Q_2. \end{array}\right\} \tag{B.18}$$

Because the majorizing arrival epochs $\{\widetilde{S}_{j,Q} : 1 \leq j \leq n\}$ are accepted independently by CIAT, we have

$$\Pr\left\{ \left|N_Q(t) - \widetilde{N}_Q(t)\right| \leq \delta \middle| \mathcal{G}_n \right\} \geq (1-\eta)^n \text{ for } Q \geq Q_2; \tag{B.19}$$

and in fact the dominated convergence theorem ensures that

$$\begin{aligned} &\lim_{Q\to\infty} \Pr\left\{ \left|N_Q(t) - \widetilde{N}_Q(t)\right| > \delta \middle| \mathcal{G}_n \right\} \\ &= 1 - \lim_{Q\to\infty} \Pr\left\{ \left|N_Q(t) - \widetilde{N}_Q(t)\right| \leq \delta \middle| \mathcal{G}_n \right\} \\ &= 1 - 1 = 0 \leq (1-\eta)^n. \end{aligned} \tag{B.20}$$

By the law of total probability, we have

$$\Pr\left\{\left|N_Q(t)-\widetilde{N}_Q(t)\right|>\delta\right\}=\sum_{n=0}^{\infty}\Pr\{\mathcal{G}_n\}\Pr\left\{\left|N_Q(t)-\widetilde{N}_Q(t)\right|>\delta\middle|\mathcal{G}_n\right\};\tag{B.21}$$

and by (B.19) and the dominated convergence theorem, we have

$$\begin{aligned}\lim_{Q\to\infty}\Pr\left\{\left|N_Q(t)-\widetilde{N}_Q(t)\right|>\delta\right\}&=\sum_{n=0}^{\infty}\Pr\{\mathcal{G}_n\}\times\lim_{Q\to\infty}\Pr\left\{\left|N_Q(t)-\widetilde{N}_Q(t)\right|>\delta\middle|\mathcal{G}_n\right\}\\&\le\sum_{n=0}^{\infty}\Pr\{\mathcal{G}_n\}\left[1-(1-\eta)^n\right]\\&=\sum_{n=0}^{\infty}\Pr\left\{\ddot{N}(t)=n\right\}\left[1-(1-\eta)^n\right]\\&=1-\ddot{\mathcal{P}}(1-\eta)\\&=\varepsilon\end{aligned}\tag{B.22}$$

But since $\varepsilon>0$ is arbitrary, we have proved (B.6) so that we have

$$N_Q(t)-\widetilde{N}_Q(t)\xrightarrow{P}0\quad\text{as } Q\to\infty.\tag{B.23}$$

Combining (B.5) and (B.23), we have by Slutsky's Theorem [4] that

$$N_Q(t)=\widetilde{N}_Q(t)+[N_Q(t)-\widetilde{N}_Q(t)]\xrightarrow{D}\ddot{N}(t)\text{ as } Q\to\infty\tag{B.24}$$

so that $N_Q(t)$ converges in distribution to $\ddot{N}(t)$.

Next we observe that the random variables $\{N_Q^2(t): Q=1,2,\ldots\}$ are *uniformly integrable*. From (B.3) we see that

$$N_Q^2(t)\le\widetilde{N}_Q^2(t)=\left\{N^\circ[\widetilde{\mu}_Q(t)]\right\}^2\le\left\{N^\circ[\widetilde{\mu}_1(t)]\right\}^2;\tag{B.25}$$

and

$$\mathrm{E}\left(\left\{N^\circ[\widetilde{\mu}_1(t)]\right\}^2\right)<\infty\tag{B.26}$$

by Equation (17) of [11].

Finally from (B.25) we see that

$$\Pr\left\{N_Q^2(t)\ge u\right\}\le\Pr\left\{\widetilde{N}_Q^2(t)\ge u\right\}\text{ for every } u>0,\ Q=1,2,\ldots\tag{B.27}$$

It follows immediately from the last paragraph on p. 348 of [5] that the random variables $\{N_Q^2(t): Q=$

$1, 2, \ldots\}$ are uniformly integrable. Combining this latter result with (B.24) and Theorem 25.12 of [5], we see that

$$\lim_{Q\to\infty} \mathrm{E}[N_Q^2(t)] = \mathrm{E}[\ddot{N}^2(t)]; \tag{B.28}$$

and combining the conclusion of Theorem 4 with (B.28), we have

$$\lim_{Q\to\infty} \mathrm{Var}[N_Q(t)] = \mathrm{Var}[\ddot{N}(t)]. \tag{B.29}$$

Now from Equation (B.3) and Equation (2.10), we have

$$\begin{aligned}
\mathrm{Var}\{\ddot{N}(t)\} &= \mathrm{Var}\{N^\circ[\mu(t)]\} \\
&= \left(\frac{\mathrm{Var}[X_2^\circ]}{\{\mathrm{E}[X_2^\circ]\}^3}\right) \cdot \mu(t) + o[\mu(t)] \\
&= C\mu(t) + o[\mu(t)]. \qquad \text{(B.30)}
\end{aligned}$$

It follows from Theorem 4, (B.29) and (B.30) that,

$$\lim_{Q\to\infty} \mathrm{Var}[N_Q(t)]/\mathrm{E}[N_Q(t)] = C + o[\mu(t)]/\mu(t) \text{ for } 0 < t \leq S, \tag{B.31}$$

which is the desired conclusion.

REMARK 1. In (B.22) we could have obtained the limiting value of zero directly from (B.16) without the intermediate results (B.17), (B.18), (B.19) and (B.20). We chose to present the intermediate results to highlight precisely the role of thinning in the argument.

Appendix C

Comprehensive presentation of results

Table C.1: CIAT-generated 95% CI estimators for $\mu(t),\ t \in (0, 8]$, in Case 2 with $C = 1.5$.

time t	0.2	0.4	0.6	0.8	1.0	1.2	1.4	1.6	1.8	2.0
$\widehat{\mu}(t)_{0.975}$	14.110	29.635	47.699	53.607	56.400	69.950	86.481	106.023	112.341	115.410
$\widehat{\mu}(t)$	11.606	25.824	42.767	48.360	51.001	63.883	79.706	98.497	104.592	107.550
$\widehat{\mu}(t)_{0.025}$	9.103	22.014	37.835	43.113	45.601	57.816	72.931	90.971	96.844	99.689
time t	2.2	2.4	2.6	2.8	3.0	3.2	3.4	3.6	3.8	4.0
$\widehat{\mu}(t)_{0.975}$	130.222	148.072	169.379	176.416	179.779	195.900	215.428	238.909	246.660	250.318
$\widehat{\mu}(t)$	121.830	139.131	159.770	166.617	169.891	185.605	204.756	227.555	235.141	238.712
$\widehat{\mu}(t)_{0.025}$	113.438	130.191	150.161	156.818	160.003	175.310	194.083	216.201	223.621	227.105
time t	4.2	4.4	4.6	4.8	5.0	5.2	5.4	5.6	5.8	6.0
$\widehat{\mu}(t)_{0.975}$	268.257	290.014	315.661	324.248	328.310	347.816	371.687	400.173	409.691	414.246
$\widehat{\mu}(t)$	256.246	277.500	302.674	311.060	315.057	334.259	357.629	385.481	394.780	399.256
$\widehat{\mu}(t)_{0.025}$	244.234	264.985	289.688	297.872	301.805	320.702	343.571	370.788	379.869	384.265
time t	6.2	6.4	6.6	6.8	7.0	7.2	7.4	7.6	7.8	8.0
$\widehat{\mu}(t)_{0.975}$	436.043	462.513	493.896	504.274	509.227	533.130	562.176	597.083	608.483	612.923
$\widehat{\mu}(t)$	420.629	446.578	477.496	487.696	492.567	516.070	544.659	579.017	590.264	594.583
$\widehat{\mu}(t)_{0.025}$	405.215	430.644	461.095	471.119	475.907	499.009	527.142	560.951	572.046	576.244

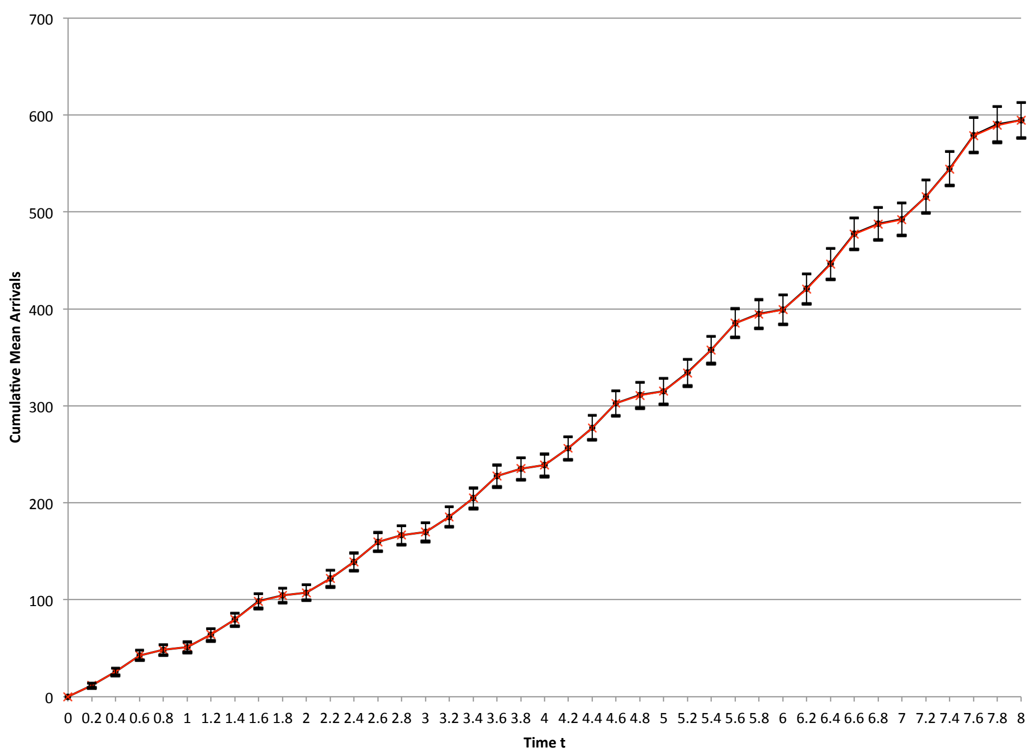

Figure C.1: CIAT-generated 95% CIs for $\mu(t),\ t \in (0, 8]$, in Case 2 with $C = 1.5$.

Table C.2: CIAT-generated 95% CI estimators for $C_Q(t)$, $t \in (0, 8]$, in Case 2 with $C = 1.5$.

time t	0.2	0.4	0.6	0.8	1.0	1.2	1.4	1.6	1.8	2.0
$\widehat{C}(t)_{0.975}$	1.521	1.609	1.621	1.618	1.619	1.623	1.604	1.629	1.635	1.634
$\widehat{C}(t)$	1.411	1.472	1.488	1.489	1.495	1.506	1.504	1.504	1.502	1.503
$\widehat{C}(t)_{0.025}$	1.302	1.334	1.355	1.360	1.371	1.388	1.403	1.379	1.369	1.373
time t	2.2	2.4	2.6	2.8	3.0	3.2	3.4	3.6	3.8	4.0
$\widehat{C}(t)_{0.975}$	1.642	1.639	1.646	1.637	1.634	1.614	1.577	1.606	1.594	1.591
$\widehat{C}(t)$	1.512	1.503	1.512	1.508	1.505	1.493	1.455	1.481	1.475	1.475
$\widehat{C}(t)_{0.025}$	1.383	1.368	1.378	1.378	1.377	1.372	1.333	1.356	1.356	1.358
time t	4.2	4.4	4.6	4.8	5.0	5.2	5.4	5.6	5.8	6.0
$\widehat{C}(t)_{0.975}$	1.608	1.613	1.579	1.582	1.573	1.544	1.552	1.582	1.595	1.596
$\widehat{C}(t)$	1.473	1.477	1.457	1.462	1.457	1.436	1.443	1.464	1.472	1.471
$\widehat{C}(t)_{0.025}$	1.339	1.341	1.334	1.341	1.341	1.329	1.335	1.345	1.349	1.347
time t	6.2	6.4	6.6	6.8	7.0	7.2	7.4	7.6	7.8	8.0
$\widehat{C}(t)_{0.975}$	1.595	1.607	1.595	1.592	1.594	1.592	1.588	1.595	1.586	1.596
$\widehat{C}(t)$	1.476	1.486	1.473	1.473	1.473	1.474	1.472	1.474	1.469	1.478
$\widehat{C}(t)_{0.025}$	1.357	1.365	1.351	1.354	1.352	1.356	1.357	1.352	1.353	1.361

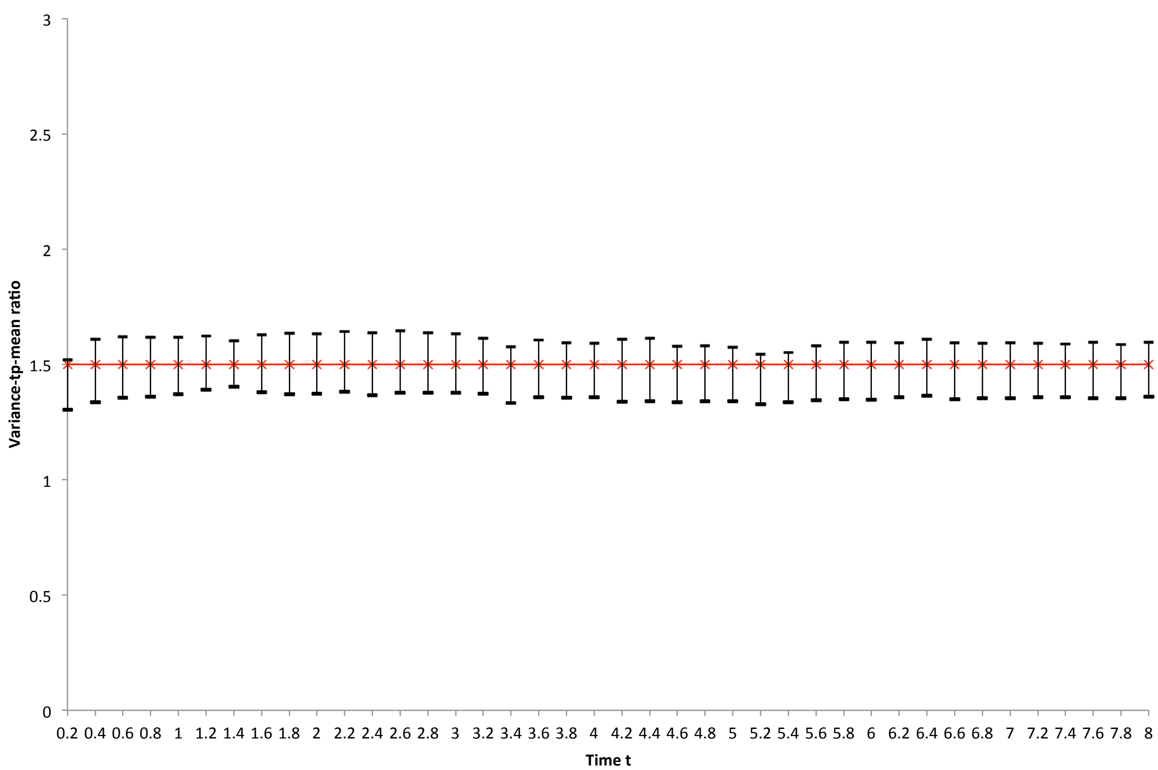

Figure C.2: CIAT-generated 95% CIs for $C_Q(t)$, $t \in (0, 8]$, in Case 2 with $C = 1.5$.

Table C.3: CIAT-generated 95% CI estimators for $\mu(t)$, $t \in (0, 8]$, in Case 2 with $C = 0.2$.

time t	0.2	0.4	0.6	0.8	1.0	1.2	1.4	1.6	1.8	2.0
$\widehat{\mu}(t)_{0.975}$	13.612	28.736	46.507	52.331	55.117	68.620	84.697	103.873	110.296	113.323
$\widehat{\mu}(t)$	11.687	25.886	42.868	48.443	51.101	64.051	79.643	98.279	104.514	107.466
$\widehat{\mu}(t)_{0.025}$	9.761	23.035	39.229	44.554	47.084	59.481	74.588	92.685	98.732	101.609
time t	2.2	2.4	2.6	2.8	3.0	3.2	3.4	3.6	3.8	4.0
$\widehat{\mu}(t)_{0.975}$	128.056	145.854	166.983	173.961	177.365	193.473	213.128	236.303	243.958	247.608
$\widehat{\mu}(t)$	121.795	139.135	159.801	166.614	169.925	185.722	204.985	227.742	235.262	238.842
$\widehat{\mu}(t)_{0.025}$	115.533	132.417	152.619	159.267	162.485	177.970	196.841	219.180	226.566	230.076
time t	4.2	4.4	4.6	4.8	5.0	5.2	5.4	5.6	5.8	6.0
$\widehat{\mu}(t)_{0.975}$	265.388	286.819	312.343	320.781	324.815	344.547	368.303	396.509	405.946	410.409
$\widehat{\mu}(t)$	256.256	277.365	302.546	310.880	314.864	334.218	357.592	385.403	394.746	399.142
$\widehat{\mu}(t)_{0.025}$	247.124	267.910	292.748	300.979	304.914	323.889	346.882	374.297	383.545	387.874
time t	6.2	6.4	6.6	6.8	7.0	7.2	7.4	7.6	7.8	8.0
$\widehat{\mu}(t)_{0.975}$	431.996	458.289	489.655	499.994	504.947	528.769	557.613	592.279	603.721	608.019
$\widehat{\mu}(t)$	420.472	446.403	477.305	487.573	492.471	516.024	544.609	578.864	590.180	594.447
$\widehat{\mu}(t)_{0.025}$	408.947	434.516	464.954	475.152	479.996	503.278	531.605	565.449	576.638	580.875

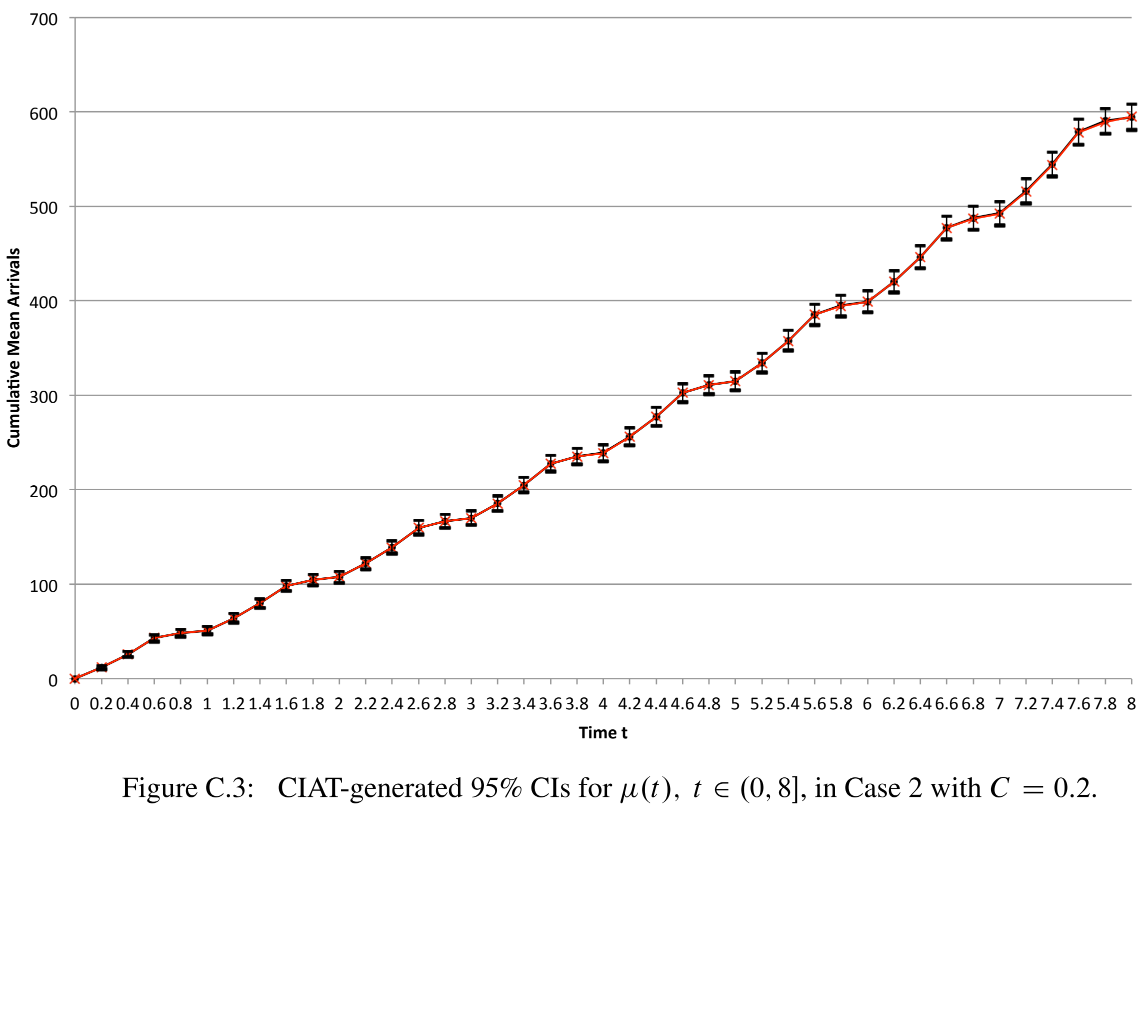

Figure C.3: CIAT-generated 95% CIs for $\mu(t)$, $t \in (0, 8]$, in Case 2 with $C = 0.2$.

Table C.4: CIAT-generated 95% CI estimators for $C_Q(t)$, $t \in (0, 8]$, in Case 2 with $C = 0.2$.

time t	0.2	0.4	0.6	0.8	1	1.2	1.4	1.6	1.8	2
$\widehat{C}(t)_{0.975}$	0.238	0.234	0.238	0.236	0.236	0.236	0.236	0.230	0.229	0.229
$\widehat{C}(t)$	0.219	0.214	0.219	0.216	0.216	0.218	0.218	0.213	0.212	0.213
$\widehat{C}(t)_{0.025}$	0.199	0.194	0.200	0.196	0.197	0.199	0.200	0.197	0.196	0.196
time t	2.2	2.4	2.6	2.8	3	3.2	3.4	3.6	3.8	4
$\widehat{C}(t)_{0.975}$	0.227	0.225	0.222	0.222	0.220	0.219	0.218	0.219	0.219	0.218
$\widehat{C}(t)$	0.210	0.207	0.204	0.204	0.203	0.201	0.201	0.202	0.202	0.201
$\widehat{C}(t)_{0.025}$	0.193	0.189	0.185	0.186	0.185	0.184	0.184	0.185	0.186	0.183
time t	4.2	4.4	4.6	4.8	5	5.2	5.4	5.6	5.8	6
$\widehat{C}(t)_{0.975}$	0.216	0.216	0.217	0.218	0.218	0.220	0.223	0.223	0.225	0.225
$\widehat{C}(t)$	0.199	0.200	0.200	0.201	0.201	0.203	0.205	0.205	0.206	0.207
$\widehat{C}(t)_{0.025}$	0.183	0.184	0.182	0.184	0.183	0.186	0.187	0.186	0.187	0.188
time t	6.2	6.4	6.6	6.8	7	7.2	7.4	7.6	7.8	8
$\widehat{C}(t)_{0.975}$	0.226	0.223	0.222	0.221	0.223	0.225	0.224	0.220	0.221	0.221
$\widehat{C}(t)$	0.207	0.205	0.205	0.204	0.205	0.207	0.208	0.204	0.205	0.205
$\widehat{C}(t)_{0.025}$	0.189	0.188	0.188	0.187	0.188	0.190	0.191	0.189	0.189	0.189

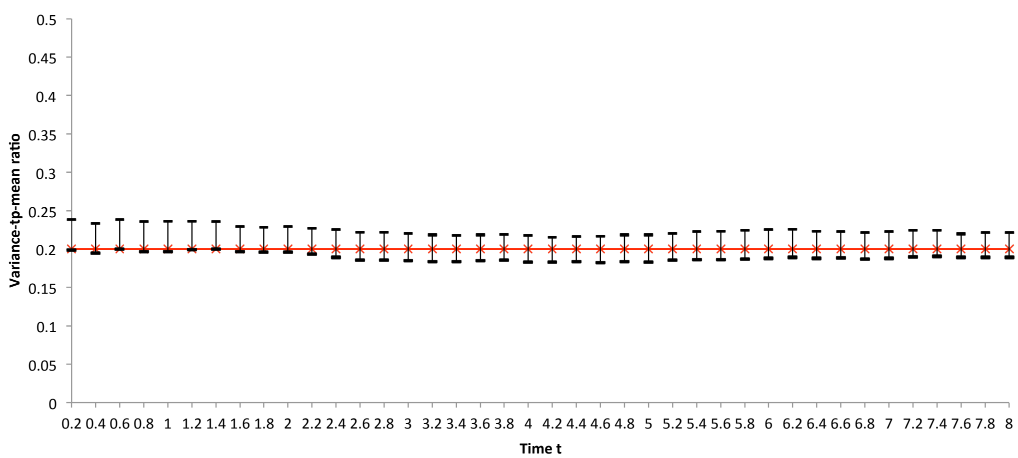

Figure C.4: CIAT-generated 95% CIs for $C_Q(t)$, $t \in (0, 8]$, in Case 2 with $C = 0.2$.

Table C.5: CIAT-generated 95% CI estimators for $\mu(t)$, $t \in (0, 8]$, in Case 3 with C=1.5.

time t	0.2	0.4	0.6	0.8	1.0	1.2	1.4	1.6	1.8	2.0
$\widehat{\mu}(t)_{0.975}$	13.947	28.592	45.127	50.281	52.643	63.801	77.101	92.238	97.176	99.399
$\widehat{\mu}(t)$	11.453	24.897	40.419	45.306	47.565	58.196	70.848	85.356	90.113	92.260
$\widehat{\mu}(t)_{0.025}$	8.959	21.202	35.710	40.330	42.487	52.592	64.595	78.475	83.050	85.120

time t	2.2	2.4	2.6	2.8	3.0	3.2	3.4	3.6	3.8	4.0
$\widehat{\mu}(t)_{0.975}$	110.008	122.498	137.119	141.823	144.008	154.603	167.264	182.268	187.110	189.378
$\widehat{\mu}(t)$	102.476	114.497	128.642	133.221	135.366	145.600	157.918	172.471	177.208	179.459
$\widehat{\mu}(t)_{0.025}$	94.944	106.497	120.165	124.619	126.723	136.596	148.571	162.674	167.306	169.541

time t	4.2	4.4	4.6	4.8	5.0	5.2	5.4	5.6	5.8	6.0
$\widehat{\mu}(t)_{0.975}$	200.331	213.509	229.322	234.588	237.064	249.094	263.743	281.057	286.812	289.652
$\widehat{\mu}(t)$	190.105	202.938	218.344	223.469	225.890	237.618	251.825	268.765	274.379	277.145
$\widehat{\mu}(t)_{0.025}$	179.880	192.368	207.366	212.351	214.717	226.143	239.907	256.473	261.946	264.639

time t	6.2	6.4	6.6	6.8	7.0	7.2	7.4	7.6	7.8	8.0
$\widehat{\mu}(t)_{0.975}$	303.216	319.734	339.469	346.188	349.391	365.426	385.213	409.104	417.110	420.289
$\widehat{\mu}(t)$	290.426	306.621	326.036	332.610	335.754	351.470	370.752	394.189	402.039	405.147
$\widehat{\mu}(t)_{0.025}$	277.636	293.508	312.602	319.031	322.117	337.513	356.291	379.273	386.969	390.005

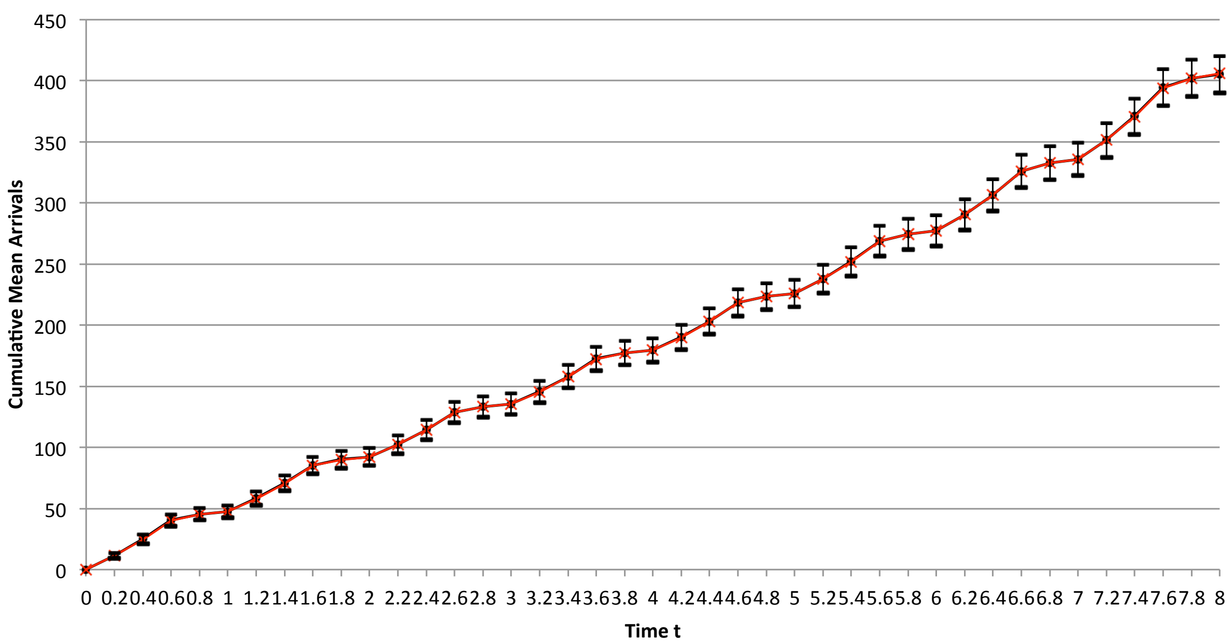

Figure C.5: CIAT-generated 95% CIs for $\mu(t)$, $t \in (0, 8]$, in Case 3 with $C = 1.5$.

Table C.6: CIAT-generated 95% CI estimators for $C_Q(t)$, $t \in (0, 8]$, in Case 3 with $C = 1.5$.

time t	0.2	0.4	0.6	0.8	1.0	1.2	1.4	1.6	1.8	2.0
$\widehat{C}(t)_{0.975}$	1.611	1.600	1.620	1.610	1.588	1.583	1.615	1.625	1.630	1.635
$\widehat{C}(t)$	1.470	1.462	1.460	1.461	1.448	1.442	1.469	1.472	1.475	1.482
$\widehat{C}(t)_{0.025}$	1.328	1.323	1.300	1.313	1.308	1.300	1.323	1.318	1.320	1.328
time t	2.2	2.4	2.6	2.8	3.0	3.2	3.4	3.6	3.8	4.0
$\widehat{C}(t)_{0.975}$	1.646	1.655	1.637	1.628	1.621	1.644	1.632	1.633	1.630	1.614
$\widehat{C}(t)$	1.493	1.504	1.499	1.491	1.482	1.502	1.488	1.492	1.488	1.475
$\widehat{C}(t)_{0.025}$	1.341	1.353	1.361	1.353	1.344	1.360	1.343	1.351	1.346	1.336
time t	4.2	4.4	4.6	4.8	5.0	5.2	5.4	5.6	5.8	6.0
$\widehat{C}(t)_{0.975}$	1.622	1.621	1.619	1.620	1.620	1.625	1.655	1.653	1.648	1.655
$\widehat{C}(t)$	1.481	1.482	1.484	1.488	1.486	1.492	1.514	1.508	1.511	1.515
$\widehat{C}(t)_{0.025}$	1.340	1.344	1.349	1.356	1.352	1.358	1.372	1.362	1.373	1.375
time t	6.2	6.4	6.6	6.8	7.0	7.2	7.4	7.6	7.8	8.0
$\widehat{C}(t)_{0.975}$	1.645	1.646	1.608	1.608	1.606	1.612	1.632	1.628	1.638	1.646
$\widehat{C}(t)$	1.511	1.502	1.477	1.480	1.479	1.480	1.504	1.503	1.508	1.513
$\widehat{C}(t)_{0.025}$	1.377	1.358	1.346	1.352	1.352	1.349	1.377	1.378	1.378	1.379

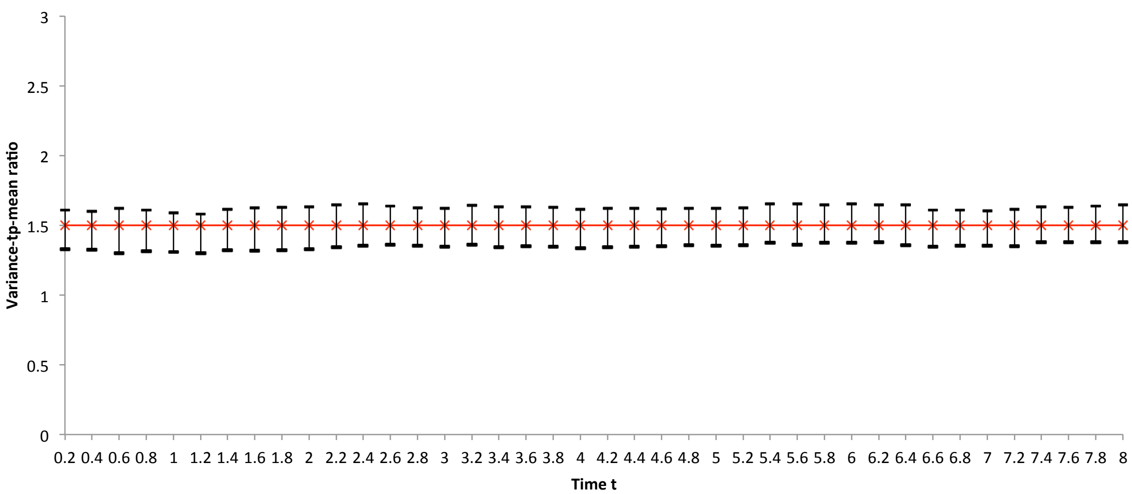

Figure C.6: CIAT-generated 95% CIs for $C_Q(t)$, $t \in (0, 8]$, in Case 3 with $C = 1.5$.

Table C.7: CIAT-generated 95% CI estimators for $\mu(t)$, $t \in (0, 8]$, in Case 3 with $C = 0.2$.

time t	0.2	0.4	0.6	0.8	1.0	1.2	1.4	1.6	1.8	2.0
$\widehat{\mu}(t)_{0.975}$	13.382	27.596	43.798	48.980	51.324	62.382	75.319	90.299	95.175	97.433
$\widehat{\mu}(t)$	11.465	24.831	40.285	45.227	47.496	58.177	70.688	85.163	89.896	92.073
$\widehat{\mu}(t)_{0.025}$	9.548	22.067	36.771	41.473	43.668	53.971	66.056	80.027	84.617	86.713

time t	2.2	2.4	2.6	2.8	3.0	3.2	3.4	3.6	3.8	4.0
$\widehat{\mu}(t)_{0.975}$	107.903	120.415	134.969	139.702	141.922	152.421	164.972	179.887	184.780	187.043
$\widehat{\mu}(t)$	102.252	114.393	128.598	133.224	135.401	145.684	157.957	172.496	177.278	179.498
$\widehat{\mu}(t)_{0.025}$	96.602	108.371	122.226	126.746	128.880	138.946	150.941	165.106	169.776	171.953

time t	4.2	4.4	4.6	4.8	5.0	5.2	5.4	5.6	5.8	6.0
$\widehat{\mu}(t)_{0.975}$	197.999	211.286	226.949	232.075	234.527	246.526	260.970	278.334	284.132	286.948
$\widehat{\mu}(t)$	190.253	203.212	218.541	223.585	225.975	237.748	251.987	269.046	274.710	277.451
$\widehat{\mu}(t)_{0.025}$	182.507	195.137	210.133	215.095	217.423	228.970	243.004	259.758	265.287	267.955

time t	6.2	6.4	6.6	6.8	7.0	7.2	7.4	7.6	7.8	8.0
$\widehat{\mu}(t)_{0.975}$	300.346	316.836	336.510	343.170	346.378	362.275	381.775	405.567	413.574	416.688
$\widehat{\mu}(t)$	290.616	306.884	326.292	332.868	336.018	351.696	370.943	394.422	402.279	405.345
$\widehat{\mu}(t)_{0.025}$	280.887	296.932	316.073	322.566	325.659	341.117	360.111	383.277	390.985	394.002

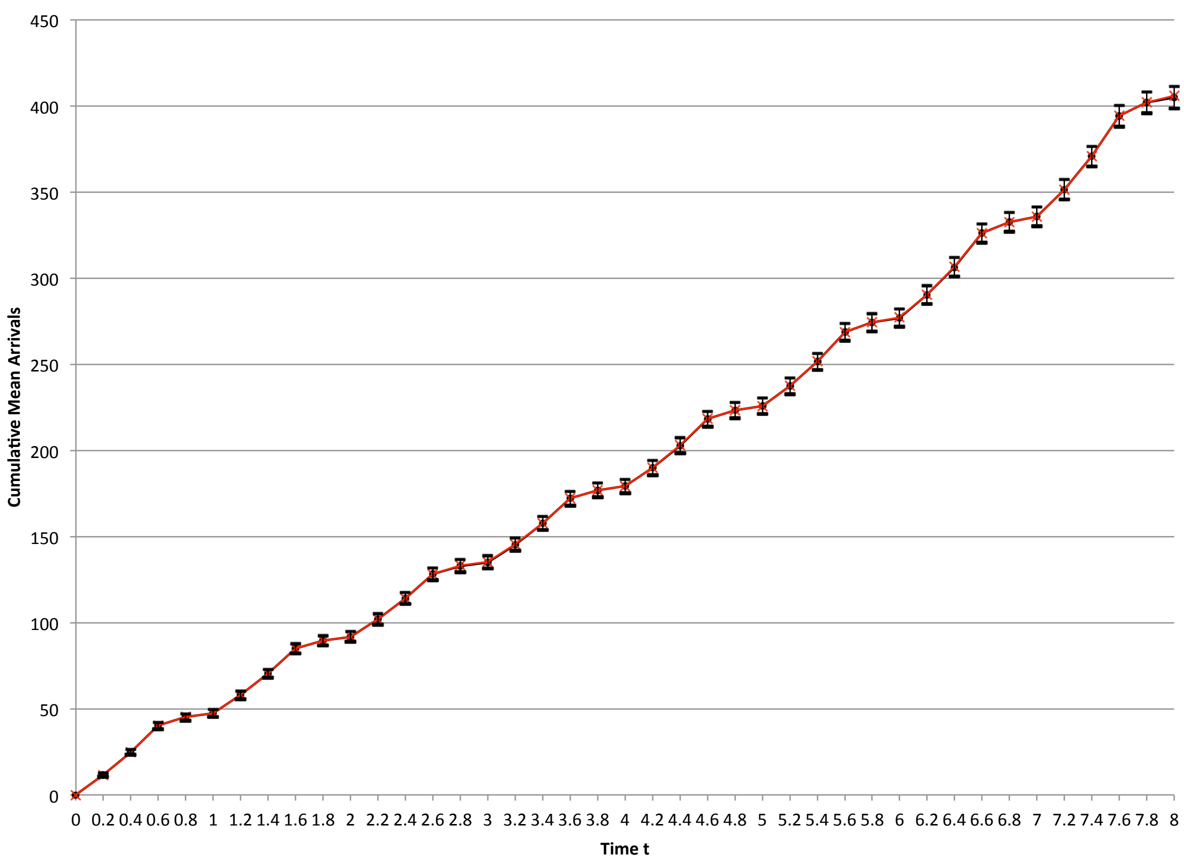

Figure C.7: CIAT-generated 95% CIs for $\mu(t)$, $t \in (0, 8]$, in Case 3 with $C = 0.2$.

Table C.8: CIAT-generated 95% CI estimators for $C_Q(t)$, $t \in (0, 8]$, in Case 3, $C = 0.2$.

time t	0.2	0.4	0.6	0.8	1.0	1.2	1.4	1.6	1.8	2.0
$\widehat{C}(t)_{0.975}$	0.227	0.216	0.213	0.217	0.216	0.215	0.214	0.217	0.219	0.218
$\widehat{C}(t)$	0.210	0.200	0.196	0.197	0.197	0.197	0.197	0.200	0.202	0.201
$\widehat{C}(t)_{0.025}$	0.193	0.183	0.180	0.177	0.178	0.179	0.179	0.183	0.185	0.184
time t	2.2	2.4	2.6	2.8	3.0	3.2	3.4	3.6	3.8	4.0
$\widehat{C}(t)_{0.975}$	0.219	0.219	0.222	0.221	0.221	0.221	0.217	0.218	0.218	0.217
$\widehat{C}(t)$	0.201	0.201	0.205	0.203	0.203	0.203	0.199	0.200	0.199	0.199
$\widehat{C}(t)_{0.025}$	0.183	0.183	0.187	0.185	0.186	0.185	0.182	0.182	0.181	0.181
time t	4.2	4.4	4.6	4.8	5.0	5.2	5.4	5.6	5.8	6.0
$\widehat{C}(t)_{0.975}$	0.216	0.216	0.215	0.215	0.215	0.214	0.213	0.214	0.216	0.216
$\widehat{C}(t)$	0.198	0.198	0.197	0.198	0.198	0.197	0.196	0.196	0.198	0.198
$\widehat{C}(t)_{0.025}$	0.180	0.180	0.179	0.181	0.181	0.181	0.179	0.178	0.180	0.180
time t	6.2	6.4	6.6	6.8	7.0	7.2	7.4	7.6	7.8	8.0
$\widehat{C}(t)_{0.975}$	0.215	0.215	0.213	0.212	0.211	0.211	0.213	0.217	0.219	0.219
$\widehat{C}(t)$	0.197	0.197	0.196	0.196	0.196	0.194	0.196	0.198	0.200	0.199
$\widehat{C}(t)_{0.025}$	0.179	0.180	0.180	0.180	0.180	0.178	0.178	0.180	0.180	0.180

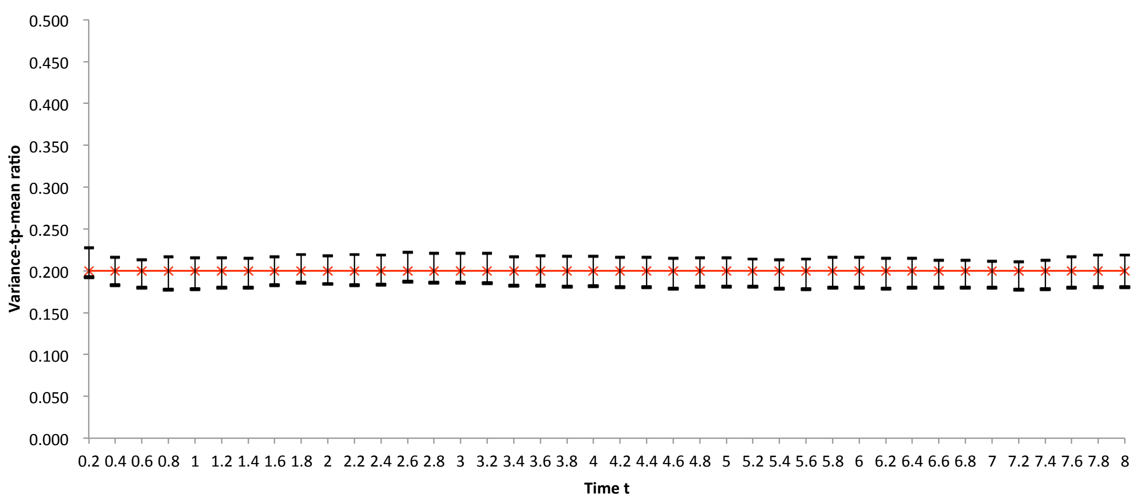

Figure C.8: CIAT-generated 95% CIs for $C_Q(t)$, $t \in (0, 8]$, in Case 3 with $C = 0.2$.

Table C.9: CIATL-generated 95% CI estimators for $\mu(t),\ t \in (0, 8]$, in Case 1 with $C = 1.5$.

time t	0.2	0.4	0.6	0.8	1.0	1.2	1.4	1.6	1.8	2.0
$\widehat{\mu}(t)_{0.025}$	13.989	29.094	46.364	51.851	54.389	66.483	80.800	97.635	103.144	105.657
$\widehat{\mu}(t)$	11.570	25.428	41.570	46.770	49.207	60.777	74.505	90.615	95.875	98.309
$\widehat{\mu}(t)_{0.975}$	9.150	21.761	36.776	41.689	44.024	55.070	68.211	83.594	88.606	90.960
time t	2.2	2.4	2.6	2.8	3.0	3.2	3.4	3.6	3.8	4.0
$\widehat{\mu}(t)_{0.025}$	117.770	131.995	148.807	154.230	156.805	168.662	182.821	199.432	204.781	207.357
$\widehat{\mu}(t)$	109.980	123.801	140.042	145.319	147.803	159.337	173.079	189.332	194.584	197.081
$\widehat{\mu}(t)_{0.975}$	102.190	115.607	131.278	136.408	138.802	150.012	163.337	179.232	184.388	186.805
time t	4.2	4.4	4.6	4.8	5.0	5.2	5.4	5.6	5.8	6.0
$\widehat{\mu}(t)_{0.025}$	219.110	233.223	249.807	255.146	257.624	269.349	283.337	299.838	305.217	307.744
$\widehat{\mu}(t)$	208.602	222.290	238.485	243.715	246.142	257.633	271.381	287.526	292.763	295.224
$\widehat{\mu}(t)_{0.975}$	198.093	211.357	227.163	232.284	234.659	245.917	259.424	275.215	280.308	282.703
time t	6.2	6.4	6.6	6.8	7.0	7.2	7.4	7.6	7.8	8.0
$\widehat{\mu}(t)_{0.025}$	319.521	333.628	350.133	355.482	357.985	369.671	383.666	400.158	405.525	407.548
$\widehat{\mu}(t)$	306.727	320.484	336.621	341.844	344.303	355.813	369.543	385.657	390.922	392.904
$\widehat{\mu}(t)_{0.975}$	293.932	307.339	323.109	328.205	330.620	341.955	355.419	371.156	376.319	378.259

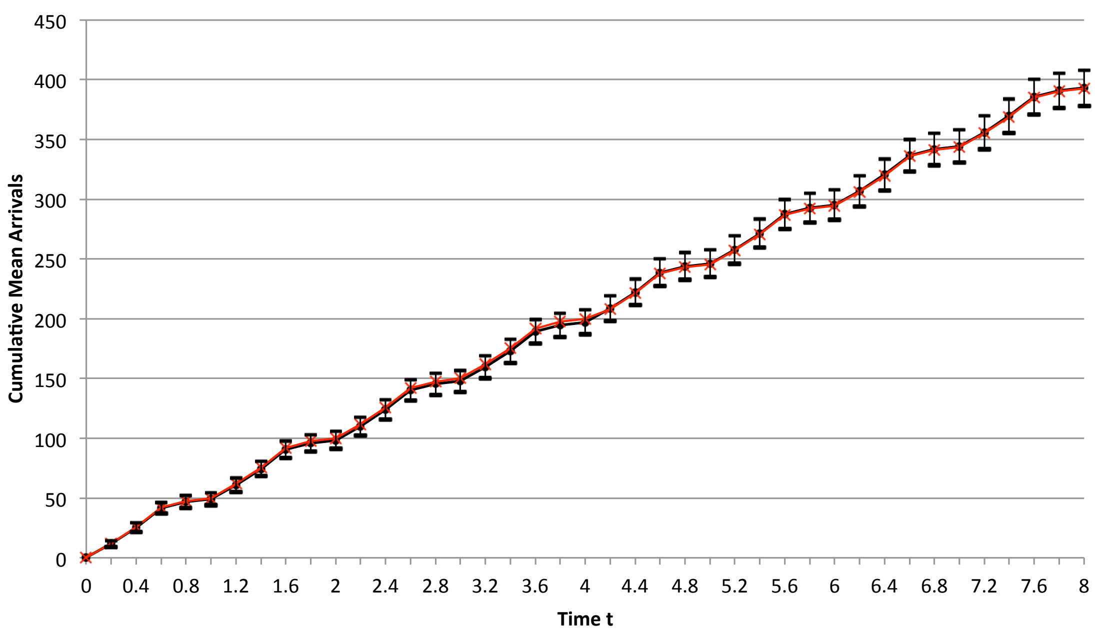

Figure C.9: CIATL-generated 95% CIs for $\mu(t),\ t \in (0, 8]$, in Case 1 with $C = 1.5$.

Table C.10: CIATL-generated 95% CI estimators for $C_Q(t)$, $t \in (0, 8]$, in Case 1 with $C = 1.5$.

time t	0.2	0.4	0.6	0.8	1.0	1.2	1.4	1.6	1.8	2.0
$\widehat{C}(t)_{0.025}$	1.439	1.490	1.547	1.530	1.525	1.509	1.483	1.517	1.537	1.533
$\widehat{C}(t)$	1.344	1.395	1.448	1.446	1.443	1.416	1.409	1.443	1.466	1.462
$\widehat{C}(t)_{0.975}$	1.248	1.300	1.349	1.363	1.361	1.323	1.334	1.369	1.395	1.392
time t	2.2	2.4	2.6	2.8	3.0	3.2	3.4	3.6	3.8	4.0
$\widehat{C}(t)_{0.025}$	1.543	1.525	1.530	1.512	1.515	1.515	1.530	1.526	1.534	1.543
$\widehat{C}(t)$	1.478	1.449	1.459	1.450	1.456	1.456	1.462	1.443	1.440	1.447
$\widehat{C}(t)_{0.975}$	1.412	1.373	1.388	1.387	1.397	1.397	1.393	1.361	1.346	1.351
time t	4.2	4.4	4.6	4.8	5.0	5.2	5.4	5.6	5.8	6.0
$\widehat{C}(t)_{0.025}$	1.530	1.573	1.565	1.561	1.555	1.564	1.540	1.531	1.538	1.538
$\widehat{C}(t)$	1.437	1.460	1.448	1.443	1.438	1.437	1.422	1.422	1.430	1.431
$\widehat{C}(t)_{0.975}$	1.343	1.347	1.331	1.324	1.321	1.310	1.305	1.313	1.321	1.324
time t	6.2	6.4	6.6	6.8	7.0	7.2	7.4	7.6	7.8	8.0
$\widehat{C}(t)_{0.025}$	1.546	1.556	1.573	1.570	1.573	1.562	1.558	1.571	1.557	1.559
$\widehat{C}(t)$	1.438	1.452	1.461	1.465	1.466	1.459	1.459	1.472	1.470	1.469
$\widehat{C}(t)_{0.975}$	1.330	1.349	1.350	1.361	1.359	1.355	1.361	1.373	1.383	1.379

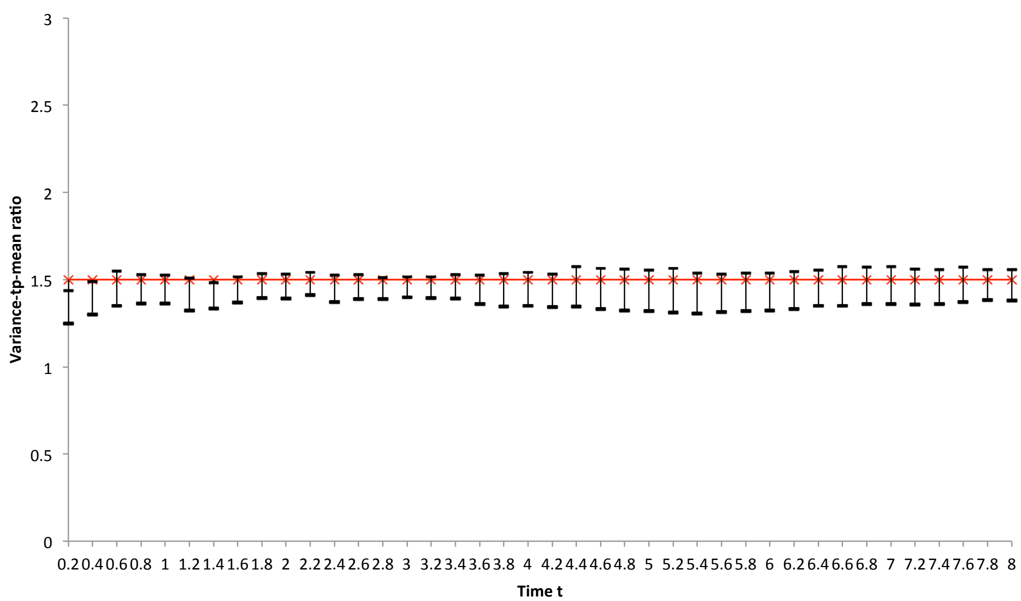

Figure C.10: CIATL-generated 95% CIs for $C_Q(t)$, $t \in (0, 8]$, in Case 1 with $C = 1.5$.